

8-2021

## Virulence and biofilm formation in *Candida albicans* are inhibited by short peptide subunits of EntV

Shane Cristy

Follow this and additional works at: [https://digitalcommons.library.tmc.edu/utgsbs\\_dissertations](https://digitalcommons.library.tmc.edu/utgsbs_dissertations)



Part of the [Medicine and Health Sciences Commons](#)

---

### Recommended Citation

Cristy, Shane, "Virulence and biofilm formation in *Candida albicans* are inhibited by short peptide subunits of EntV" (2021). *The University of Texas MD Anderson Cancer Center UTHealth Graduate School of Biomedical Sciences Dissertations and Theses (Open Access)*. 1122.  
[https://digitalcommons.library.tmc.edu/utgsbs\\_dissertations/1122](https://digitalcommons.library.tmc.edu/utgsbs_dissertations/1122)

This Thesis (MS) is brought to you for free and open access by the The University of Texas MD Anderson Cancer Center UTHealth Graduate School of Biomedical Sciences at DigitalCommons@TMC. It has been accepted for inclusion in The University of Texas MD Anderson Cancer Center UTHealth Graduate School of Biomedical Sciences Dissertations and Theses (Open Access) by an authorized administrator of DigitalCommons@TMC. For more information, please contact [digitalcommons@library.tmc.edu](mailto:digitalcommons@library.tmc.edu).

VIRULENCE AND BIOFILM FORMATION IN  
*CANDIDA ALBICANS* ARE INHIBITED BY SHORT PEPTIDE SUBUNITS OF ENTV

by

Shane Alan Cristy, B.S.

APPROVED:

---

Michael C. Lorenz, Ph.D.

Advisory Professor

---

Danielle A. Garsin, Ph.D.

---

Theresa M. Koehler, Ph.D.

---

Jennifer Walker, Ph.D.

---

William Margolin, Ph.D.

---

APPROVED:

---

Dean, The University of Texas

MD Anderson Cancer Center UTHHealth Graduate School of Biomedical Sciences

VIRULENCE AND BIOFILM FORMATION IN *CANDIDA*  
*ALBICANS* ARE INHIBITED BY SHORT PEPTIDE SUBUNITS OF ENTV

A

Thesis

Presented to the Faculty of

The University of Texas

MD Anderson Cancer Center UTHealth

Graduate School of Biomedical Sciences

in Partial Fulfillment

of the Requirements

for the Degree of

Master of Science

by

Shane Alan Cristy, B.S.  
Houston, Texas

August 2021

## **Acknowledgements**

I would like to acknowledge my advisor Mike Lorenz who has been incredibly supportive and helpful throughout this journey. He has challenged me to do my best, and I look forward to starting a new project and a new degree in the lab next fall. I'd also like to acknowledge Danielle Garsin for her leadership on the EntV project. Her creativity and ambition have been instrumental in the success of this study.

I would like to acknowledge the current and former Lorenz and Garsin lab members who have been so kind and helpful these past 18 months.

To my family for always supporting me.

Lastly, to my loving partner, Raven, for supporting me throughout all of graduate school. I couldn't have done this without you.

# **Virulence and biofilm formation in *Candida albicans* are inhibited by short peptide subunits of EntV**

Shane Alan Cristy, B.S.

Advisory Professor: Michael C. Lorenz, Ph.D.

*Candida albicans*, the most clinically significant fungal pathogen, commonly causes topical mucosal infections such as oral cavity and urogenital tract infections. It also less frequently causes severe invasive and bloodstream infections. Invasive infections are most prevalent amongst patients with compromised innate immune responses, such as those receiving chemotherapy or recovering from surgery. *C. albicans* can also form biofilms on implanted medical devices. Fungal infections are difficult to treat due to the paucity of therapeutic options, and this problem is compounded by the resistance properties of biofilm infections.

*Candida albicans* exists as a member of the commensal flora of the skin and gut where many complex polymicrobial interactions occur with genera such as *Pseudomonas* and *Streptococcus*. Some of these interactions potentiate or inhibit virulence. One such interaction is with *Enterococcus faecalis*, a bacterial gastrointestinal commensal species. *E. faecalis* produces a small peptide, EntV, that modulates *C. albicans* virulence. The mature 68-amino acid EntV peptide inhibits biofilm formation *in vitro* and attenuates fungal virulence in a *Caenorhabditis elegans* infection model and a murine oral candidiasis model.

In this work, I sought to identify the regions of EntV responsible for the anti-fungal activity, and based on structural information, I hypothesized that the activity is localized to a single helix of the mature peptide. In this study, I report that smaller peptides derived from this helix ranging from 12 to 16 amino acids have equal or improved efficacy in inhibiting *C. albicans* virulence and biofilm formation. These smaller peptides inhibit initial adhesion to abiotic surfaces, reduce final biofilm biomass, and reduce the size of mature biofilms as measured by confocal microscopy. Further trimming of these peptides to fewer than 11 amino acids reduces and eventually eliminates activity. These data indicate that EntV-derived peptides warrant further investigation as potential non-fungicidal additives to medical devices and antifungal therapeutics.

## Table of Contents

Approval Sheet .....	i
Title Page.....	ii
Acknowledgements.....	iii
Abstract.....	iv
Table of Contents.....	vi
List of Figures .....	ix
List of Tables .....	xi
<b>Chapter 1: Background and Significance.....</b>	<b>1</b>
<i>Candida albicans</i> .....	2
Pathology of Candidiasis .....	2
Polymorphism .....	6
Biofilms .....	7
Antifungal Treatment and Clinical Practice .....	11
Antimicrobial Peptides .....	15
Interspecies interactions with <i>Candida albicans</i> .....	19
EntV .....	22
<b>Chapter 2: Materials and Methods.....</b>	<b>25</b>
Strain, media, and growth conditions .....	26
Peptides.....	26
Growth Assay.....	28
Adhesion Assay .....	28
Crystal Violet Biofilm Assay .....	30

Biofilm confocal microscopy .....	31
Epithelial invasion assay .....	32
<b>Chapter 3: EntV derivatives inhibit <i>in vitro</i> adhesion .....</b>	<b>35</b>
Introduction .....	36
Results .....	38
Discussion .....	63
<b>Chapter 4: EntV derivatives reduce biofilm biomass and disrupt biofilm structure .....</b>	<b>68</b>
Introduction .....	69
Results .....	71
Discussion .....	104
<b>Chapter 5: Hyphal invasion of epithelial cells is inhibited by EntV in an <i>ex vivo</i> co-culture assay.....</b>	<b>107</b>
Introduction .....	108
Results .....	110
Discussion .....	115
<b>Chapter 6: Discussion .....</b>	<b>116</b>
Efficacy of C-terminal derived peptides.....	117
Translating to <i>in vivo</i> work .....	118
An examination of important residues .....	119
Determination of mechanism of action .....	120
Future Development .....	121
Future Applications .....	123



Evolution of EntV .....	126
Appendix.....	128
Bibliography .....	131
Vita.....	162

## List of Figures

Figure 3.1: Structure of a 16aa peptide derived from the C-terminal region of EntV ....	39
Figure 3.2: The 16aa EntV peptide is a non-fungicidal inhibitor of <i>C. albicans</i> adhesion .....	42
Figure 3.3: The 16aa EntV peptide has a sequence specific inhibitory effect on <i>C. albicans</i> adhesion .....	46
Figure 3.4: Similar bacteriocins do not greatly inhibit <i>C. albicans</i> adhesion.....	50
Figure 3.5: Glutamine substitution variants have different activities.....	54
Figure 3.6: Small EntV peptides form helices and are non-fungicidal.....	57
Figure 3.7: The 12aa EntV peptide has superior activity compared to the other small peptides .....	60
Figure 4.1: Untreated biofilms have a regular structure with vertical hyphae .....	73
Figure 4.2: EntV disrupts biofilm structure .....	76
Figure 4.3: 16aa EntV disrupts biofilm structure .....	79
Figure 4.4: 68aa EntV and 16aa EntV reduce biofilm biomass <i>in vitro</i> after 48 hours .....	83
Figure 4.5: The 16aa EntV peptide has a sequence specific inhibitory effect on <i>C. albicans</i> biofilm development.....	85
Figure 4.6: Similar bacteriocins Sam57 and YpkK are less effective than EntV at inhibiting biofilm development.....	88
Figure 4.7: Inhibition of biofilm development by small EntV peptides .....	92
Figure 4.8: 12aa EntV is a potent inhibitor of biofilm development .....	96
Figure 4.9: Biofilms treated with 11aa EntV .....	98

Figure 4.10: Biofilms treated with the 10aa EntV peptide .....	100
Figure 4.11: The 9aa EntV peptide does not disrupt biofilm structure.....	102
Figure 5.1: The C-terminal helix of EntV inhibits hyphal formation and epithelial invasion in an <i>ex vivo</i> co-culture assay .....	112
Figure A.1: DMSO does not inhibit adhesion at relevant concentrations .....	129

## List of Tables

Table 2.1: Peptides used in this study .....	26
Table 2.2: <i>Candida albicans</i> strains in this study .....	34

## **Chapter 1: Background and Significance**

## ***Candida albicans***

*Candida albicans* is an opportunistic fungal pathogen that causes oropharyngeal, vulvovaginal, and systemic disseminated infections (1, 2). *C. albicans* is commonly isolated from the commensal flora of the oral cavity, genitourinary tract, and gastrointestinal tract (3). As such, it is generally not communicated from person to person; rather, the source of infection is often the patient's own microbiota (4). As a member of the commensal microbiota, *C. albicans* has many complex interactions with other microbes in the host environment that potentiate or inhibit virulence (5–7). In healthy individuals, the phagocytes of the innate immune system and barrier defenses of mucosal surfaces prevent *C. albicans* overgrowth and infection (8).

This pathogen is remarkable for its phenotypic polymorphism, a key virulence trait. In response to environmental conditions, it can switch between growing as a budding ovoid yeast, elongated segmented pseudohyphae, and multinucleated filamentous hyphae (9). Additionally, *C. albicans* can form biofilms on abiotic and host surfaces (10). For some critically ill patients, the growth of a biofilm on a contaminated central venous catheter is the greatest risk factor for developing a dangerous bloodborne *C. albicans* infection (11–13). Due to a paucity of options in effective antifungal therapies to treat *C. albicans* infections, drug discovery is an important subject of active research in the field (10, 14, 15).

## **Pathology of Candidiasis**

*Candida albicans* causes many different infections in the human host. These include skin infections such as candidal intertrigo (16) and eye infections such as endogenous endophthalmitis (17). Some chronic mucocutaneous candidiasis

disorders even have host genetic predispositions (18). However, oropharyngeal, vulvovaginal, and disseminated candidiasis are the most clinically important infections caused by *C. albicans*.

### Oropharyngeal Candidiasis

Oropharyngeal candidiasis, or thrush, is a mucosal infection of the tongue and palate caused by an overgrowth of *Candida* species, of which *C. albicans* is the most common (1). These infections are common in neonates, especially those delivered preterm, due to their immature immune systems and lack of a healthy and diverse microbiome (19, 20). Adults with healthy immune systems and microbiomes rarely experience oropharyngeal infections (1, 20). However, persons with weakened immune systems, such as those living with HIV, are much more likely to develop an oropharyngeal candidiasis infection. Thrush is described as an AIDS-defining illness, meaning if a patient presents to the clinic with thrush and is otherwise healthy, they should additionally be tested for HIV (21). Lastly, other factors that may put a person at risk for an oral thrush infection include the presence of dental implants, radiation therapy or chemotherapy to the head or neck, and the use of broad-spectrum antibiotics (1, 20). Generally, the prognosis for these infections is good. If a relapse infection occurs, this is often due to poor compliance with prescribed therapy or because the predisposing factors still exist (1).

### Vulvovaginal Candidiasis

*Candida* species are the second most frequent cause of vulvovaginitis behind the overgrowth of bacterial species such as *Gardnerella vaginalis* and *Mycoplasma hominis* (22). Vulvovaginal candidiasis infections are caused by the overgrowth of

*Candida* species. Estimates have indicated up to 75% of women will experience at least one infection in their lifetime. The vast majority of these infections are caused by *Candida albicans*, but *Candida glabrata* is also etiological (22). In addition to overgrowth of *Candida* species, vulvovaginal candidiasis is characterized by irritation and inflammation of the vulva and vaginal mucosa and neutrophil infiltration to the site of infection (2, 23).

Vulvovaginal candidiasis is generally not considered to be a sexually transmitted disease as it is typically caused by the overgrowth of native flora (22). Several risk factors have been indicated including underlying diabetes, immunosuppressive therapies, antibiotic treatment, pregnancy, and oral contraceptive use (2, 22). Infections caused by *C. albicans* are typically uncomplicated and can be cleared by treatment with fluconazole. Recurring vulvovaginal candidiasis, defined as at least four infection events in a single year, is an idiopathic chronic overgrowth of *Candida* species that results in irritation and inflammation and requires maintenance therapy with antifungals to control symptoms (22). Of women who experience vulvovaginal candidiasis infections, only approximately 5-8% will contract a recurring infection (24).

#### Disseminated Candidiasis

Unlike the mucosal infections, disseminated candidiasis infections are rarer and more dangerous. In the year 2000 the United States diagnosed approximately 10,000 candidemia cases with a 10% attributable mortality in pediatric patients and a 14.5% attributable mortality in adult patients with a median crude mortality rate of 32% (25). Furthermore, the incidence of bloodstream infections (BSIs) caused by *Candida* species has risen since that measure, making *Candida* species the fourth leading



cause of nosocomial BSIs in the United States (26). There are two main sources of the infection: the gastrointestinal tract and the skin (8).

*C. albicans* can translocate from the gastrointestinal tract to the bloodstream due to abdominal surgery or the introduction of medical devices that disrupt the mucosal barrier (4). The gastrointestinal tract also tends to be the origin of disseminated infections in patients receiving treatment that affects quickly dividing cells. Patients with a hematological malignancy, receiving chemotherapy, or undergoing a hematopoietic stem cell transplant are at elevated risk for these infections. These patients are usually taking antibiotics, may have mucositis from chemotherapy, are immunosuppressed generally, and specifically may be neutropenic (25, 27, 28). Together, these conditions create an environment conducive to *Candida* overgrowth in the intestinal lumen and translocation to the bloodstream (29). Once bloodborne, the fungal cells invade host tissue. For the vast majority of these patients, the major organs most affected are the liver and spleen, while the kidneys are affected to a lesser degree (30).

Candidemia due to a translocation of fungal cells from the skin to the bloodstream is most often found in nonneutropenic acutely ill patients in intensive care units (25). Fungal contamination of central venous catheters is the primary route of translocation from the skin into the bloodstream of these patients (8, 11). Central venous catheters are an essential medical device, and over 5 million devices are inserted into patients annually in the United States (11). However, they are a major risk factor because they compromise the skin barrier and are infected frequently. There is a strong correlation, but not a strictly causal relationship, such that of all the

candidemia cases, 65 – 90% of these patients have a central venous catheter (12).

Autopsy results have shown that the kidneys are the primary organs affected by skin-derived candidemia (8).

In addition to the liver, spleen, and kidneys (8, 30), bloodborne *C. albicans* can invade the heart and central nervous system (31, 32). Once the infection is spread across the deep tissues of the host, it can be extremely difficult to treat. The infection may manifest into sepsis, meningitis, endocarditis, or total organ failure accompanied by crude mortality rates of 25 – 60% (31–34).

### **Polymorphism**

There is a common but oversimplified view in the field that yeast is the commensal, noninvasive, even nonpathogenic morphology of *C. albicans* while hyphae are the pathogenic form of medical concern (9). Rather, it is the switching between yeast and hyphal forms that is essential for full *C. albicans* virulence (35). This is evidenced by the attenuated virulence of mutants locked in either the yeast ( $\Delta/\Delta$  *efg1/efg1*  $\Delta/\Delta$  *cph1/cph1* (36)) or the hyphal ( $\Delta/\Delta$  *tup1/tup1*,  $\Delta/\Delta$  *nrg1/nrg1* (37)) forms.

Hyphal formation is characteristic of invasive infections (38–41). In mucosal infections, hyphae have been shown to adhere to the surface of epithelial cells and puncture the tissue; this activity has been shown in esophageal infections (40), vulvovaginal infections (38), and in the intestines (41). In disseminated infections, hyphae cause tissue damage throughout the body including the heart (31), kidneys, and the blood-brain barrier (39). Additionally, after phagocytosis by a macrophage, hyphal morphogenesis promotes *C. albicans* escape from the phagosome and

macrophage lysis (42). Hyphal morphogenesis is not induced after phagocytosis by a neutrophil, however, and no such escape or cell killing occurs (43).

The yeast form has been shown to be advantageous in the early stages of dissemination by establishing infection sites throughout the body of the host (35). It is unlikely that yeast cells in circulation arise from invading hyphal cells transitioning to yeast, as serum is a potent inducer of hyphal morphogenesis (44). Rather, these yeast cells may enter systemic circulation by translocation from where *C. albicans* grows commensally in the gut (45) and on the skin (46). Disperser cells from a mature biofilm are another source of yeast that can enter the circulation if the biofilm is growing on an implanted medical device such as a central venous catheter (9).

## **Biofilms**

*C. albicans* can form biofilms on a variety of biotic and abiotic surfaces including medical devices. *C. albicans* can easily colonize and form biofilms on devices introduced to places in the body where it grows as a commensal, such as dentures in the oral cavity or a urinary catheter to the urogenital tract (11, 13, 47). Regular and thorough cleaning are usually sufficient to limit biofilm growth on dentures (1), but infected urinary catheters must be removed and a subsequent antifungal regimen is sometimes required (11, 13). *Candida* biofilm infections of surgically implanted medical devices such as mechanical heart valves, pacemakers, and hip and knee joint prostheses are comparatively rare, but these infections carry higher rates of associated mortality. The infected device must be removed in an invasive surgery, unless doing so puts the patient at undo hazard (11, 13), followed by a lengthy regimen of antifungal treatment (48).

For nonneutropenic immunocompetent patients, the use of a central venous catheter is the greatest risk factor for developing candidemia (11–13). Additionally, of these infections caused by *C. albicans* and *C. parapsilosis*, biofilm production has been shown to correlate with a significant increase in mortality (49). For patients receiving nutrition by intravenous hyperalimentation, these two fungal species are of particular concern because the glucose in the media promotes biofilm formation (49). Disperser cells from these biofilms are given instant access to the bloodstream (9), and treatment necessitates removal of the catheter and a lengthy antifungal regimen (13, 48, 49).

#### Biofilm Structure and Development

The structure of a *C. albicans* biofilm is remarkably heterogenous. Typical biofilms grown on an approximately level surface have a densely packed foundational layer of yeast and pseudohyphal cells. Hyphae encased in extracellular matrix components grow out from the foundation (50–53). The total structure can be variable in size, but biofilms have been measured up to 450 µm thick (50).

The first step of biofilm development is adhesion to the substrate. This interaction is mediated by adhesins, proteins that protrude from the fungal cell wall to bind to the substrate either electrostatically or with specific cell surface receptors (54–57). Many *C. albicans* adhesins are glycosylphosphatidylinositol-dependent cell wall proteins with N-terminal domains that mediate substrate binding and characteristic serine/threonine-rich tandem repeat domains. *C. albicans* adhesins include Eap1 (56), Hwp1 (58), Iff4 (59), Hyr1 (60), and several of the Als proteins, notably Als1 and Als3 (54).

Of the adhesins mentioned, yeast cells express Eap1 and Als1 (55–57). Hyphal cells additionally produce the Hwp1, Iff4, Hyr1, and Als3 adhesins (57–59, 61, 62). There is a logical assumption in the field that all these adhesins are strong promoters of virulence due to their activity in fungal attachment to host tissue and establishment of invasive infections and biofilms (63). There is evidence that Iff4 and Hwp1 are essential for virulence in murine disseminated or oroesophageal models, respectively (58, 59). This evidence remains somewhat circumstantial. This uncertainty is likely because there are many adhesins in *C. albicans*, potentially some unknown as well, and deletion of only one allows for compensation by others.

Having established contact with the surface, the yeast cells rapidly change their transcription regulation framework. This process is dynamic with many overlapping pathways and yet undiscovered factors, but the end result of this change is to activate biofilm specific genes and stimulate hyphal morphogenesis (54, 55, 64, 65).

One of the first changes to occur is activation of the cell integrity mitogen-activated protein (MAP) kinase pathway by accumulating active MAP kinase Mpk1p (also called Slk2p). This initial contact-dependent step activates the PKC pathway with Pkc1, and a downstream target of Pkc1 is MAPK Mkc1 (66). Mkc1 is a critical effector that is necessary for virulence in systemic infections (67) and putatively interacts with Bcr1 and Efg1 (55, 64). Bcr1 is one of a set of a master biofilm regulators that has several downstream targets including Als1, Als3, and Hwp1 (54). In the context of biofilms, all three of these adhesins are important for fungal cell-cell adherence, creating a more cohesive structure (57, 62).

There are three well characterized signaling cascade pathways that serve as the primary positive promoters of hyphal morphogenesis in *C. albicans*: the cyclic AMP (cAMP) pathway, MAP-kinase pathway, and Rim101 pH response pathway (64, 65, 68). Of these, the cAMP pathway is most influential for clinically relevant biofilm development (69). The cAMP pathway responds to many different environmental conditions including the accumulation of CO<sub>2</sub> in the form of bicarbonate (70). Ras1 activates Cyr1, an adenylate cyclase, which produces cAMP. Two isoforms of cAMP-dependent protein kinase, Tpk1 and Tpk2, then phosphorylate Efg1 (65, 68, 69, 71).

The master regulators of biofilm formation identified so far are Efg1, Bcr1, Brg1, Rob1, Ndt80, Tec1, Flo8, Rfx2, and Gal4 (51, 72). These regulators have an intricate web of interactions with each other and regulate approximately 1,000 target genes (51). Efg1 has multiple functional domains and regulates transcription in response to various environmental cues (73). Deletion of *efg1* results in a mutant that is still capable of forming hyphae, but further manipulation to create a  $\Delta/\Delta$  *efg1/efg1*  $\Delta/\Delta$  *cph1/cph1* mutant locks *C. albicans* in a yeast form (36).

As the hyphae continue to grow, the filamentation transcription framework is maintained by Ume6 (74–76), a transcription factor that has been shown to work downstream of several of the master regulators (75). Ume6 has an oppositional equilibrating relationship with two transcriptional repressors, Nrg1 and Rfp1, along with their mutual co-repressor, Tup1. This creates a negative feedback loop without which *C. albicans* uncontrollably forms hyphae under non-inducing conditions (74, 75, 77).

In addition to forming hyphae, as the biofilm grows it produces extracellular matrix (ECM) components. The majority of the ECM is made of polysaccharides

similar in composition to the fungal cell wall (50). Biofilm cells have been found to have cell walls with a greater proportion of  $\beta$ -1,3 glucan, and the surrounding matrix contains significant amounts of  $\beta$ -1,3 glucan (78). The  $\beta$ -1,3 glucan in the biofilm matrix is most likely due to increased  $\beta$ -glucan synthase (Fks1p) activity. The matrix is successful in sequestering antifungal drugs, including drugs from all three major classes of antifungals, thus rendering *C. albicans* biofilms less susceptible to antifungal treatment (79, 80).

The final development stage of biofilm formation is when the biofilm seeds disperser cells into the media. In the context of a biofilm growing in an implanted central venous catheter, these cells will be the ones to cause a disseminated infection (9, 81). Interestingly, disperser cells have been shown to be phenotypically distinct from *C. albicans* cells grown planktonically. Disperser cells more readily adhere to new substrates and are more virulent in a disseminated model of disease (81).

### **Antifungal Treatment in Clinical Practice**

There are currently three classes of antifungal drugs approved for clinical use against invasive or systemic candidiasis by the FDA. These drugs target either ergosterol, a unique fungal membrane component, or the production of the fungal cell wall (82). There are few available antifungal drugs because fungi are more closely related to mammals evolutionarily than bacteria or viruses, thus we share more common cellular features. This similarity increases the odds of toxicity and off target effects (83).

## Polyenes

Polyenes were the first class of antifungals approved for clinical use and are derived from natural products of the bacterial genus *Streptomyces* (84). This class includes nystatin, a common topical treatment for mucocutaneous candidiasis. The polyenes used to treat invasive or systemic infections are amphotericin B and its lipid formulations (83). Amphotericin B interacts with ergosterol in the fungal membrane and forms an eight-member ring-shaped pore. Accumulation of these pores results in fungal membrane permeability and ultimately cell death (85, 86).

Amphotericin B is typically reserved for patients with special situations such as *Candida* meningitis or those who cannot tolerate or are not responding to therapy with echinocandins (82). This is because amphotericin B frequently causes adverse effects ranging from mild symptoms such as nausea and fever (83) to severe and potentially chronic symptoms including nephrotoxicity. Reports of acute renal failure can be as high as between 50 – 65% of patients receiving treatment. Amphotericin B continues to be used as a last line of defense despite the severe side effects due to its potent efficacy against most *Candida* species (82, 87).

## Azoles

Azole drugs inhibit fungal growth and alter membrane integrity by directly inhibiting the ergosterol biosynthesis enzyme lanosterol 14 $\alpha$ -demethylase (85, 88). The azole class can be separated into two subclasses: the imidazoles and the triazoles. The imidazoles include miconazole, clotrimazole, and ketoconazole and are used to treat mucocutaneous candidiasis (83). The triazoles approved by the FDA to treat systemic infections are fluconazole and voriconazole (82), however there are



many new drugs of this class in development (83). These drugs have generally good safety profiles and low toxicity (88). Per the current clinical guidelines, fluconazole may be used as a front-line drug for invasive candidiasis, especially against a *C. parapsilosis* infection. Furthermore, once laboratory results have positively identified the fungal agent, fluconazole is recommended against *C. albicans* and *C. tropicalis* species, and voriconazole may be appropriate for treating *C. krusei* and *C. glabrata* infections (89). While there has not been a significant shift in the incidence of azole resistant *C. albicans* isolates, that has not been the case across the rest of the *Candida* genus as other species develop resistance to these widely used drugs (90).

### Echinocandins

Echinocandins are the most recently developed class of antifungals. These drugs are fungicidal and are active to a narrower spectrum of mostly *Candida* and *Aspergillus* species. Echinocandins inhibit fungal wall biosynthesis by inactivating  $\beta$ -1, 3-D-glucan synthase (Fks1) (91). Of this class, caspofungin, micafungin, and anidulafungin are all FDA approved for treatment of systemic candidiasis (82), and all three of these drugs have excellent safety profiles with little to no adverse effects (92). These drugs are the current preferred front-line options available to treat any moderate to severe invasive candidiasis infection (89).

### Combination therapy

It remains unclear if combinations of the antifungal drugs listed thus far would provide any benefit when treating invasive candidiasis. A randomized clinical trial tested combinations of amphotericin B and fluconazole against monotherapy fluconazole and showed positive results for the combination therapy (93). However,

many leaders in the field have suggested this study had some methodological flaws (82, 94). Further study is necessary to determine if a combination of antifungal drugs would be advantageous for the treatment of invasive candidiasis (82); unfortunately, clinical trials of this kind are difficult to conduct due to many challenges including expense, time, low enrollment numbers, and the critical nature of the disease (95). *In vitro* and *in vivo* studies have been conducted, but these studies have produced inconsistent results, occasionally finding antagonism between different drugs (96).

For *Candida* meningitis, endophthalmitis, and endocarditis, current guidelines suggest a combination of amphotericin B and flucytosine, an antimetabolite drug (89). Flucytosine is not used as a monotherapy due to concerns about the development of resistance (83). From a survey of approximately 400 patients in the United States, 11 – 35% of *C. albicans* isolates have developed resistance to flucytosine (97).

#### Prophylactic treatment

In the recent decades, clinicians have used prophylactic administration of antifungals, especially azoles, to protect vulnerable patients from fungal infections. Many different types of patients may receive this therapy ranging from those with a recent abdominal surgery or a chronic hematological disease to recipients of stem cell or organ transplants (48, 98, 99). This treatment has been effective in reducing the incidence of invasive fungal infections in this vulnerable population (98–100); however, there are concerns about the development of resistance against these drugs.

Prophylactic azole treatment has been associated with an increase in the risk of colonization with resistant isolates and an increase in colonization with non-*albicans*

*Candida* species such as *C. glabrata* or *C. krusei*, which are innately resistant to fluconazole, or *C. dubliniensis* which has largely acquired fluconazole resistance (100).

#### Current Antifungal Limitations and Future Directions

Currently there are few options available for treatment of invasive candidiasis. Current guidelines in the United States outline only the nine drugs mentioned previously, and of those choices, four are amphotericin B formulations that carry severe risk of adverse effects, and the others comprise only two chemical classes (89), thus making the chance of resistance a critical concern. To address the urgent need of new antifungal agents, one possibility to pursue is the targeting of fungal virulence factors such as the formation of hyphae or biofilms. An agent created for this strategy would attenuate virulence rather than inhibit fungal growth and thus reduce the selective pressure for the generation of resistant mutants. Small molecule inhibitors have already been identified that show promising results exemplifying these key characteristics (14).

#### **Antimicrobial Peptides**

Antimicrobial peptides (AMPs) have been previously broadly defined as chemicals with either killing or static activity against microbes and that are comprised of amino acids with peptide bonds (101). AMPs can be conjugated with non-amino acid moieties and can range in size from large proteins to a few amino acids. The field of antifungal AMPs is less developed than that for antibacterial AMPs (101), but AMPs have been established as a legitimate avenue for future pharmacological discoveries (102).

Most AMPs can be categorized into one of three groups based upon their target and mechanism of action. AMPs that are active against *C. albicans* typically target either the membrane, the fungal cell wall, or nucleic acid biosynthesis and metabolism (101, 103). I have curated a noncomprehensive list of AMPs that are active against *C. albicans* for the purpose of emphasizing important discoveries in the field and demonstrating the state of antifungal peptide research.

#### Membrane-active peptides

AMPs that form pores in the cell membrane are common in nature. Production of these peptides has been identified in a wide variety of species including plant-associated bacteria, sheep, and honey bees (101). Pore-forming AMPs tend to be effective against a broad range of microorganisms. This lack of specificity can manifest as high toxicity when used in clinical applications (104). Amphotericin B and LL-37, an AMP produced by neutrophils, are both AMPs that interact with fungal cell membranes to form pores (86, 105). Human neutrophils and epithelial cells produce  $\beta$ -defensins that are secreted from the salivary glands (106).  $\beta$ -defensins HBD-1 and HBD-3 permeabilize membranes via an ATP-independent mechanism (107).

Not all AMPs that target the cell membrane form pores. One such example of interest is aureobasidin A, a cyclic depsipeptide produced by *Aureobasidium pullulans* (108). Aureobasidin A is a noncompetitive inhibitor of the essential sphingolipid biosynthesis enzyme inositol phosphorylceramide synthase (109, 110). This enzyme is not present in mammalian cells, so the peptide has a low toxicity profile (111). Aureobasidin A is potent against *Candida* species, but it has minimal efficacy against *Aspergillus* species due to increased efflux activity in *Aspergillus* (110, 112).

### Cell Wall targeting AMPs

The echinocandin class of antifungals discussed previously are AMPs synthetically derived from secondary metabolites produced by several fungal species (113). The echinocandins approved to treat candidemia, caspofungin, micafungin, and anidulafungin, are all cyclic lipopeptides with two proline residues (114). While isolates resistant to these drugs are rare, there are concerns about resistance because modification of a few amino acids of the target enzyme, Fks1, can increase the MIC of these drugs 100 to 1,000-fold (115). *In vitro* resistance studies of these drugs with *C. albicans* have shown a paradoxical effect where growth is reduced at the MIC, but then continues at concentrations above the MIC, and then halts at much higher concentrations. A leading hypothesis to explain this effect is that activation of stress response pathways can compensate to maintain cell wall stability, but whether this has any clinical relevance is undetermined as there is insufficient evidence of this effect in clinical datasets or *in vivo* models (114)

Another cell wall targeting AMP of interest is nikkomycin Z. This dipeptide synthesized by *Streptomyces tendae* is a competitive inhibitor of chitin synthases (116). Chitin is formed from  $\beta$ -(1,4) linkages of *N*-acetylglucosamine and is an essential component of the fungal cell wall (117). Chitin is of particular interest for fungal pathogenesis because hyphal cell walls contain approximately 10 times more chitin than yeast cells (118). Nikkomycin Z is fungicidal against *C. albicans*, but when used as a monotherapy it is lacking in potency. When used in combination with fluconazole, itraconazole, caspofungin, or micafungin, however, the drug synergizes to improve the

efficacy of these existing antifungals against *C. albicans* growing planktonically and as a biofilm (119, 120).

#### AMP nucleic acid inhibitors

Bovine neutrophils produce a tridecapeptide amide, indolicidin, that binds DNA and potentially has activity against DNA processing and repair (121, 122). This peptide causes some toxicity to human cells, so recent studies have investigated potential formulations with gold nanoparticles and graphene to develop the peptide into a potential pharmaceutical product (123, 124).

#### Other AMPs

Histatin 5 is a cationic peptide found in human salivary glands that is effective against many *Candida* species (125). This peptide binds to Ssa1/2 on the fungal cell wall and induces reactive oxygen species formation upon translocation into the cell (126–129). A 12-amino-acid product of Histatin 5 has been created that retains the anti-*Candida* activity (130, 131).

#### Current developments in AMP research

In recent years three antifungal peptides have been tested in clinical trials: aureobasidin A, nikkomycin Z, and VL-2397, which is primarily active against *Aspergillus* species (132). If approved for clinical use, these drugs would make available entirely new classes of antifungals.

The AMPs discussed here target fundamental properties of the cell, such as the charge of the membrane, that are typically difficult to alter, and any alterations made are often metabolically taxing (133). Additionally, the concentration range of AMPs that is conducive to selection of single-step, drug-resistant mutants is narrower than that of

conventional antimicrobials (134). The total of these effects is an overall lower probability of developing resistance (135). Therefore, AMPs are an attractive source for potential antifungal drugs and agents for use in combination therapy with conventional antifungals (133).

Resistance is not impossible, however. Resistance events have been described against both naturally occurring and pharmaceutical AMPs (103, 136, 137). The resistance strategies used against AMPs are not dissimilar to those used against conventional antimicrobials. *C. albicans* may acquire resistance to AMPs by secreting effectors to degrade the peptide, producing AMP efflux pumps, or by differential regulation of signaling pathways (138). Due to the threat of resistance, a strategy of particular interest would be to combine the advantages of AMPs with those of attenuation therapies. This strategy could potentially further reduce the selective pressure for development of resistance.

In general, the selective pressure to evolve AMPs stems from competition. From the perspective of the host, AMPs are used to protect against infection and cultivate the commensal microbiota (139). Many members of the commensal gut microbiota are intrinsically resistant to AMPs produced by the host in response to infection (140). For microbes, AMPs present a means to gain a competitive edge in their environment (141).

### **Interspecies interactions with *Candida albicans***

*C. albicans* has many complex interactions with other microbes in the host environment that potentiate or inhibit virulence (5–7). These interactions occur as both

direct physical contact (5, 142) and chemical signaling with quorum sensing mechanisms (142).

#### *Pseudomonas aeruginosa* and *Candida albicans*

*P. aeruginosa* is a Gram-negative opportunistic pathogen that produces several virulence factors (143). It is motile, rod-shaped, and capable of forming biofilms (144). *P. aeruginosa* and *C. albicans* are often co-isolated in cystic fibrosis lung infections and burn wound infections (6, 145–147). In *in vitro* studies, *P. aeruginosa* physically interacts with *C. albicans* by adhering to hyphal cells and then secreting phospholipases and phenazines, killing the fungal cells (148–150). *P. aeruginosa* also interacts with *C. albicans* chemically. A *P. aeruginosa* quorum sensing signaling molecule, 3-oxo-12 homoserine lactone is chemically similar to farnesol, a *C. albicans* quorum sensing signal molecule (55, 151). This signaling molecule from *P. aeruginosa* can trigger an inactivation of the Ras1-cAMP-PKA pathway, thus reducing the expression of hyphal and biofilm genes (151–154). In turn, farnesol from *C. albicans* has been shown to interact with *P. aeruginosa* quorum sensing and reduce the production of phenazines (155).

#### *Streptococci* and *Candida albicans*

*Streptococcus mutans* is a Gram-positive colonizer of the oral cavity that is commonly co-isolated with *C. albicans* from the denture plaques of healthy individuals and pediatric dental caries (156, 157). *S. mutans* produces a competence-stimulating peptide and a signaling molecule, *trans*-2-decenoic acid, that both inhibit hyphal formation in *C. albicans*. In turn, *S. mutans* quorum sensing is stimulated by *C. albicans* (158).



When forming dental plaques, *C. albicans* adheres to and aggregates with *Streptococci* such as *S. mutans*, *S. salivarius*, and *S. gordonii*. This physical interaction is mediated by the Als adhesins (159). *S. gordonii* directly interacts with Als1 and Als3 with its SspA and SspB surface proteins. Interaction with *S. gordonii* promotes *C. albicans* hyphal morphogenesis and biofilm formation (160–162).

#### *Enterococcus faecalis* and *Candida albicans*

*Enterococcus faecalis* is a Gram-positive opportunistic pathogen that causes several infections including endocarditis, bacteremia, urinary tract, and intra-abdominal infections. It is a member of the commensal gut microbiome as early as infancy (163). *C. albicans* and *E. faecalis* are commonly co-isolated likely due to their shared niche in the gastrointestinal tract (164–166). These species have been co-isolated from infected root canal samples (167) and blood samples from patients in intensive care (168). Intra-abdominal infections, typically the result of loss of gastrointestinal tract integrity, are the most frequent source of polymicrobial blood stream infections (169–172).

In the gut of healthy individuals, *E. faecalis* and *C. albicans* grow as benign commensals (3, 163). This type of growth can be demonstrated in *in vivo* models. In a *Caenorhabditis elegans* infection model, monocultures of *C. albicans* and *E. faecalis* were found to cause disease, but co-cultures of the two microbes attenuated the virulence of each (173). Furthermore, the addition of spent *E. faecalis* supernatant to *in vitro* cultures of *C. albicans* inhibited hyphal formation and reduced the biomass of biofilms (173). The inhibition of *C. albicans* by *E. faecalis* was found to be mediated by an antimicrobial peptide, EntV (15).

## EntV

EntV is the product of *E. faecalis* gene *ef1097* (15, 174). This bacteriocin has bactericidal activity against members of the Gram-positive genera *Lactobacilli* and *Staphylococcus*, including *Staphylococcus aureus* (174, 175). Its production is regulated by the Fsr quorum-sensing system (173, 175), and it is secreted from the cell as a 136-amino-acid (-aa) propeptide (176). A putative *E. faecalis* thioredoxin, DsbA, then catalyzes the formation of disulfide bond between C106 and C167, and the amino-terminus is cleaved by the extracellular *E. faecalis* metalloprotease GelE. This processing is necessary to produce the antifungally active 68aa EntV peptide (176).

This peptide is non-toxic to *C. albicans* but has been shown to attenuate fungal virulence traits. *In vitro* analyses showed EntV to have activity in reducing *C. albicans* hyphal morphogenesis and biofilm formation. EntV showed protection in a *C. elegans* infection model; treatment with concentrations of EntV ranging from 10 nM to 0.001 nM were all effective in reducing hyphal penetration into the cuticle of the nematodes and extending the lifespan relative to untreated infected nematodes. EntV also showed protection in a murine macrophage coculture model and was non-toxic toward the macrophages or HeLa cells. Lastly, EntV has been shown to reduce pathology in a murine oropharyngeal candidiasis model. In this experiment, the authors gave mice a sublingual inoculation of *C. albicans* and then allowed them to drink freely from water that either contained EntV or the vehicle control. After three and five days the mice were euthanized and tongues were collected for histology and fungal burden analysis. The mice provided with water containing 100 nM EntV showed fewer signs of fungal invasion into the epithelium, less disruption of the epithelium, and a significant

decrease in fungal burden (15). These results indicate that EntV is a potent inhibitor of *C. albicans* virulence and a strong candidate for further study as a potential antifungal therapy. The mechanism of action for the attenuation activity of EntV against *C. albicans* is undefined, but this is an active subject of research.

Our lab is interested in optimizing the EntV peptide into a viable pharmaceutical product. One objective in service to this goal is to find a substructure within the 68aa peptide that achieves the antifungal activities. The 68aa structure is suboptimal because of the necessity of the disulfide bond and its large size, but a single peptide structure of approximately twelve amino acids would be more in accordance with other antimicrobial peptides currently in clinical use or under investigation (101).

Our lab conducted an analysis of the structure of EntV that is currently unpublished. In this analysis, we found that the 136aa structure consists of a ring of helices around a central helix which happens to be the C-terminal region. Upon cleavage of the N-terminus by GelE, the ring is opened up, resulting in a 68aa structure, and the central C-terminal helix is exposed. This insight led to my central hypothesis that small peptides derived from this central helix will have equal to improved efficacy in inhibiting *C. albicans in vitro* biofilm formation and *ex vivo* virulence.

In this thesis I show that a 16aa peptide derived from the C-terminal central helix of EntV had greater potency in inhibiting *C. albicans* adhesion than the 68aa EntV peptide. This 16aa peptide had similar activity to the 68aa EntV peptide in altering *C. albicans* biofilm structure, reducing biofilm biomass, and inhibiting virulence in an *ex vivo* epithelial tissue invasion model. The EntV peptide and the C-terminal helix-

derived peptide were found to be highly specific for inhibiting biofilm formation in *C. albicans*. Lastly, a peptide of minimum size that retains the efficacy of the C-terminal helix was determined.

## **Chapter 2: Materials and Methods**

## Strain, media, and growth conditions

All strains used in this work are detailed in Table 2.2. For general growth and propagation, *C. albicans* strains were grown in yeast extract peptone dextrose (YPD) medium (1% yeast extract, 2% peptone, 2% glucose) (177) at 30°C and shaking at 200 rpm. Biofilm assays were performed in artificial saliva media (YNB-AS) modified from Wong & Sissions (178) (0.17% yeast nitrogen base without ammonium sulfate and amino acids (YNB) (w/v), 0.5% casamino acids (w/v), 0.25% mucin (porcine stomach mucin type III, Sigma) (w/v), 14mM potassium chloride, 8 mM sodium chloride, 100  $\mu$ M choline chloride, 50  $\mu$ M sodium citrate, 5  $\mu$ M ascorbate) (15).

## Peptides

The peptides in this study were designed by members of the Garsin and Lorenz labs and synthetically made and purchased from Bio-Synthesis, Inc, Lewisville, Texas, USA. These peptides were dissolved in dimethyl sulfoxide (DMSO) at a concentration of 1 mM for stocking purposes and stored at -80°C. The peptide solution in DMSO can be diluted directly into media for use in the assays described in this section. Table 2.1 describes the amino acid sequences of each peptide in the study starting from the amino terminus and ending at the carboxy terminus.

**Table 2.1: Peptides used in this study**

Peptide Identity	Amino acid sequence
68 amino acid EntV derivative (68aa)	LGSCVANKIKDEFFAMISISAIVKAAQKKAWKELAVTVLRFAKA NGLKTNAIIVAGQLALWAVQCGLS
16 amino acid EntV derivative (16aa)	AIIVAGQLALWAVQCG

12 amino acid EntV derivative (12aa)	VAGQLALWAVQC
11 amino acid EntV derivative (11aa)	AGQLALWAVQC
10 amino acid EntV derivative (10aa)	GQLALWAVQC
9 amino acid EntV derivative (9aa)	QLALWAVQC
16 amino acid helical peptide	VGALWICGLAVIQAAQ
16 amino acid disordered peptide	AAAAQQGGIICLLVWW
Q – I variant	AIIVAGILALWAVICG
Q – E variant	AIIVAGELALWAVECG
Sam57	KVVADEKTSITSEYTIEEQRQIDEVAAVLEKMFADGVTEENLK QYAQANYSEEELIADNELNTNLSQIQDENAIMYKVDWGALG NCMANKIKDELLAMISVGTIIKYAQKKAWKELAKIVIKYVAKAG VKTNAALIAGQLAIWGLQCGINF
YpkK	AETPAAVESAGTVDEQALAQYFAKVDNAQTEKEAHDALVDFL GEDAANQAIKENSATGQSVSTRGAGTFLTCIKGKASDDIKSV FDVNVVAAAIGQKDYAKAAKEAVKYLAKQGVKRNAAALAGM FAYWGWQCRGSW

## **Growth Assay**

Growth of *C. albicans* strain SC5314 with the peptides used in this study was assayed using a similar technique as described previously (179) with the following modifications. SC5314 was grown overnight in YPD at 30°C and shaking at 200 rpm and subsequently subcultured for 4 hours in the same growth conditions. Cells were then collected and washed twice in phosphate-buffered saline (PBS). The cell concentration was adjusted in YPD such that the starting OD<sub>600</sub> of the assay would be 0.01. Each peptide was added to YPD media for a final concentration of 100 nM. Cells and peptides were added together to clear 96 well polystyrene plates (Falcon) with a total media volume of 200 µl along with a media only contamination/negative control and a DMSO vector control. The plate was incubated at 30°C with continuous shaking for 16 hours, and OD<sub>600</sub> measurements were taken automatically every 15 minutes on a Synergy H1 plate reader (BioTek) with Gen5 version 3.08 software (BioTek).

## **Adhesion Assay**

The *C. albicans* adhesion assay was developed using similar techniques as described previously (180) with the following specifications. *C. albicans* strains SC5314 and  $\Delta/\Delta$  *efg1*  $\Delta/\Delta$  *cph1* were grown overnight at 30°C and shaking at 200 rpm and subsequently subcultured for 4 hours in the same growth conditions. Cells were then collected, washed twice in phosphate-buffered saline (PBS), and adjusted to a concentration of  $1 \times 10^7$  cells/ml in PBS (or PBS with peptide additions) (measured with Countess II, Life Technologies). The peptides were prepared in a dilution series with final concentrations of 100 nM, 10 nM, 1 nM, 0.1 nM, 0.01 nM, and 0.001 nM. The *C. albicans* cells were then soaked in the PBS peptide solution for 60 minutes at 30°C and



shaking at 200 rpm. Then 100 µl of this solution was added to wells of a 96 well tissue culture treated polystyrene plate (Falcon) (for a concentration of  $1 \times 10^6$  cells/well). Technical replicates of each test condition were performed in 6 total adjacent wells. 100 µl of YNB-AS media with peptide additions at the same concentration was then added to each well, and then the plate was incubated for 90 minutes at 37°C and shaking at 200 rpm. After this incubation, the media was gently removed along with any cells that failed to adhere. The remaining cells were then stained for 20 minutes with 40 µl of 0.08% crystal violet solution (diluted, Sigma) added to each well. The crystal violet stain was removed and the wells were washed three times with sterile water to remove any excess dye. The cells were then destained with 200 µl of 200 proof ethanol for 20 minutes, and 100 µl of the ethanol solution was transferred to a new well for analysis. The optical density at 595 nm ( $OD_{595}$ ) was measured using a Synergy H1 plate reader (BioTek) with Gen5 version 3.08 software (BioTek).

For data analysis, the background absorbance was determined by including a series of media only control wells. This background was then subtracted from the values of all the samples, and the data was normalized against the untreated control. For the experimental wells, the data was presented as a percentage relative to the untreated control. These experiments were replicated in at least biological triplicate, and the normalized data was analyzed in a two-way ANOVA with a Dunnett's test to determine differences between the untreated control and the experimental samples. Statistical analysis was performed using GraphPad Prism 9.1 software.

## Crystal Violet Biofilm Assay

The crystal violet biofilm assay was developed using a similar technique as described previously (15, 180) with the following specifications. *C. albicans* strains SC5314 and  $\Delta/\Delta$  *efg1*  $\Delta/\Delta$  *cph1* were grown overnight in YPD medium at 30°C and shaking at 200 rpm. Cells were then collected, washed twice in phosphate-buffered saline (PBS), and adjusted to a concentration of  $5 \times 10^6$  cells/ml in PBS (or PBS with peptide additions) (measured with Countess II automated cell counter, Life Technologies). The peptides were prepared in a dilution series with final concentrations of 100 nM, 10 nM, 1 nM, and 0.1 nM. The *C. albicans* cells were then soaked in the PBS peptide solution for 60 minutes at 30°C and shaking at 200 rpm. Then 100  $\mu$ l of this solution was added to wells of a 96 well tissue culture treated polystyrene plate (Falcon) (for a concentration of  $5 \times 10^5$  cells/well). Technical replicates of each test condition were performed in 6 total adjacent wells, and duplicate plates were made to ensure against the chance of contamination. The plate was then incubated for 60 minutes at 37°C and shaking at 200 rpm. The PBS and cells that failed to adhere were gently removed, and 200  $\mu$ l of YNB-AS media with the same peptide dilution series was added to each well. The plate was then incubated statically at 37°C for 48 hours. After incubation, the remaining media, planktonic cells, and pellicle were removed, leaving only the surface associated biofilm. This was stained with 50  $\mu$ l of 0.08% crystal violet solution (diluted, Sigma) for 30 minutes. The crystal violet staining solution was removed, and then the plate was washed 4 times using an automated 405 TS Microplate washer (BioTek). The program parameters were set with an aspiration travel speed of 4.1 mm / second and 300  $\mu$ l wash volume dispensed at

flow rate setting 3. The biofilms were then destained with 200  $\mu$ l of 200 proof ethanol for 20 minutes, and 50  $\mu$ l of the resultant was transferred to a new well, diluted with 100  $\mu$ l of ethanol, and analyzed. The optical density at 595 nm ( $OD_{595}$ ) was measured using a Synergy H1 plate reader (BioTek) with Gen5 version 3.08 software (BioTek).

For data analysis, the background absorbance was determined by including a series of media only control wells. This background was then subtracted from the values of all the samples, and the data was normalized against the untreated control. For the experimental wells, the data was presented as a percentage relative to the untreated control. These experiments were replicated in at least biological triplicate, and the normalized data was analyzed in a two-way ANOVA with a Dunnett's test to determine differences between the untreated control and the experimental samples. Statistical analysis was performed using GraphPad Prism 9.1 software.

### **Biofilm confocal microscopy**

*C. albicans* biofilms were examined with confocal microscopy using a similar technique as described previously (15) with the following specifications. *C. albicans* strain *HWP1p-GFP, ADH1p-mCherry* was grown overnight at 30°C and shaking at 200 rpm. Cells were then collected, washed twice in phosphate-buffered saline (PBS), and adjusted to a concentration of  $5 \times 10^6$  cells/ml in PBS (or PBS with peptide additions) (measured with Countess II, Life Technologies). The peptides were prepared at a concentration of 300 nM. The *C. albicans* cells were then soaked in the PBS peptide solution for 60 minutes at 30°C and shaking at 200 rpm. Then 100  $\mu$ l of this solution was added to wells of a tissue culture treated 8 well chamber slide (Ibidi) (for a concentration of  $5 \times 10^5$  cells/well). At least 2 technical replicates were performed for

each biological replicate. Then 200 µl of YNB-AS media with peptide additions at the same concentration was added to each well, and the slide was incubated statically for 48 hours at 37°C. After incubation, the biofilms were washed once with PBS to remove planktonic cells.

Z-stacked microscopic images were taken of the biofilms using an Olympus IX83 inverted microscope with cellSens Dimension 2.3 (Olympus) software. The z-stack images were taken at 20x magnification and had 101 vertical frames. Each frame was separated by 3 µm, creating an image of totaling 300 µm in depth. Each image was created using fluorescence microscopy, and if possible, these images were deconvoluted for final presentation.

### **Epithelial invasion assay**

Human pharyngeal carcinoma cells (FaDu) of cell line HTB-43 (ATCC, Manassas, Virginia, USA) were cultured in Dulbecco's Modified Eagle's Medium (DMEM) (GE Life Sciences) + 10% fetal bovine serum (FBS), phenol red pH indicator, penicillin, and streptomycin at 37°C in a 5% CO<sub>2</sub> humidified incubator. These cells were washed with PBS, counted (measured with Countess II, Life Technologies), and adjusted to a concentration of  $1.5 \times 10^5$  cells/ml in fresh DMEM culture media. 100 µl of these cells (for a concentration of  $1.5 \times 10^4$  cells/well) were added to each well of an 8 well chamber slide (Ibidi) along with 200 µl of fresh DMEM culture media. These cultures were allowed to grow for 2 to 3 days until each well contained a completely confluent single layer of cells.

A *C. albicans* strain (JRC58B) constitutively producing mCherry from the *ACT1* promoter (*ACT1p-mCherry*) was grown overnight at 30°C and shaking at 200 rpm.

Cells were then collected, washed twice in phosphate-buffered saline (PBS), and adjusted to a concentration of  $2.5 \times 10^5$  cells/ml in PBS (or PBS with peptide additions) (measured with Countess II, Life Technologies). The peptides were prepared at a concentration of 300 nM. The *C. albicans* cells were then soaked in the PBS peptide solution for 60 minutes at 30°C and shaking at 200 rpm. Then 100 µl of this solution was added to wells of a tissue culture treated 8 well chamber slide (Ibidi) (for a concentration of  $2.5 \times 10^4$  cells/well). At least 2 technical replicates were performed for each biological replicate. Then 200 µl of DMEM media with peptide additions only (no FBS, phenol red, etc.) at the same concentration was added to each well, and the slide was incubated statically for 2 hours at 37°C in a 5% CO<sub>2</sub> humidified incubator.

After incubation the media was removed and the cells were fixed with 2.7% paraformaldehyde for 20 minutes. The cell layer was then washed three times with PBS and then incubated with PBS-diluted NucBlue Fixed Cell Stain (Thermo Fisher – Life Technologies Corp. Eugene, Oregon, USA) and a polyclonal anti-*Candida*-FITC antibody (LifeSpan BioSciences, Inc) overnight at 4°C and gentle rocking. The following day, fluorescent and differential interference contrast images were taken using an Olympus IX83 inverted microscope with cellSens Dimension 2.3 (Olympus) software.

**Table 2.2 – *Candida albicans* strains in this study**

Strain	Designation	Relevant Genotype	Source /
			Reference
SC5314	Wild Type	Prototroph	(181)
HLC54	$\Delta/\Delta$ <i>efg1</i> $\Delta/\Delta$ <i>cph1</i>	<i>ura3::1 imm434/ura3:: 1 imm434</i> <i>cph1::hisG/cph1::hisG</i> <i>efg1::hisG/efg1::hisG-URA3-hisG</i>	(36)
CEGC1	<i>HWP1p-GFP</i> , <i>ADH1p-mCherry</i>	<i>ura3/ura3ENO1/eno1::HWP1p-GFP-URA3</i> <i>RPS10/rps10::ADH1p-mCherry-SAT1</i>	(15)
JRC58B	<i>ACT1p-mCherry</i>	<i>RPS10/rps10::ACT1p-mCherry-SAT1</i>	Unpublished from John R. Collette

The three mutant strains, HLC54, CEGC1, and JRC58B were all created from the SC5314 parent strain.

### **Chapter 3: EntV derivatives inhibit *in vitro* adhesion**

## Introduction

The first step of biofilm formation is adhesion to the substrate. *C. albicans* uses adhesins that bind to specific cell surface receptors or interact electrostatically with an abiotic substrate to mediate adhesion (54–57). Many *C. albicans* adhesins are glycosylphosphatidylinositol-dependent cell wall proteins with N-terminal domains that mediate substrate binding. Yeast cells produce adhesins such as Eap1 and Als1, while hyphae produce additional adhesions including Als3 and Hwp1 (55–57). Once a cell establishes contact with a surface, it will rapidly change its transcription regulation framework. There are many different transcription factors and pathways involved in this change, some of which remain poorly understood, that ultimately initiate the activation of biofilm specific genes and stimulate hyphal morphogenesis and biofilm formation (54, 55, 64, 65).

The data presented in this chapter focus on the analysis of a novel peptide inhibitor of the initial adherence to an abiotic substrate, specifically a tissue culture treated polystyrene 96 well plate. The adhesion assays were conducted in artificial saliva media (YNB-AS) as modified from Wong & Sissions (178). This medium contains amino acids as the sole carbon source and 0.25% mucin (w/v) (15) (for further information, refer to Chapter 2). The presence of amino acids as a carbon source has been shown to stimulate hyphal development in *C. albicans* (179), and this exact medium has been previously shown to be capable of stimulating hyphal development (15).

The YNB-AS medium is intended to be a sufficient representation of the oral environment (178). The range of catabolites available in the human oral environment is



quite vast and variable between persons (182–184). However, the full range of catabolites is not necessary to grow physiologically relevant microbial structures. The medium used in Wong & Sissions was shown to support physiologically relevant representations of oral biofilms such as dental plaque (178). The importance of using YNB-AS in this study is that this media replicates a clinically important niche of *C. albicans* infection and has direct relevance to murine oropharyngeal candidiasis, the dominant *in vivo* infection model used in our lab.

An important component of the YNB-AS media is the dissolved porcine stomach type III mucin. *C. albicans* is able to bind and adhere to mucins, although the molecular mechanism remains unknown (185, 186). Mucins contain fucose glycans, a known binding partner of the N-terminal region of Als1 (187) and likely binding partner of the structurally similar Als3 adhesin (185). Hwp1 also has the potential to bind to mucins as it is known to bind to host buccal epithelial cells (188) and have complementary activity with Als1 and Als3 in surface adhesion (57).

In this chapter, the activity of peptides derived from the C-terminal helix domain of EntV are tested in inhibiting *C. albicans* adherence to an abiotic substrate. This analysis includes examinations of the predicted structures of these derived peptides and an examination of structure and sequence specificity of the interaction between *C. albicans* and the derived peptides. The specificity of the interaction between *C. albicans* and EntV is examined using alternative bacteriocin peptides. Lastly, a peptide of optimal activity and minimal length is determined.

## Results

It has been previously shown that the 68aa EntV peptide does not inhibit the growth of *C. albicans* but has a potent effect on inhibiting fungal virulence and the development of *C. albicans* biofilms (15). I hypothesized that the C-terminal helix of EntV causes the attenuation activity. Figure 1.1A shows the amino acid sequence starting with the N-terminus of the 68aa peptide (15, 174, 175) with the derived 16aa peptide in red font. I used PEP-FOLD 3 (189–191), a *de novo* peptide structure prediction software available online, to predict the structure of the 16aa peptide. The dominant model predicted a helix that incorporated all available residues (Figure 3.1B), which is consistent with the conformation of these residues in the 68aa structure (data unpublished). However, three alternative models were generated that collectively indicated instability at the N-terminus with disagreement on whether the valine at position 4 would be included in the helix. Thus, these models produced peptides with the first 3 to 4 residues forming a disorganized N-terminal tail (Figure 3.1C).

A) 68aa EntV

LGSCVANKIKDEFFAMISISAIVKAAQKKAWKELA 35

VTVLRFKANGGLKTN**AIIVAGQLALWAVQCGLS** 68

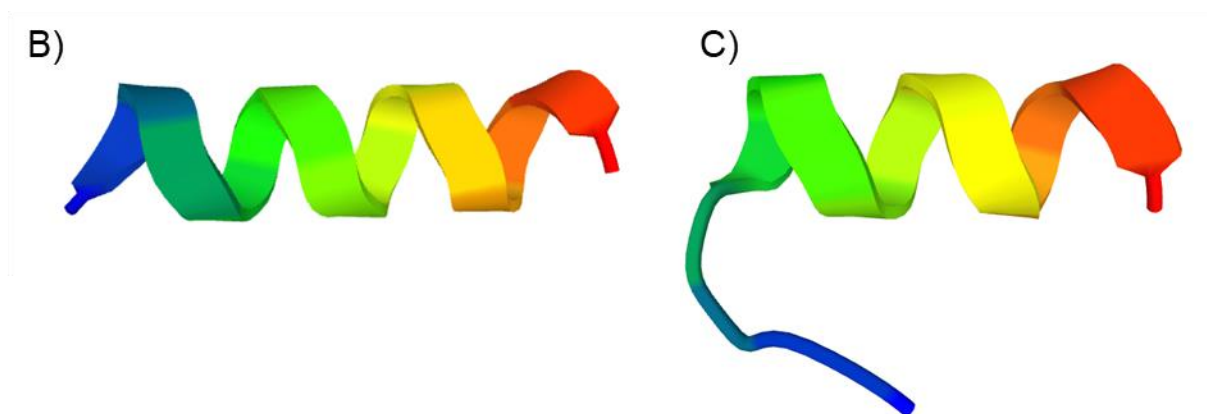


**Figure 3.1: Structure of a 16aa peptide derived from the C-terminal region of EntV.** The portion of the full EntV peptide responsible for the attenuation activity against *C. albicans* was hypothesized to be the C-terminal helix. A) The amino acid sequence of the fully processed C-terminal region of EntV is listed with the 16aa region of interest identified in red text. B) The structure of this 16aa peptide in physiological conditions was predicted using PEP-FOLD 3 (189–191). The dominant model indicated a structure with all the residues forming a helix. C) From this same analysis, alternative models predicted a structure with the first 3-4 residues forming a disorganized N-terminal tail.

---

### **The 16aa EntV peptide is a non-fungicidal inhibitor of *C. albicans* adhesion**

To determine if the central, C-terminal helix of EntV is responsible for the attenuation activity, I compared the 68aa EntV peptide with the 16aa peptide derived from the C-terminus thereof in biofilm development assays. The 68aa peptide has been previously shown to have no cytotoxic effect on *C. albicans* (15), so I verified that this was true of the 16aa peptide as well. I performed a growth assay to assess any toxic effects that may exist against the *C. albicans* prototrophic strain SC5314 cultured in YPD media. The 68aa and 16aa peptides were diluted to a final concentration of 100 nM in YPD media, and a volumetrically equivalent DMSO only control was included to verify that the DMSO solvent did not contribute to any toxicity. By this analysis, the peptides cause no toxicity to the planktonic *C. albicans* cells (Figure 3.2A), so any differences in biofilm development found in subsequent assays are from legitimate inhibition effects.

The first step of biofilm development is adhesion to the substrate. I performed adhesion inhibition assays to compare the effect of the 68aa and 16aa peptides. These were compared against the untreated control. In addition, a  $\Delta/\Delta$  *efg1*  $\Delta/\Delta$  *cph1* mutant sample was included to serve as a negative control because this mutant is known to be deficient in biofilm formation and virulence (36). These assays measured adhesion to an abiotic substrate, i.e., the base of the well of a tissue culture treated 96-well plate, and artificial saliva media was used to improve the assay's practical relevance. The adhesion step takes place during a 90-minute incubation period at 37°C with rotation at 200 rpm. Adhesion is measured by staining the adhered cells with crystal violet and then ultimately measuring absorbance. The results are normalized

relative to the untreated sample, and these normalized results can be compared across multiple biological replicates.

The 68aa peptide effectively reduced fungal adherence at concentrations of 100 nM and 10 nM (Figure 3.2B). The 16aa peptide, however, outperformed the larger peptide at the 100 nM and 10 nM concentrations; the 16aa peptide was sufficiently active at these concentrations to result in adhesion inhibition comparable to the  $\Delta/\Delta$  *efg1*  $\Delta/\Delta$  *cph1* mutant. Additionally, the 16aa peptide showed potent inhibition at a concentration of 1 nM (Figure 3.2C). For a clear and thorough comparison of the two peptides, the mean relative adhesion values for the 100 nM to 0.1 nM treated samples from both adhesion assays are depicted in Figure 3.2D.

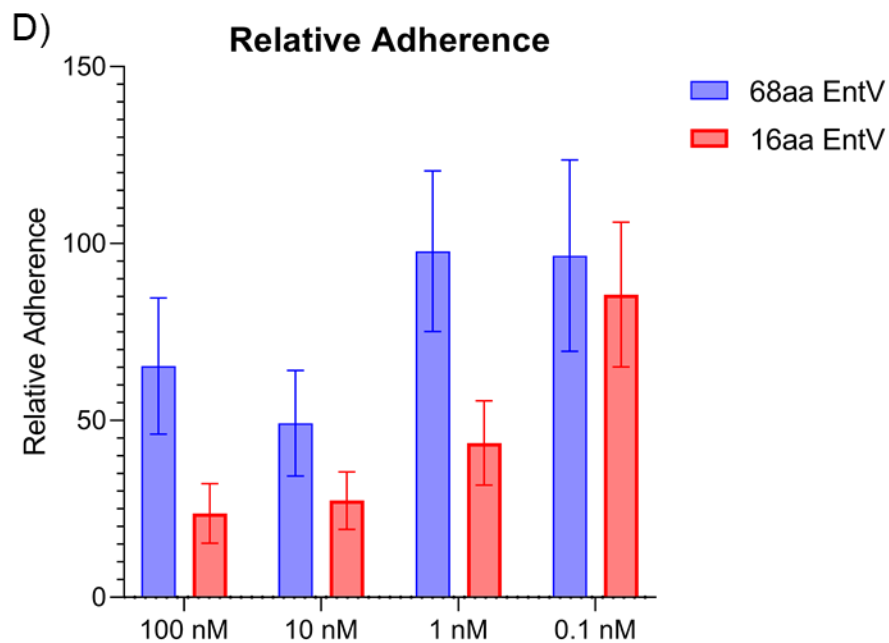
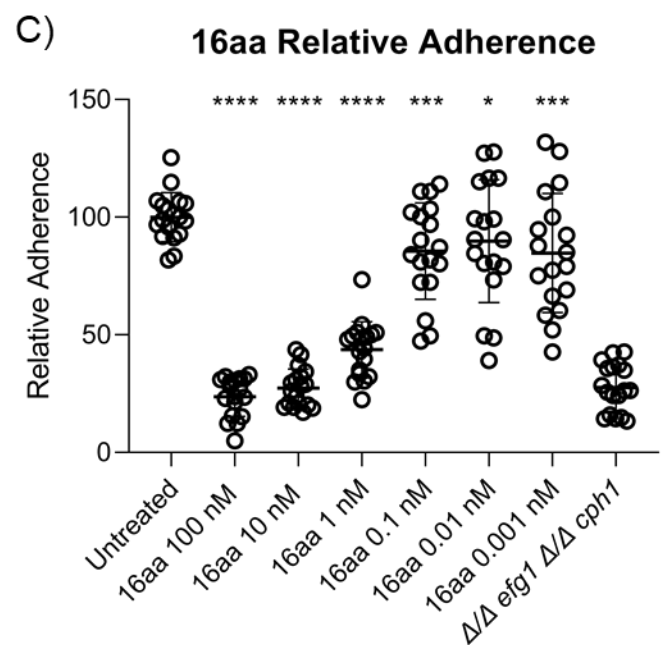
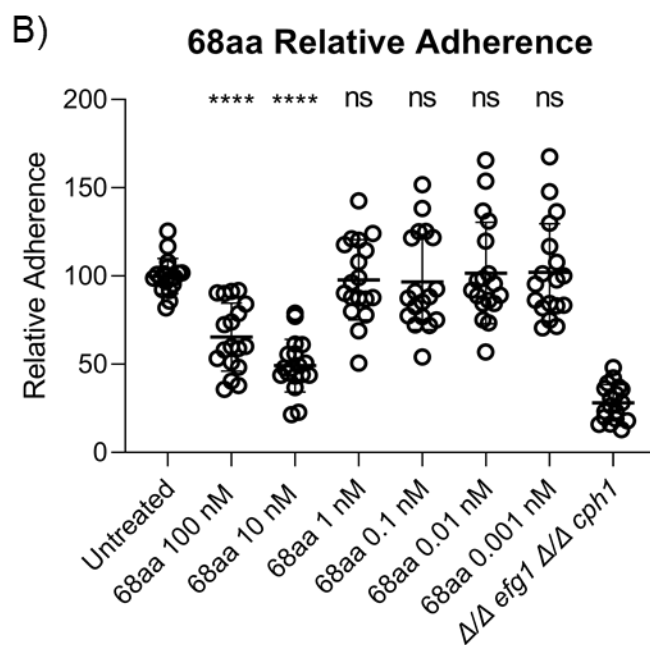
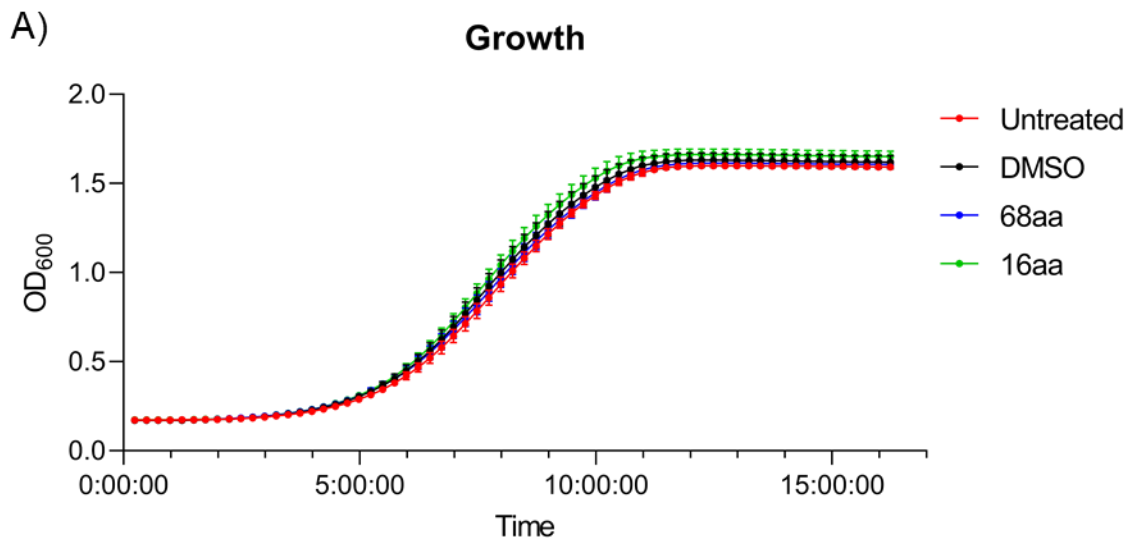


**Figure 3.2: The 16aa EntV peptide is a non-fungicidal inhibitor of *C. albicans***

**adhesion.** A) The 16aa and 68aa peptides at 100 nM and a DMSO vector control were tested for inhibition of planktonic growth in YPD. Readings were done automatically at 15 minute intervals on a plate reader. B) Adhesion to an abiotic substrate was tested in tissue culture treated 96 well plates with artificial saliva during a 90-minute incubation period. The 68aa peptide significantly reduced adhesion at concentrations of 100 nM and 10 nM. C) Using the same adhesion assay conditions, the 16aa peptide was effective in reducing adhesion at concentrations of 100 nM, 10 nM, and 1 nM, and additionally this peptide was more effective at the higher concentrations than the 68aa peptide. D) The mean relative adhesion values for the 100 nM to 0.1 nM treated samples from both adhesion assays are displayed for comparison. Adhesion assays were analyzed by normalizing each experimental technical replicate against the untreated mean. Results represent data collected across three biological replicates, and a two-way ANOVA with a Dunnet's test was used to determine differences between the untreated control and the experimental groups. N=3, \*  $P < 0.05$ , \*\*  $P < 0.01$ , \*\*\*  $P < 0.001$ , \*\*\*\*  $P < 0.0001$ .

---

### **The effect of the 16aa EntV peptide is sequence-specific**

In the interest of rigor, two alternative hypotheses were generated to explain the inhibition demonstrated in Figure 3.2. These alternative hypotheses challenged the specificity of the 16aa EntV peptide. The first hypothesis is that any peptide of similar amino acid composition and overall charge would elicit the same response. To test this hypothesis, our lab created a disordered peptide with the same amino acid composition as the 16aa EntV peptide, but the sequence was arranged such that all the distinct amino acids were grouped together. This peptide is predicted to have a highly disorganized structure according to my analysis with the PEP-FOLD 3 (189–191) software. All models generated agreed that the only significant secondary structure is an N-terminal helix consisting of the alanine residues and, in the dominant model, the first glutamine (Figure 3.3A).

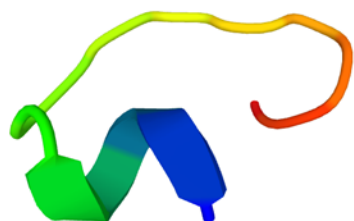
The second alternative hypothesis is that any peptide of similar amino acid composition, charge, and the ability to form a helix would elicit the same response. As before, a peptide was created from the same amino acids as the 16aa EntV peptide, but this time carefully rearranged such as to create a peptide that is predicted to form a similar helix as the 16aa EntV peptide. The dominant model predicted by PEP-FOLD 3 (189–191) produced a helix that incorporated all the available amino acid residues (Figure 3.3B). Alternative models suggested instability in the helix at the tryptophan residue, thus creating an N-terminal tail of 5 amino acid residues. Thus, this engineered 16aa sequence variant peptide is predicted to have a structure very similar to the EntV derived 16aa peptide.



These peptides were tested in a growth assay as before to ensure neither caused any cytotoxic effects (Figure 3.3C). In the adhesion assay, the disordered peptide showed a mean inhibition of approximately 19% at the 100 nM concentration (p-value < 0.0001) and 9% at the 10 nM concentration (p-value = 0.0434) (Figure 3.3D). The helical peptide had slightly better efficacy at the 100 nM concentration with a mean inhibition of 27% (p-value < 0.0001), but the 10 nM concentration showed no significant inhibition (Figure 3.3E). Overall, neither of these peptides had an inhibitory effect comparable to the 16aa EntV peptide (Figure 3.3F). Thus, the two alternative hypotheses were rejected. This demonstrates that the 16aa EntV peptide has a sequence specific activity against *C. albicans* adhesion.

A) 16aa Disordered

AAAAQQGGIICLLVW

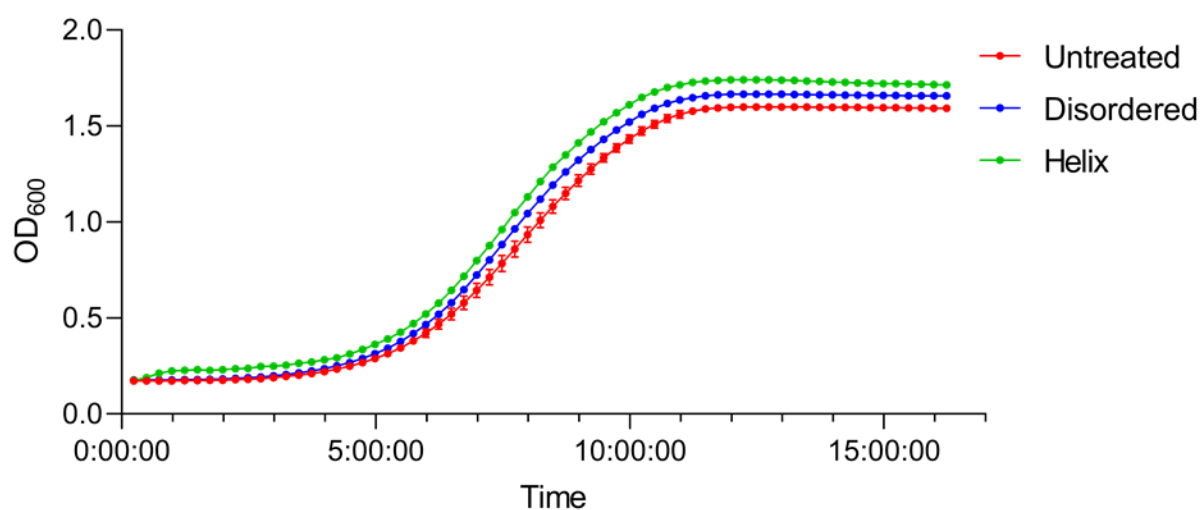


B) 16aa Helix

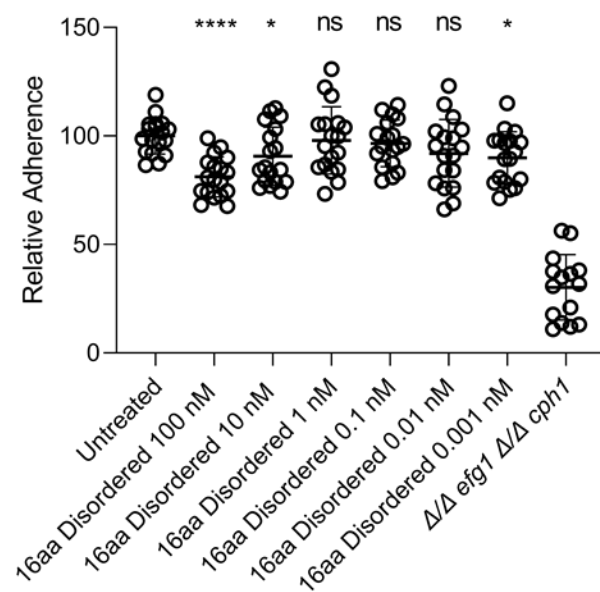
VGALWICGLAVIQAAQ



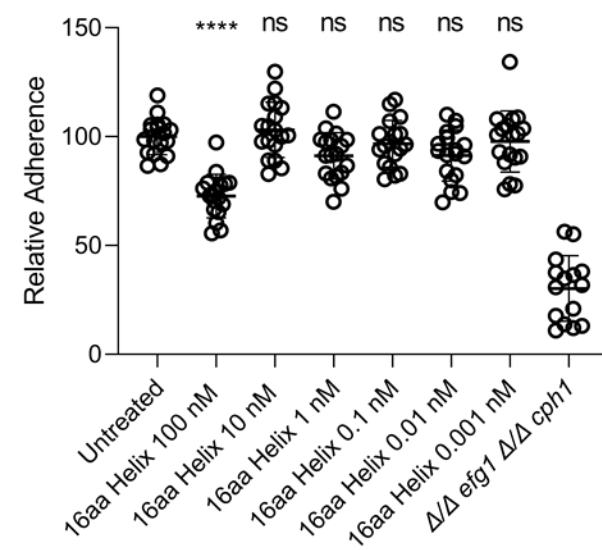
C) **Growth**



D) **16aa Disordered Relative Adherence**



E) **16aa Helix Relative Adherence**



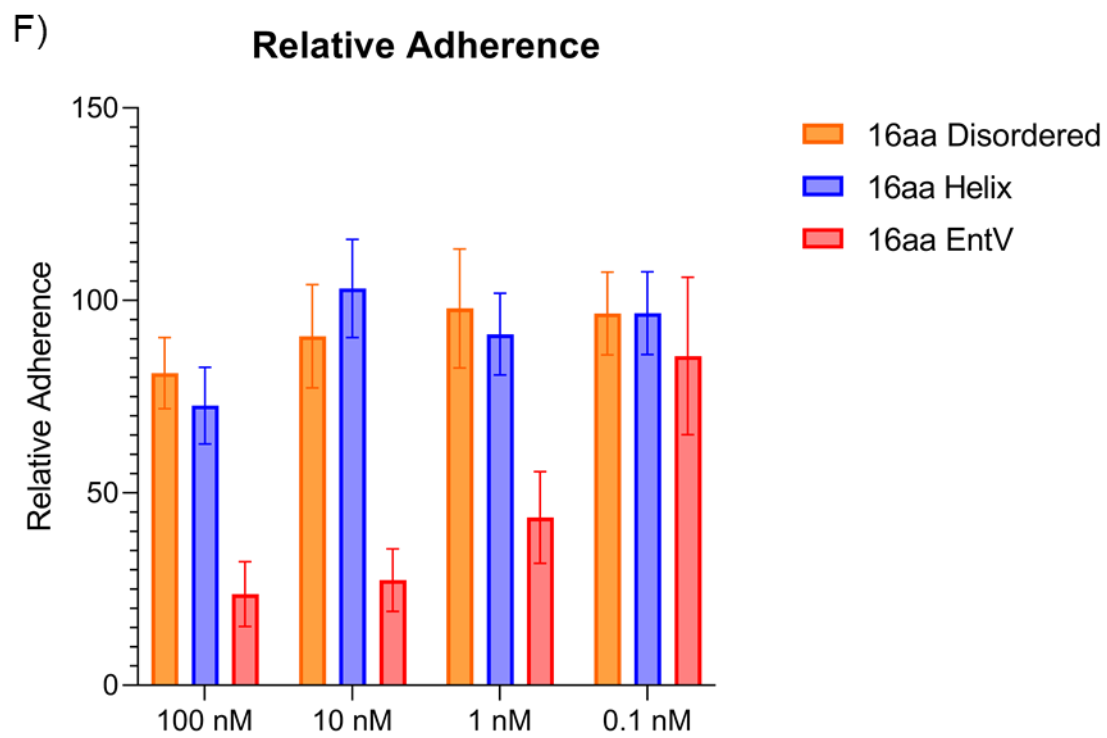


**Figure 3.3: The 16aa EntV peptide has a sequence specific inhibitory effect on *C. albicans* adhesion.** To test the sequence specificity of the interaction with the 16aa EntV peptide, two alternative peptides were designed using reordered sequences of the same amino acids as the 16aa EntV peptide. A) The disordered peptide is predicted to be highly disorganized with only a small N-terminal helix predicted by PEP-FOLD 3 (189–191). B) The helical peptide is predicted to form a helix that is likely to incorporate the full peptide sequence but with some N-terminal instability similar to the results with the 16aa EntV peptide. C) The peptides cause no cytotoxic effects at 100 nM concentrations against *C. albicans* growing planktonically in YPD. D and E) Adhesion assays were performed with the disordered and helical peptides, respectively. F) The activities of the disordered and helical peptides are compared with the native 16aa EntV peptide. Adhesion assays were analyzed by normalizing each experimental technical replicate against the untreated mean. Results represent data collected across three biological replicates, and a two-way ANOVA with a Dunnet's test was used to determine differences between the untreated control and the experimental groups. N=3, \*  $P < 0.05$ , \*\*  $P < 0.01$ , \*\*\*  $P < 0.001$ , \*\*\*\*  $P < 0.0001$ .

---

### **The attenuation activity of EntV is unique amongst similar bacteriocins**

There are few antibacterial peptides produced by Gram-positive bacteria similar to EntV that have been described previously in the literature. Two bacteriocins, Sam57 and YpkK, produced by *Streptococcus pyogenes* and *Corynebacterium jeikeium*, respectively, share similarities of size and structural motifs with EntV. While these peptides have only small sequence similarities, they all feature essential disulfide bonds and C-terminal helical structures (174). I performed adhesion assays to determine if these peptides had the same attenuation activity against *C. albicans* as EntV.

Figure 3.4 depicts the results of the experiments with Sam57 and YpkK. Like EntV, these bacteriocins had no cytotoxic effects against *C. albicans* (Figure 3.4A). Both peptides showed slight efficacy at high concentrations, but neither peptide reduced adhesion by more than 20% (Figure 3.4B and C). These results demonstrate the specificity of EntV against *C. albicans*, indicating that attenuation of *C. albicans* biofilm formation is a characteristic of EntV in particular, rather than of bacteriocins in general.

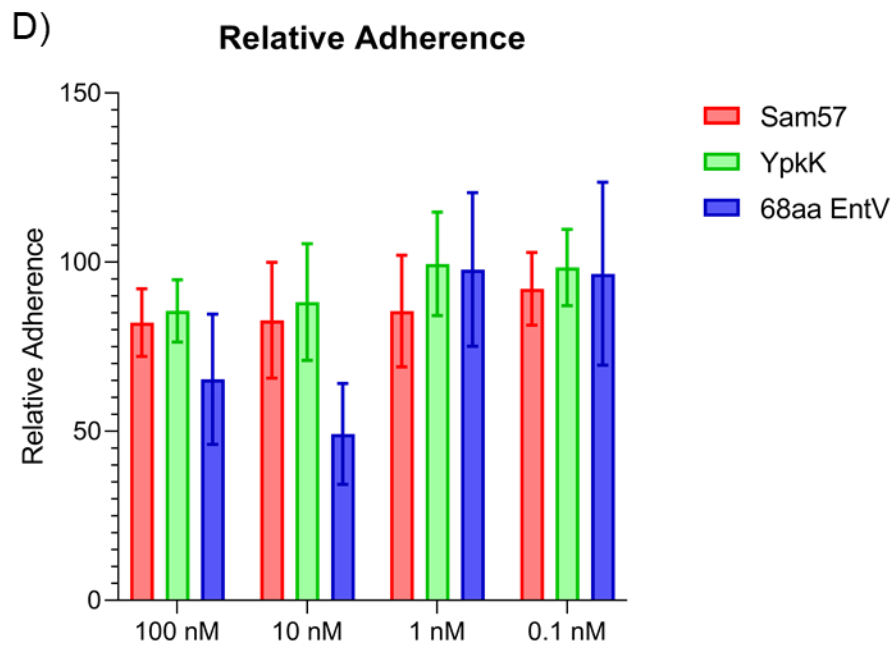
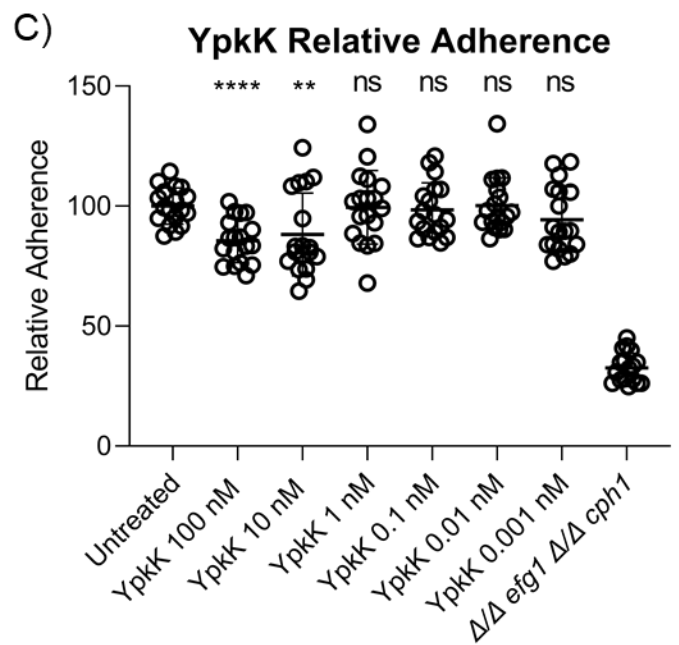
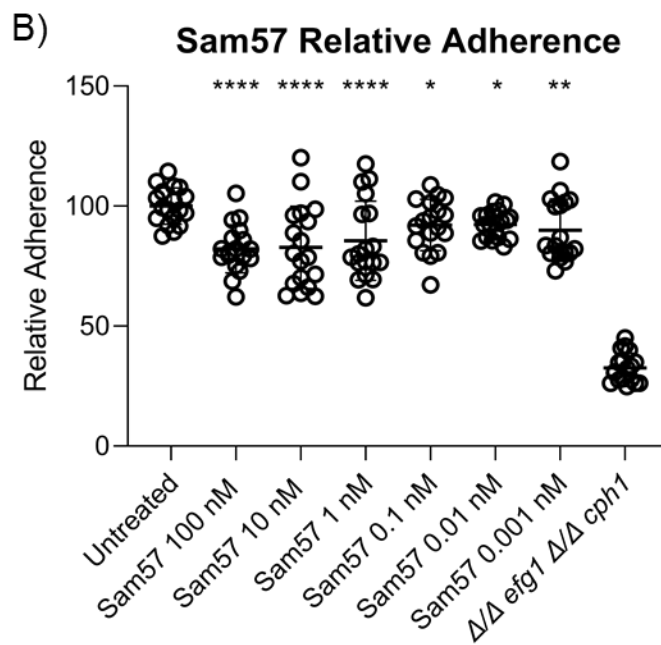
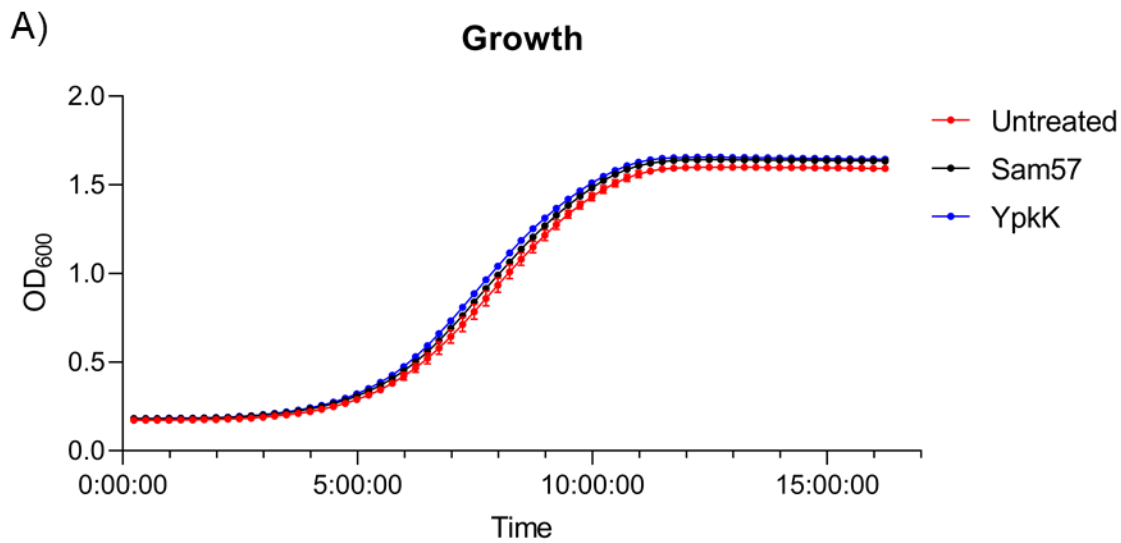


**Figure 3.4: Similar bacteriocins do not greatly inhibit *C. albicans* adhesion.** To test the specificity of EntV compared to other similar bacteriocins, adhesion assays were performed with the peptides Sam57 and YpkK. A) Growth in YPD was tested with 100 nM treatments of each peptide. Like EntV, these bacteriocins have no cytotoxic effect on *C. albicans*. B and C) Adhesion assays were performed with the Sam57 and YpkK peptides, respectively. D) The activities of the Sam57 and YpkK peptides are compared to the 68aa EntV peptide. Adhesion assays were analyzed by normalizing each experimental technical replicate against the untreated mean. Results represent data collected across three biological replicates, and a two-way ANOVA with a Dunnet's test was used to determine differences between the untreated control and the experimental groups. N=3, \* P < 0.05, \*\* P < 0.01, \*\*\* P < 0.001, \*\*\*\* P < 0.0001.

---

## **Examination of the Glutamine residues in the 16aa EntV peptide**

The 16aa EntV peptide consists mostly of amino acid residues with hydrophobic side chains. The exceptions to this are the two glutamine residues at positions 7 and 14 and the cysteine residue at position 15. The two glutamine residues are predicted to be on the same face of the 16aa EntV peptide separated by one turn of the helix with the leucine and tryptophan residues at positions 10 and 11 between them. The cysteine residue has been determined to be necessary for activity in unpublished work from the Garsin lab using the *C. elegans* infection assay (M. Cruz and D. Garsin, personal communication). I hypothesized that the conspicuously placed glutamine residues would also be necessary for EntV activity. To explore the importance of the glutamine residues, our lab purchased two synthetic peptides with substituted amino acid residues in the 7 and 14 positions.

The Q – I variant replaces the glutamine residues with isoleucine, a non-polar and hydrophobic amino acid. Isoleucine was chosen because of the naturally occurring amino acids with hydrophobic side chains, isoleucine is closest in size and shape to glutamine. The amino acid sequence of the Q – I variant is described in Figure 3.5A along with a predicted structure from PEP-FOLD 3 (189–191). The substituted isoleucine residues are identified in red font, and in the structure the bright green and red residues facing the viewer are the substituted isoleucine residues. Like the 16aa EntV peptide, this variant peptide was predicted to form a helix that incorporated all available amino acid residues, however unlike the 16aa EntV peptide, none of the models generated in the prediction of this structure indicated any instability in the helix. This variant peptide should overall be uncharged and generally be hydrophobic.



The Q – E variant replaces the glutamine residues with glutamate, a negatively charged amino acid. Figure 3.5B depicts the amino acid sequence of this variant peptide along with its predicted structure. In the structure, the first member of the helix facing the viewer (bright green) and the last member of the helix facing the viewer (red) are the substituted glutamate residues. Interestingly, this variant peptide was predicted to have an unstable N-terminal tail, similar to the alternative models of the 16aa EntV peptide. All the models produced indicated instability in the N-terminus, but there was some disagreement on if the valine at position 4 would be incorporated into the helix. The structure depicted in Figure 3.5B does not include the valine in the helix.

The variant peptides were compared in adhesion assays depicted in Figures 3.5 C and D. The Q – I variant successfully inhibited adhesion with a reduction of approximately 50% from the 10 nM treatment. The Q – E variant however had only a minimal impact on adhesion with a reduction of only approximately 12% from the 100 nM treatment. The Q – I variant had activity in the same range as the 68aa EntV and 16aa EntV peptides (Figure 3.5E). The Q – E variant, however, was inactive in this assay, but whether this is due to the permanent instability in the N-terminus of the variant peptide or the altered overall charge of the peptide has yet to be determined. These results indicate my hypothesis is false. The glutamine residues are not essential for activity in inhibition of adhesion.

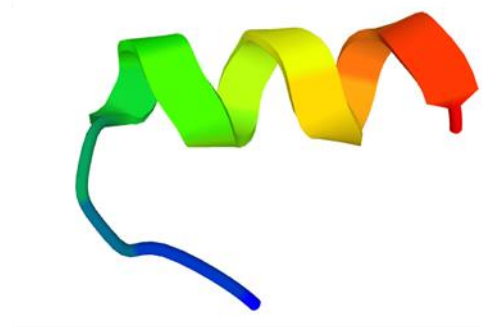
A) Q – I variant

AIIVAGILALWAVICG

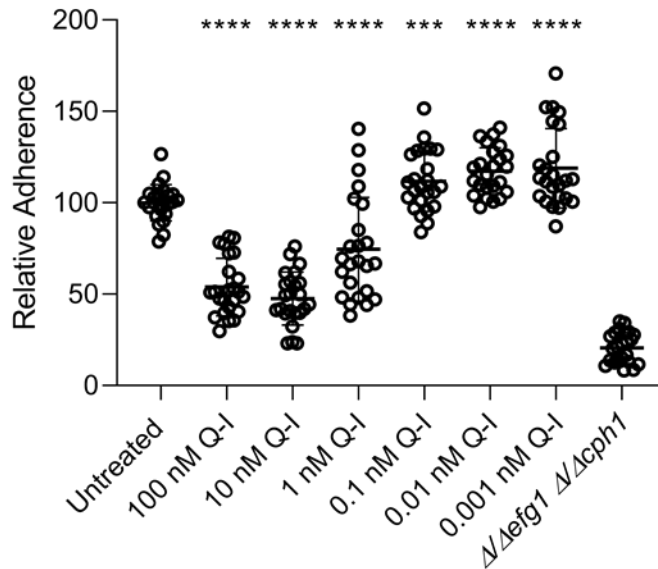


B) Q – E variant

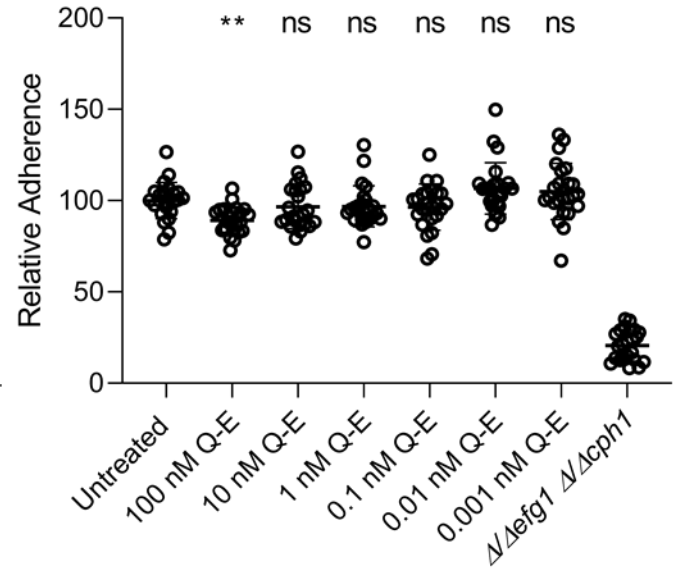
AIIVAGELALWAVECG



C) **Q - I Variant**  
**Relative Adherence**



D) **Q - E Variant**  
**Relative Adherence**



E) **Relative Adherence**

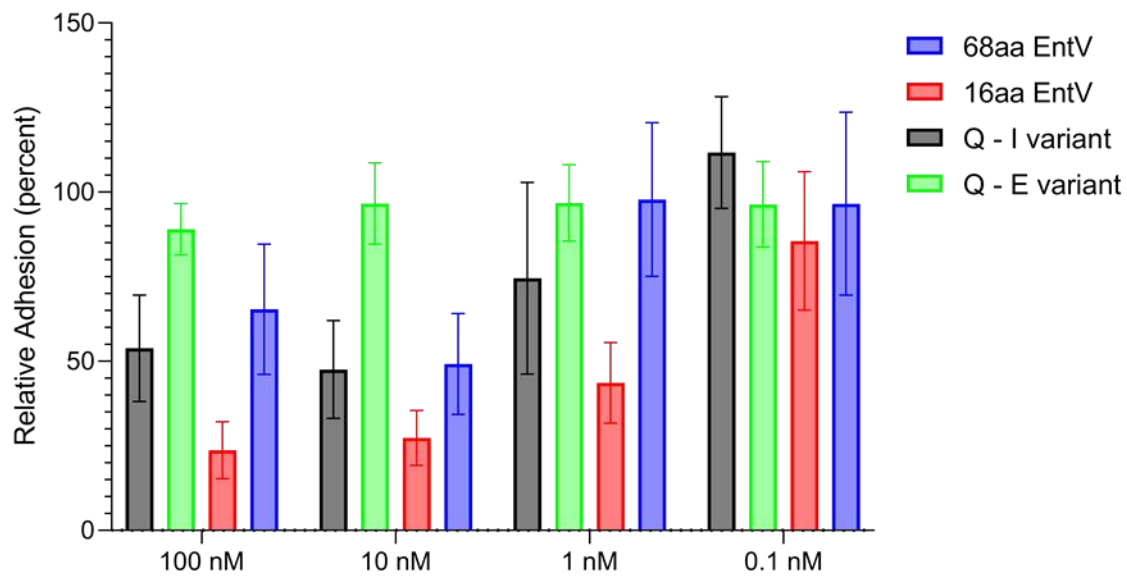


**Figure 3.5: Glutamine substitution variants have different activities.** The activity of the glutamine residues at positions 7 and 14 was explored using variant peptides that substituted either isoleucine residues or glutamate residues at those positions (indicated by red font in A and B). A) The Q – I variant is predicted to form a helix similar to the 16aa EntV peptide. B) The Q – E variant is predicted to have an N-terminal tail consisting of at least the first three residues. C and D) Adhesion assays were performed with the Q – I and Q – E variant peptides, respectively. E) The Q – I variant performs in the same general range as the 68aa EntV and 16aa EntV peptides, indicating the glutamine residues are not essential for activity. The Q – E variant peptide, however, has only minimal activity in the assay. Adhesion assays were analyzed by normalizing each experimental technical replicate against the untreated mean. Results represent data collected across four biological replicates, and a two-way ANOVA with a Dunnet's test was used to determine differences between the untreated control and the experimental groups. N=4, \* P < 0.05, \*\* P < 0.01, \*\*\* P < 0.001, \*\*\*\* P < 0.0001.

---

### **An effective peptide of minimal size**

Lastly, I hypothesized that there existed a minimum size peptide derived from the C-terminal helix of EntV that would retain the efficacy of the 16aa EntV peptide in inhibiting *C. albicans* adhesion. Previously mentioned unpublished *C. elegans* infection assays from the Garsin lab indicated that the C-terminal cysteine residue is essential for activity (M. Cruz and D. Garsin, personal communication), so the only residue that could be removed from the C-terminus is the glycine at position 16 of the 16aa EntV peptide. Thus, I tested peptides with progressively shorter N-termini for activity in the adhesion assay. The amino acid sequences and predicted structures (PEP-FOLD 3 (189–191)) of the shorter peptides used in this study are depicted in Figures 3.6A through D. All these peptides are predicted to form helices that incorporate all available residues. The different models produced in each analysis only have minor disagreements such as the pitch of the helix on each terminus. The peptides were tested for cytotoxicity against *C. albicans* growing in YPD as before (Figure 3.6E), and none were found to be cytotoxic.

A) 12aa EntV

**VAGQLALWAVQC**



B) 11aa EntV

**AGQLALWAVQC**



C) 10aa EntV

**GQLALWAVQC**



D) 9aa EntV

**QLALWAVQC**



E)

**Growth**

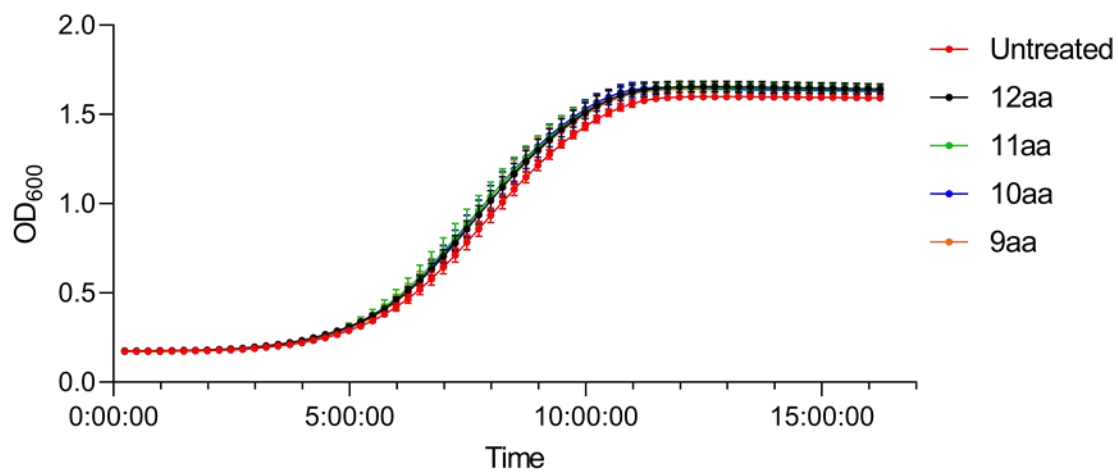


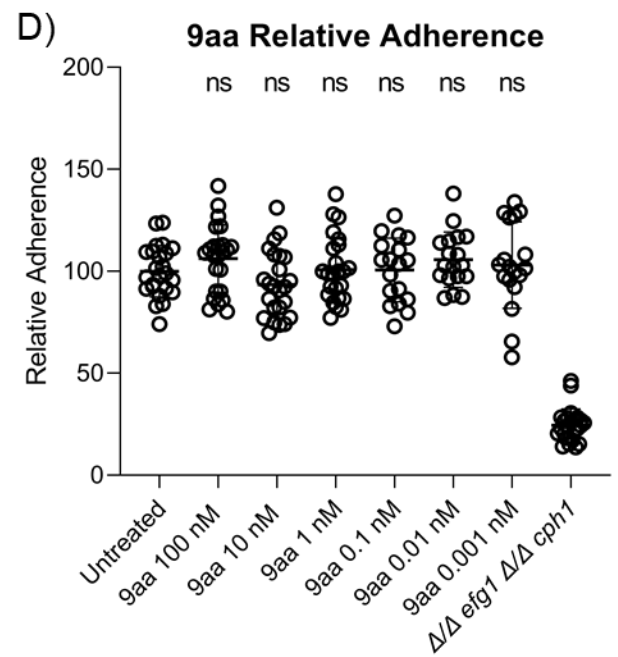
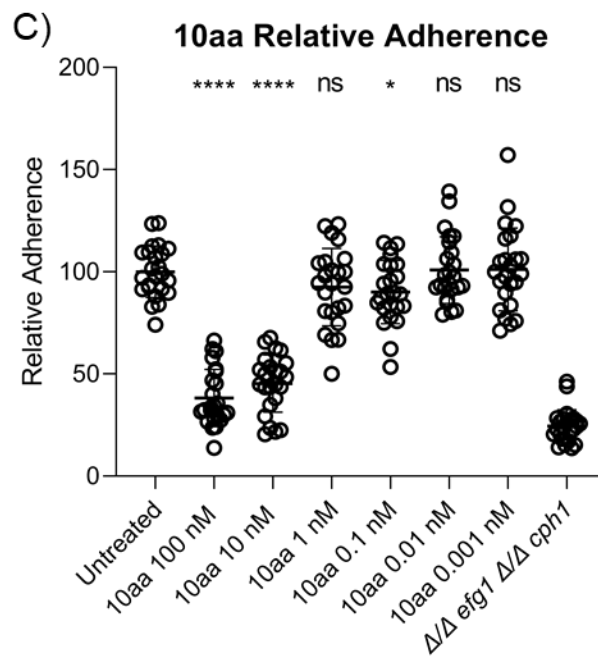
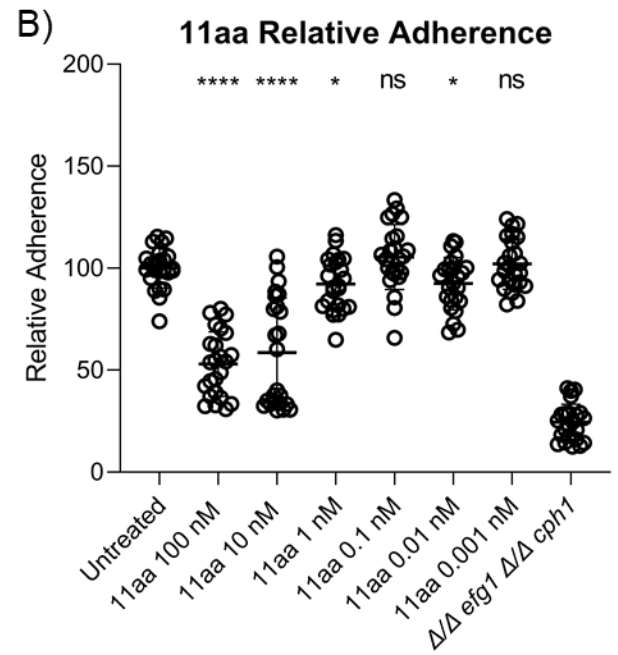
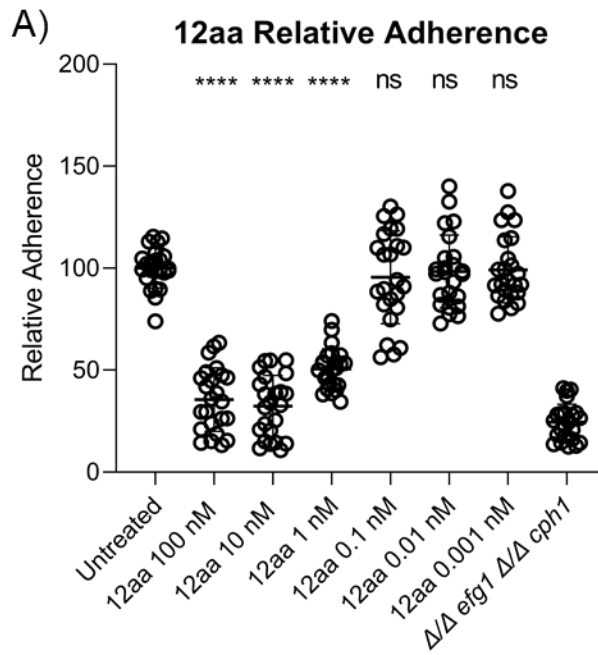
**Figure 3.6: Small EntV peptides are predicted to form helices and are non-fungicidal.** An effective peptide of minimal size was hypothesized to exist, so several smaller peptides were described and tested for cytotoxicity against *C. albicans*. A through D) The amino acid sequences and predicted structures (PEP-FOLD 3 (189–191)) of the small peptides indicate that all these peptides form helices. E) The small peptides were tested for cytotoxicity against *C. albicans* growing in YPD, and none were found to be cytotoxic.

---

### Activity of small EntV peptides

The peptides described in Figure 3.6 were tested for activity in inhibiting *C. albicans* adhesion. The results from the adhesion assay with the 12aa EntV peptide (Figure 3.7A) were very similar to that of the 16aa EntV peptide (Figure 3.2C, Figure 3.7E). The 12aa EntV peptide inhibited adhesion by approximately 70% for both the 100 nM and 10 nM concentrations, and this peptide retained some efficacy at the 1 nM concentration, inhibiting adhesion by approximately 46%. The 11aa EntV peptide was less effective at the 100 nM concentration with an approximate inhibition of 44%, and it lost efficacy at the 1 nM concentration level (Figure 3.7B). The 10aa EntV peptide had a similar activity profile with slightly higher activity at the 100 nM concentration (approximately 62% inhibition), but it lost activity at the 1 nM concentration level (Figure 3.7C). Lastly, the 9aa EntV peptide was ineffective in inhibiting *C. albicans* adhesion at any concentration (Figure 3.7D).

Figure 3.7E depicts a comparison between the small peptides and the 68aa EntV and 16aa EntV peptides. It is interesting to note from this comparison that the 12aa EntV peptide closely matched the activity of the 16aa EntV peptide while the 11aa EntV and 10aa EntV peptides more closely matched the 68aa EntV peptide. The most important distinctions between these peptides are potency of their activity at the 100 nM concentration and loss of activity for the 68aa EntV, 11aa EntV, and 10aa EntV peptides at concentrations of 1 nM. In conclusion, these data indicate a peptide of minimum size that retains the activity of the 16aa EntV peptide does exist in the 12aa EntV peptide.





E)

# Relative Adherence

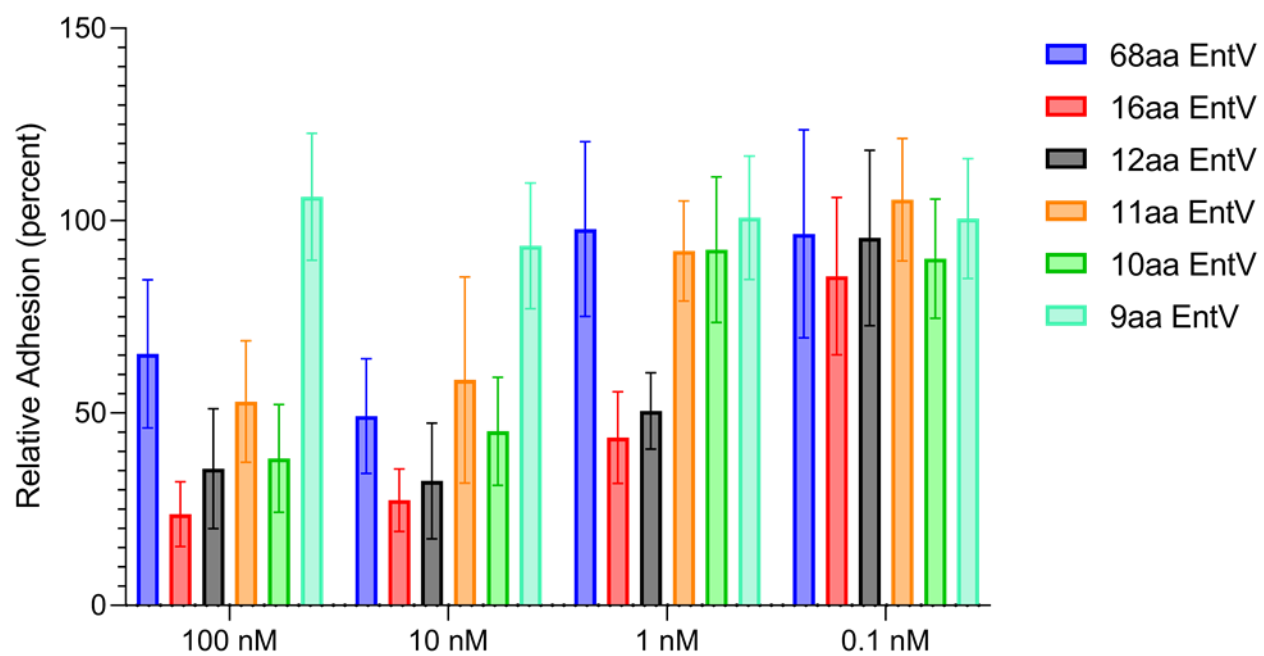


**Figure 3.7: The 12aa EntV peptide has superior activity compared to the other small peptides.** The small EntV peptides were tested in the adhesion assay to determine if a minimum size peptide derived from the C-terminus of EntV existed that retained EntV activity. A) The 12aa EntV peptide was a potent inhibitor of *C. albicans* adhesion with similar activity to the 16aa EntV peptide. B and C) The 11aa and 10aa EntV peptides were less effective than the 12aa EntV peptides and had activity profiles more closely matching that of the 68aa EntV peptide. D) The 9aa EntV peptide was ineffective at any concentration tested in inhibiting *C. albicans* adhesion. E) All the activities of the small peptides are compared along with the 68aa EntV and 16aa EntV peptides. Adhesion assays were analyzed by normalizing each experimental technical replicate against the untreated mean. Results represent data collected across four biological replicates, and a two-way ANOVA with a Dunnet's test was used to determine differences between the untreated control and the experimental groups. N=4, \*  $P < 0.05$ , \*\*  $P < 0.01$ , \*\*\*  $P < 0.001$ , \*\*\*\*  $P < 0.0001$ .

---

## Discussion

In this chapter I demonstrated that small peptides derived from the C-terminal helix of EntV are capable of matching and even outperforming the activity of the 68aa EntV peptide in inhibiting *C. albicans* adhesion to an abiotic substrate (Figure 3.7E). Like the 68aa EntV peptide, these small peptides are non-fungicidal (Figures 3.2A and 3.6E). The adhesion assay provided an *in vitro* metric by which to compare these peptides, and by that comparison the 12aa EntV peptide was found to be the best candidate for future study for potential pharmaceutical applications. The 12aa EntV peptide was superior to all other peptides tested in that it was the smallest optimally effective peptide and predicted to form a stable helix. This result informed follow-up experiments performed by other members of the Lorenz and Garsin labs in which the 12aa EntV peptide was tested in the murine oropharyngeal candidiasis model. In this infection model, mice are given a sublingual inoculation of *C. albicans* and allowed to drink freely from a 100 nM peptide solution in water. The mice are later euthanized and the tongues are excised and analyzed for fungal burden and histology. In this model the 12aa EntV peptide virtually eliminated fungal burden and performed as well as the 68aa EntV and 16aa EntV peptides (G. Buda de Cesare, M. Cruz, and S. Guha, personal communication).

The Introduction of this chapter included a discussion of *C. albicans* adhesins and how those adhesins might interact with mucin in the YNB-AS media used in the assay or mucin present in an *in vivo* oral environment. The exact molecular mechanisms of the complex interactions between *C. albicans*, mucin, the substrate surface, and EntV have yet to be elucidated. I will briefly propose a hypothetical model

to explain the relationship between these factors and the results of the assays in this chapter. *C. albicans* at the start of the adhesion stage of the experiment should be almost uniformly in the yeast form after growth in YPD and a 1-hour soak in PBS. These cells should begin forming hyphae due to the exposure to the YNB-AS media. During the adhesion stage, fungal cells may bind to mucin or the substrate surface or exist in equilibrium with both, and dissolved mucin in the media may serve as a nucleation site for several fungal cells to bind together. Hyphae, with their greater surface area and potentially enhanced binding to mucin and other *C. albicans* cells in a mucin-centered cluster, may be able to bind to both mucin and the substrate surface, thus depositing whole clusters of cells on the substrate surface. Cells treated with EntV, in comparison to untreated cells, may form fewer hyphae, as has been seen in previous studies (15, 173). With a reduction in hyphal cells, fewer independent EntV treated cells or clustered cells around a mucin particle would adhere to the substrate. This *in vitro* model would be roughly consistent with a proposed hypothetical host mucin-shedding model whereby the host uses excess mucin shedding from the mucosal layer to remove pathogenic microbes from a potential infection site (185).

In this chapter I extensively explored the 16aa EntV peptide and its interaction with *C. albicans* adhesion, including examinations of the peptide's predicted structure, specificity, and potentially important residues. In Figure 3.1 I discuss that alternative models of the 16aa EntV peptide predict that it forms an N-terminal tail consisting of 3-4 residues, which is distinct from its structure in the 68aa EntV peptide (unpublished data). A likely hypothesis is that the unstable N-terminal residues exist in an equilibrium between forming a tail or joining in the helical structure. This equilibrium

state may explain some of the unique spreading of the data for the 16aa EntV adhesion activity at low concentrations (Figure 3.2C).

In Figure 3.3 I demonstrated that the adhesion inhibition activity is sequence-specific to the 16aa EntV peptide. This is important because it indicates that *C. albicans* is having a specific reaction to the presence of the C-terminal EntV peptide sequence, and these data imply that EntV interacts with a specific, as yet unknown, binding partner. This is further evidenced by the results in Figure 3.4 that demonstrate that the *C. albicans* anti-adhesion activity of EntV is unique amongst its similar bacteriocins.

Lastly, I explored the importance of the glutamine residues at positions 7 and 14 in the 16aa EntV peptide (Figure 3.5). Changing these residues to isoleucine residues (Q - I variant) showed that glutamine is not necessary in these positions for activity. However, altering the glutamine residues to glutamate residues of the opposite charge (Q - E variant) removed activity. These results are consistent with results from *in vivo C. elegans* infection assays performed in the Garsin lab (M. Cruz and D. Garsin, personal communication). One potential explanation for this effect is that the glutamine residues do not directly interact with the binding site, but could assist in getting the peptide in the right position for binding. The loss of activity in the Q – E variant could be due to the substituted glutamate residues disrupting the helical structure as predicted by the model presented in Figure 3.5B or the change in overall charge of the peptide.

In Figures 3.6 and 3.7 I examined the structure and activity of smaller peptides derived from the C-terminal helix of EntV. The pattern of activity with the 12aa EntV

peptide displaying optimal activity, the 11aa and 10aa EntV peptides displaying suboptimal activity, and the 9aa EntV peptide being inactive is completely consistent with *in vivo* experiments from the Garsin and Lorenz labs (unpublished data). This pattern has been found in *C. elegans* infection assays measuring longevity of nematodes infected with *C. albicans* and in the murine oropharyngeal candidiasis model measuring fungal burden on the tongues of mice infected with *C. albicans* (G. Buda de Cesare, M. Cruz, S. Guha, and D. Garsin, personal communication).

The structures of these smaller peptides, unlike the 16aa EntV peptide, were predicted to form very stable helices. It is reasonable that the 12aa EntV peptide would match the activity of the 16aa EntV peptide considering that the 12aa EntV essentially consists of the portion of the 16aa EntV helix predicted to be most stable. The 12aa EntV peptide omits the first three residues (alanine-isoleucine-isoleucine) that were predicted to form the N-terminal tail of the 16aa EntV peptide.

A possible explanation for why the 11aa and 10aa EntV peptides exhibit suboptimal activity compared to the 16aa and 12aa EntV peptides is that the valine in position 1 of the 12aa EntV peptide is necessary for optimal activity either due to direct interaction with the binding partner or by facilitating binding with the binding partner. The 9aa EntV peptide however has no inhibitory effect at all. The likely explanation for this is that having the glutamine, an amino acid with a polar sidechain, at the N-terminus of the peptide creates a dipole moment that is sufficiently strong to be incompatible with the binding site of the peptide.

Finally, one might observe a pattern that the data in Figures 3.3 and 3.4 indicate the non-specific 16aa helix, 16aa disordered, Sam57, and YpkK peptides generally

have slight efficacy at only the 100 nM concentrations. This likely is due to a slight interaction with *C. albicans*. To rigorously ensure the DMSO vehicle could not be explained to cause this effect, I tested the 68aa EntV and 12aa EntV peptides with extra DMSO at each concentration to attempt to replicate the normally established activity pattern in addition to a DMSO control. I added 0.5  $\mu$ l of DMSO to each peptide solution and the DMSO control, a larger amount than is usually present in these experiments. The results replicated the established pattern and can be found in Appendix Figure A.1, thus verifying that the DMSO vector does not contribute to adhesion inhibition.

## **Chapter 4: EntV derivatives reduce biofilm biomass and disrupt biofilm structure**



## Introduction

The previous chapter examined effects of EntV derivatives on adhesion, the earliest stage of biofilm development. In this chapter, the focus is instead turned to mature biofilms in the late stages of development.

As discussed in the first chapter of this work, *C. albicans* creates large, complex biofilms with heterogeneous structures consisting of *C. albicans* in both its yeast and hyphal forms along with an extracellular matrix (ECM) composed primarily of carbohydrates (50, 78). These biofilms are of particular clinical importance when they grow on medical devices such as central venous catheters. These biofilms produce disperser cells that can create systemic infections (9, 81) as well as a reservoir with increased antimicrobial recalcitrance that can cause persistent infections (52, 53).

Previous work to describe the structure of *C. albicans* biofilms has shown that biofilms grown on level surfaces under static conditions develop an overall architecture characterized by a dense bed of yeast cells with hyphae growing generally vertically out of the bed. These hyphae are encased in ECM, providing structural support to the biofilm (50–53). However, most medical devices are not level surfaces with a static supply of nutrients. Biofilms grown under these conditions tend to be more disordered but are still composed of yeast and hyphae encased in a protective layer of ECM (50).

It has been shown previously that 68aa EntV is a potent inhibitor of biofilm development. When added to either planktonic cells or young biofilms, the 68aa EntV showed potent activity in reducing overall biomass after 48 hours (15). This previously published work performed by members of the Garsin and Lorenz labs examined statically grown biofilms. Our lab has since established a collaboration with David

Andes, M.D., a leader in the field of *C. albicans* biofilm formation on medical devices. Dr. Andes examined the potency of EntV in inhibiting biofilm development in the less hospitable environment of a central venous catheter model in rats. This work (unpublished) revealed that the 68aa EntV peptide was a potent inhibitor of biofilm formation in this environment.

In this chapter I will compare the efficacy of 68aa EntV to derivatives of the C-terminal helix in inhibiting the development of mature biofilms. This chapter begins with a qualitative discussion on the architecture of *C. albicans* biofilms, starting with untreated biofilms and then comparing the effect of continuous treatment with 68aa EntV and 16aa EntV on biofilm structure. Then follows a quantitative comparison of the biomass of treated biofilms. The specificity of the effect of EntV is analyzed using alternative peptides in quantitative biomass experiments, and lastly, the 12aa – 9aa peptides are tested for efficacy in both the biomass and biofilm structural analyses.

## Results

To determine the efficacy of EntV derivatives against *C. albicans* biofilms, first I characterized the structure of untreated biofilms. I used fluorescence microscopy to build three-dimensional images of biofilms with *C. albicans* strain CEGC1 (15). This strain produces green fluorescent protein (GFP) dependent upon activation of the *HWP1* promoter and an mCherry fluorophore dependent upon activation of the *ADH1* promoter. Hwp1 is a cell wall protein expressed by hyphal cells that has adhesin activity and is necessary for biofilm formation (57, 62). Therefore, this strain produces mCherry constitutively and GFP only upon induction of the hyphal morphogenesis pathways. I grew these biofilms on tissue culture treated chamber slides (Ibidi) for 48 hours in YNB-AS at 37°C. Before imaging, the biofilms were washed once with PBS to remove planktonic cells. For the microscopy, I took z-stacked images at 20x magnification with 101 frames and 3 µm between each frame, creating a total image 300 µm in depth. If possible, depending on signal strength, these images were deconvoluted using cellSens Dimension 2.3 (Olympus) to increase resolution.

Figure 4.1 depicts representative images of untreated biofilms. In this figure and subsequent microscopy figures in this chapter (Figures 4.2, 4.3, 4.8, 4.9, 4.10, and 4.11), horizontally adjacent images, e.g., 4.1A and 4.1B, depict the same image from either a topological or *y*-axis viewpoint, respectively.

Overall, these untreated biofilms can be characterized as having a regular structure with hyphae that generally extend upward into the structure of the biofilm. The samples in Figures 4.1A/B and C/D were not deconvoluted, but from the *y*-axis view of these figures (4.1B and D) it can be seen that the hyphae in these biofilms are

generally growing vertically. Figures 4.1E – H were successfully deconvoluted, and with this increased resolution, many more hyphae can be distinguished. In these figures, it is clear that the hyphal network is a dense structure consisting of hyphae that initially grow vertically out from the yeast bed before diverging with no clear uniform direction. Taken together, these data indicate that the upper layers of these biofilms are dense structures that are likely well supported by ECM components. From the topographical view images (Figures 4.1A, C, E, and G) it is clear that the biofilm structure as a whole is cohesive with no large holes or gaps.

Topographical view

y-axis view

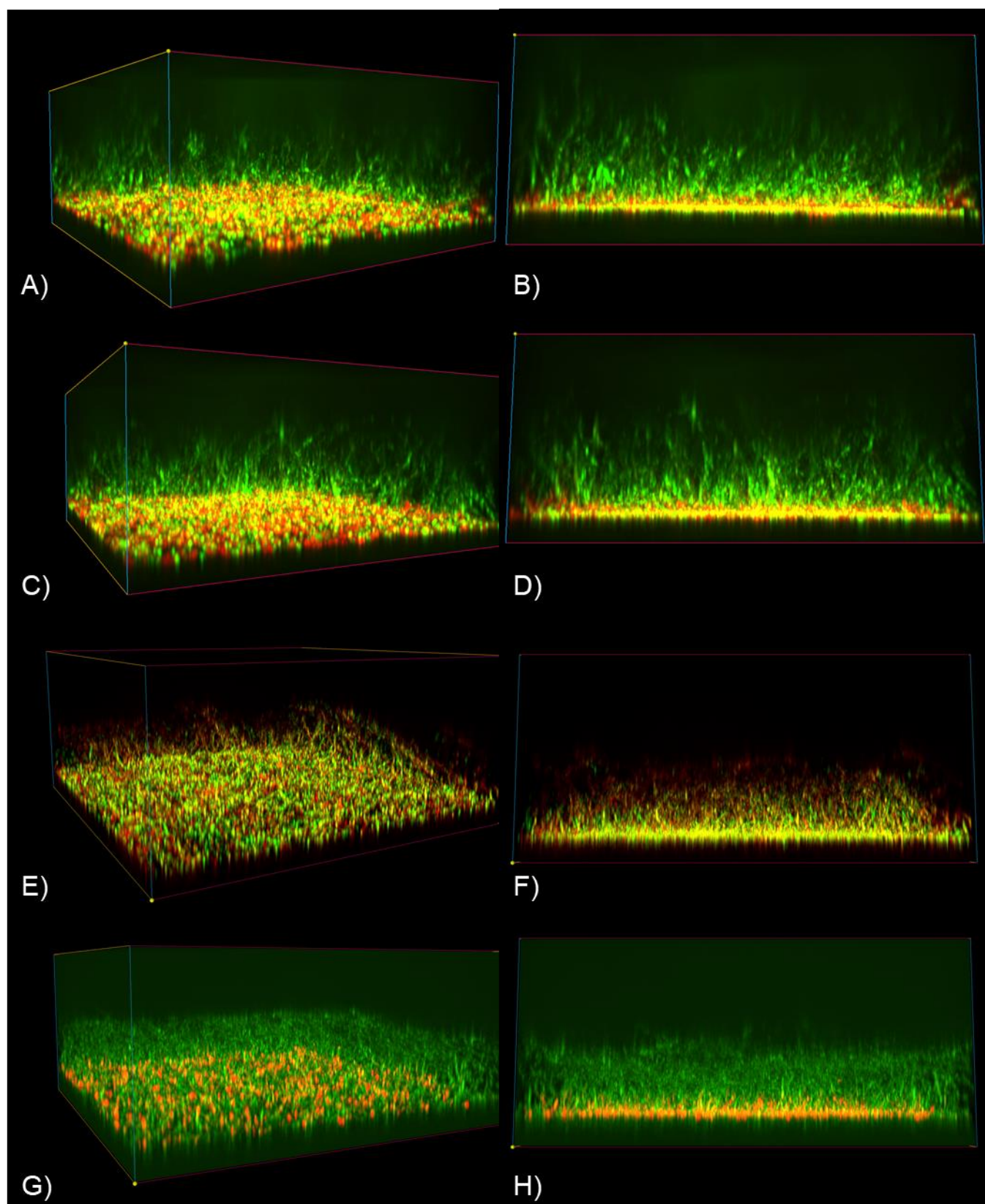


**Figure 4.1: Untreated biofilms have a regular structure with vertical hyphae.**

Representative three-dimensional images of untreated *C. albicans* CEGC1 biofilms collected by fluorescence microscopy. These biofilms were grown statically for 48 hours at 37°C in YNB-AS media and then washed. Microscopy was performed using z-stacked images at 20x magnification with 101 frames and 3 µm between each frame, creating a total image 300 µm in depth. If possible, depending on signal strength, these images were deconvoluted using cellSens Dimension 2.3 (Olympus) to increase resolution. Horizontally adjacent figures represent different perspective views of the same image. A and B) This image is not deconvoluted. This biofilm is large with hyphae that generally grow vertically out of the yeast layer. C and D) This image is not deconvoluted. As with the previous image, the biofilm is large with vertical hyphae. E and F) This image was successfully deconvoluted, and the increased resolution allows for individual hyphae to be seen. G and H) This image was deconvoluted. This image depicts a smaller than average untreated biofilm, but this biofilm is notable for its dense hyphal layer.

---

## **EntV disrupts biofilm structure**

Previous studies have shown that EntV is effective in inhibiting biofilm growth and reducing the size of young biofilms (addition of EntV after 24 hours) (15). For this study of the effect of EntV on biofilm structure, biofilms were prepared and grown as described previously but were treated with 300 nM EntV before and through the duration of incubation. Figure 4.2 depicts representative images of biofilms treated with 68aa EntV. From this figure, 68aa EntV treated biofilms can be broadly characterized as less cohesive and smaller with a flattened hyphal structure.

The hyphal layer for the biofilm depicted in Figures 4.2A and B is laying over nearly horizontally, creating the characteristic flattening effect. The images in Figures 4.2C-H were successfully deconvoluted, and in Figure 4.2D the hyphae appear to start folding over and growing horizontally almost immediately out of the yeast bed. In Figure 4.1H, the hyphae appear to initially grow vertically from the yeast layer before folding over. Treatment with EntV also appears to reduce the cohesiveness of the biofilms. The biofilms in Figures 4.2A and E appear more disordered than those of the untreated samples in Figure 4.1.

Topographical view

y-axis view

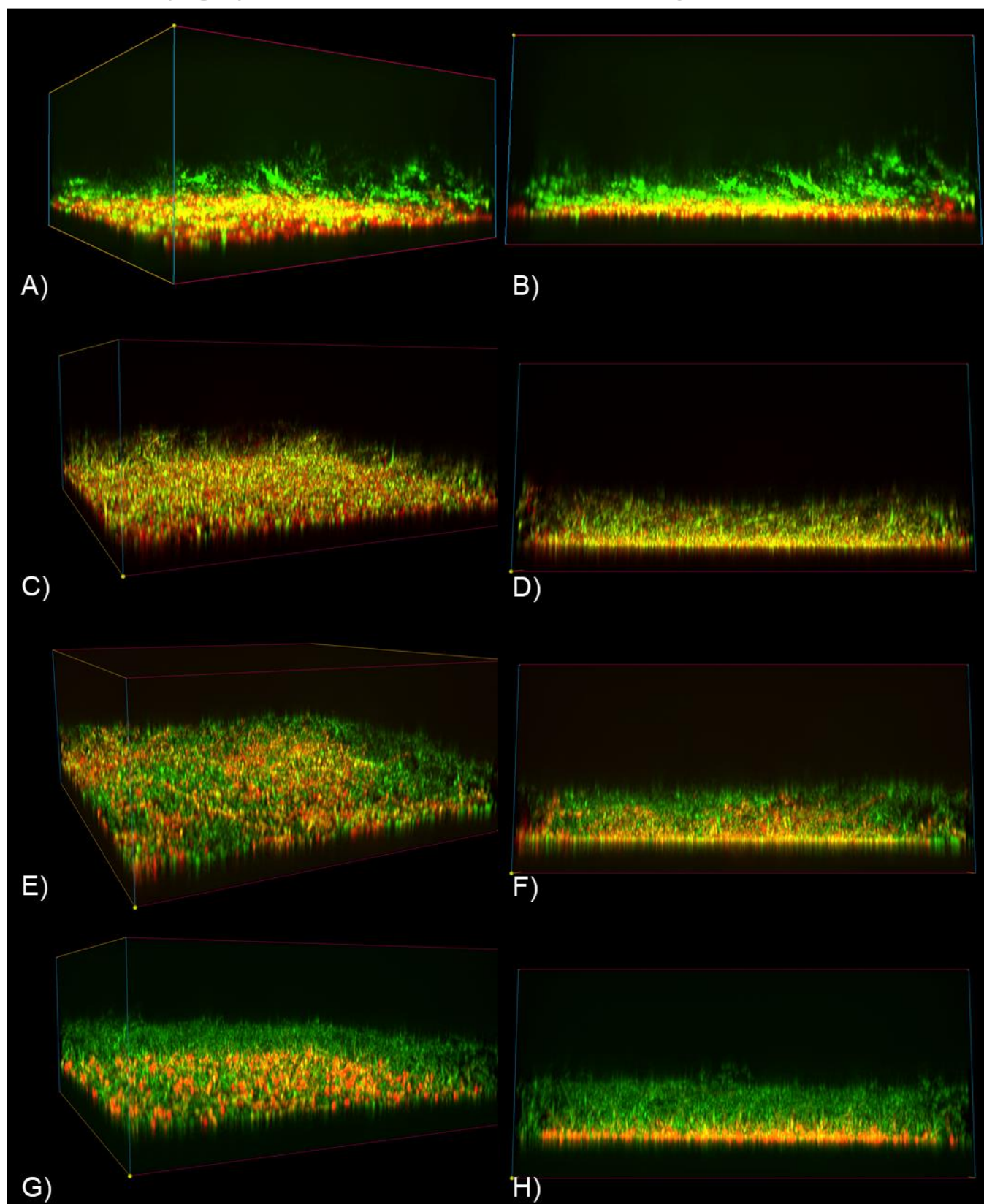




#### **Figure 4.2: EntV disrupts biofilm structure**

Representative three-dimensional fluorescence microscopy images of *C. albicans* CEGC1 biofilms treated with 300 nM 68aa EntV. These biofilms were grown statically for 48 hours at 37°C in YNB-AS media with 68aa EntV and then washed. Microscopy was performed using z-stacked images at 20x magnification with 101 frames and 3 µm between each frame, creating a total image 300 µm in depth. If possible, depending on signal strength, these images were deconvoluted using cellSens Dimension 2.3 (Olympus) to increase resolution. Horizontally adjacent figures represent different perspective views of the same image. A and B) This image was not deconvoluted. The hyphal layer can be seen folding over and growing generally horizontally on top of the yeast bed. C and D) This image was deconvoluted. This biofilm appears to be generally flattened, and the hyphae grew horizontally out of the yeast bed. E and F) This image was deconvoluted. This biofilm appears disorganized. G and H) This image was deconvoluted. This biofilm appears flattened. From the y-axis view (H), it appears that the hyphae initially grew vertically from the yeast bed before falling over and growing horizontally.

---

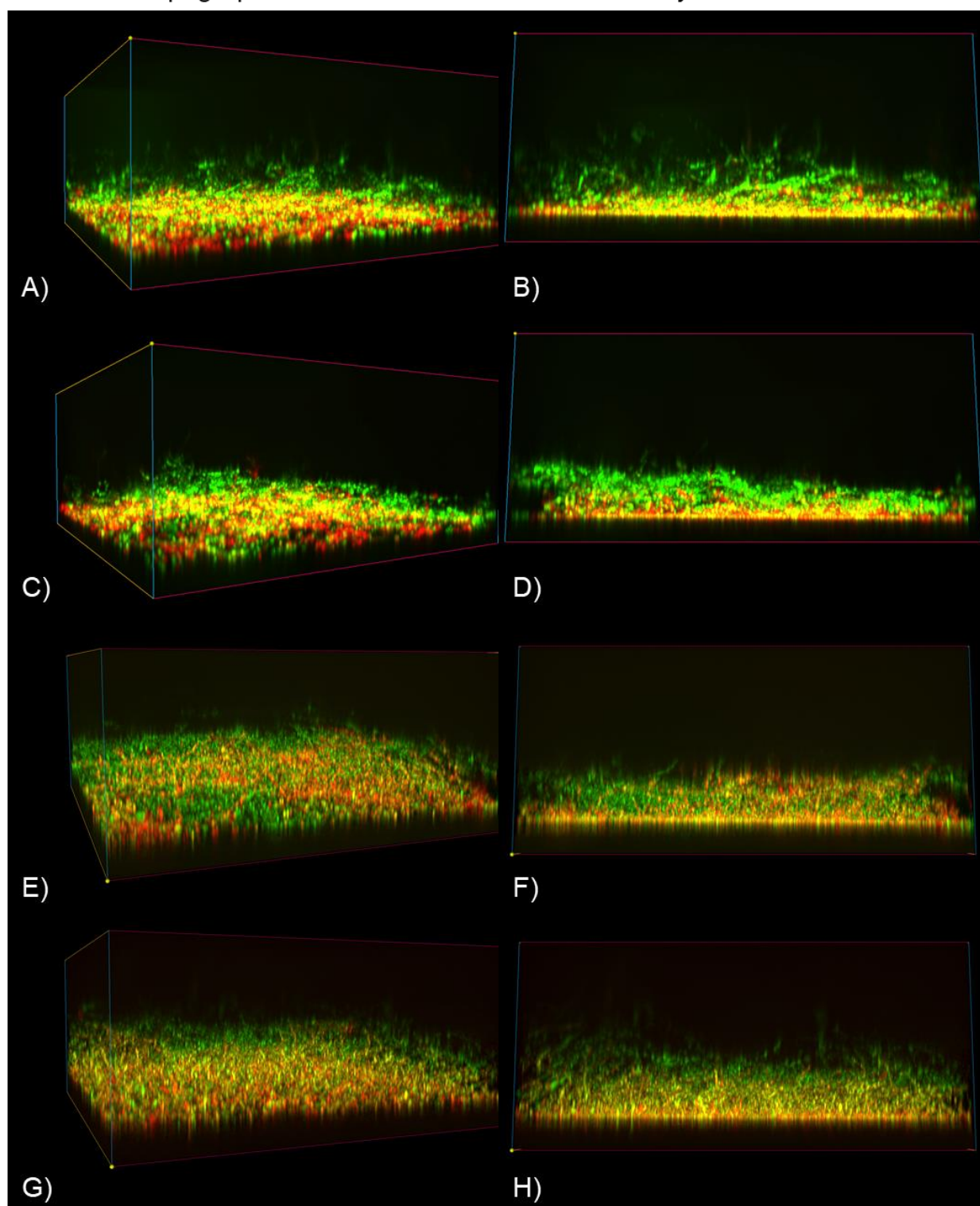
### **16aa EntV derivative is effective in disrupting biofilm structure**

To test my hypothesis that a peptide derived from the C-terminal helix of EntV will be equally effective in inhibiting biofilm formation, I prepared biofilms as before and treated them with the 16aa EntV peptide. Figure 4.3 depicts representative images of the 16aa EntV treated biofilms. In general, the same characteristics that described the biofilms treated with the 68aa EntV peptide can be applied to these biofilms. Biofilms treated with the 16aa EntV peptide were generally less cohesive, smaller, and flattened compared to untreated biofilms.

Much like the 68aa EntV treated biofilms, the samples depicted in Figures 4.3A-D have hyphae that are lying down horizontally almost as a mat on top of the yeast bed. The biofilm in Figure 4.3E appears to be highly disorganized, and the flattening effect can be seen in the y-axis view of this biofilm (Figure 4.3F). Furthermore, in Figure 4.3F, hyphae can be seen growing out of the yeast bed at all angles, but the uppermost hyphae appear to lie across the whole structure as a mat. The biofilm in Figures 4.3I and J is cohesive with a dense and orderly hyphal structure, and it shows the characteristic flattening effect, almost identical to the biofilm depicted in Figures 4.2G and H. Lastly, the biofilm in Figures 4.3G and H shows some stochastic variation amongst these samples. The hyphal layer of this biofilm appears more disorganized than that of the untreated biofilms in Figures 4.1E-H, but the size appears to be approximately the same. In summary, treatment with the 16aa EntV peptide produces biofilms similar to those treated with the 68aa EntV peptide, which can be characterized as being smaller, flattened, and less organized and cohesive than untreated biofilms.

Topographical view

y-axis view



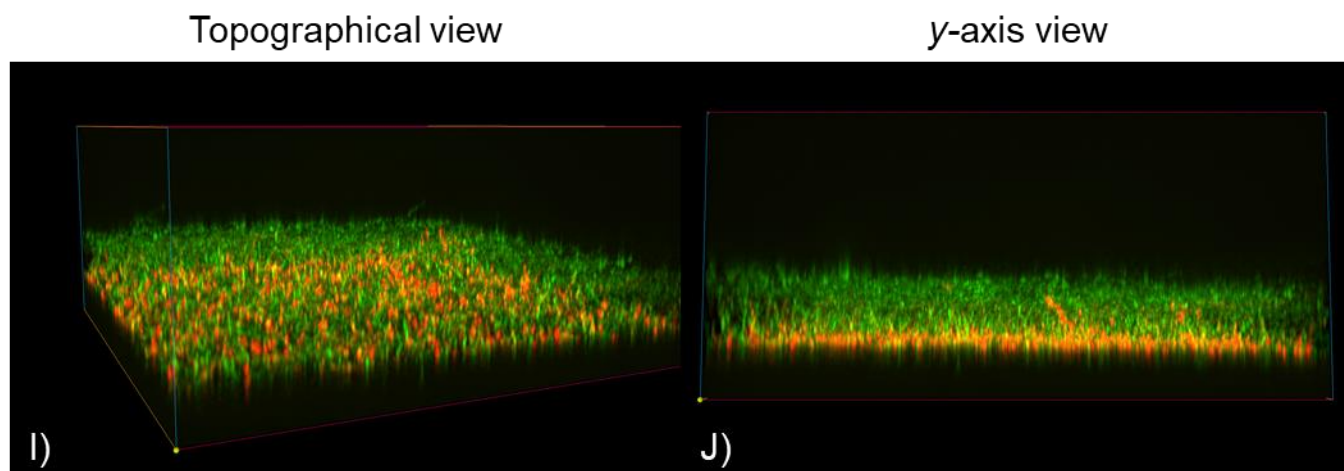


**Figure 4.3: 16aa EntV disrupts biofilm structure**

Representative three-dimensional fluorescence microscopy images of *C. albicans* CEGC1 biofilms treated with 300 nM 16aa EntV. These biofilms were grown statically for 48 hours at 37°C in YNB-AS media with 16aa EntV and then washed. Microscopy was performed using z-stacked images at 20x magnification with 101 frames and 3  $\mu\text{m}$  between each frame, creating a total image 300  $\mu\text{m}$  in depth. If possible, depending on signal strength, these images were deconvoluted using cellSens Dimension 2.3 (Olympus) to increase resolution. Horizontally adjacent figures represent different perspective views of the same image. A – D) These two images were not deconvoluted. These biofilms appear disorganized with hyphae laying horizontally, forming a mat over the yeast bed layer. E and F) This image was deconvoluted. This biofilm appears disorganized with the uppermost layer of hyphae laying as a mat over the whole structure. G and H) This image was deconvoluted. This biofilm shows the variation in the 16aa EntV treated samples. This biofilm is large but highly disorganized. I and J) This image was deconvoluted. This biofilm shows the characteristic flattening effect.

### **68aa EntV and 16aa EntV are effective in reducing biofilm biomass**

I also developed a quantitative biomass assay to pair with the microscopy data presented thus far. This assay measured the biomass of biofilms using a crystal violet stain. Briefly, this experiment was performed by growing *C. albicans* strains SC5314 and  $\Delta/\Delta$  *efg1*  $\Delta/\Delta$  *cph1* statically for 48 hours at 37°C in a 96-well tissue culture treated polystyrene plate. After incubation the remaining media, planktonic cells, and pellicle were removed, leaving only the surface associated biofilm. This biofilm was stained with crystal violet solution for 30 minutes, and then excess dye was washed away using an automated Microplate washer. The biofilms were destained with 200 proof ethanol and crystal violet absorbance was measured at OD<sub>595</sub>.

For each biological replicate I prepared 2 separate plates with 6 technical replicates each. This was to mitigate the chance of loss due to contamination. For the data analysis, I determined the background by including a medium-only well and subtracted the average from the values of the samples. Data were normalized as a percentage relative to the untreated control. A two-way ANOVA with a Dunnett's test was used to determine differences between the untreated control and the experimental samples.

Figure 4.4 shows the data from the biomass assays conducted with 68aa EntV and the 16aa EntV derivative. The 100 nM treatment with the 68aa EntV peptide reduced biomass by approximately 24%, and this effect is roughly consistent for the 10 nM and 1 nM concentrations. The efficacy decreases at 0.1 nM with a reduction of only approximately 12%, however the statistical difference and p-values are equivalent for all tested concentrations ( $p < 0.0001$ ) (Figure 4.4A). The 16aa EntV peptide shows a

similar pattern of efficacy. The 100 nM treatment with 16aa EntV reduced biomass by approximately 21%, and the effect only drops to 15% at the 0.1 nM concentration (Figure 4.4B). Similar to the data collected from the adhesion assays in Figure 3.2C, the lower concentrations of the 16aa EntV treatment show a spreading trend with a greater deviation from the mean. Overall, the biomass assays show highly similar results between treatment with the 68aa EntV peptide and 16aa EntV peptide, thus the 16aa EntV peptide is capable of producing the same inhibition effect as the full 68aa EntV peptide.

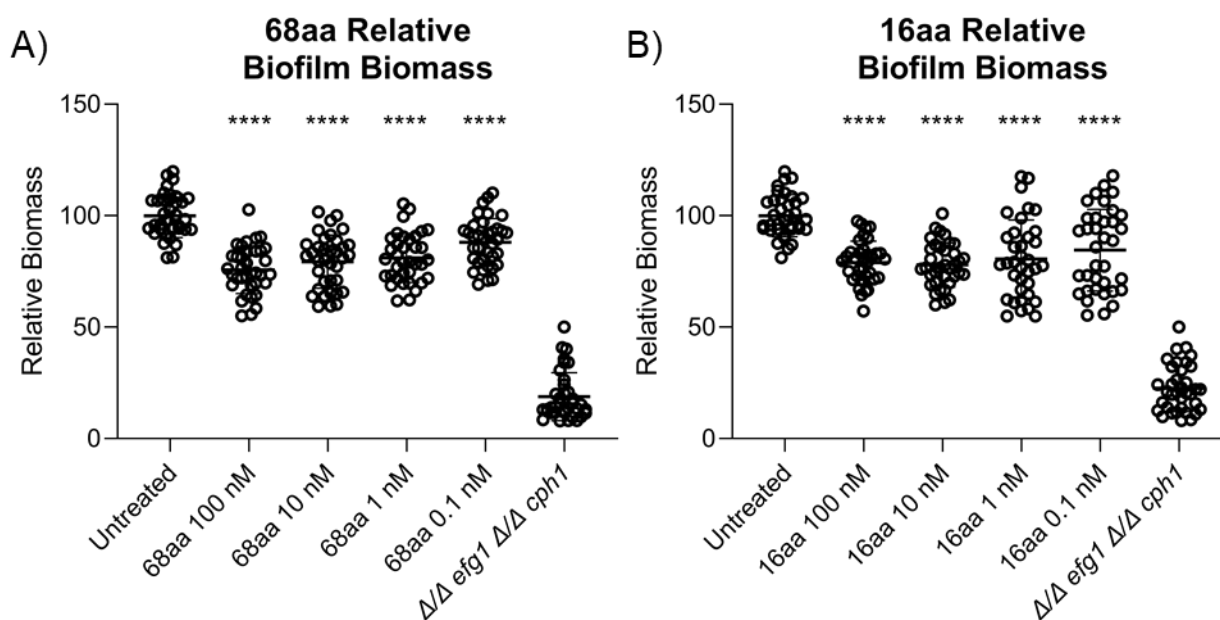


**Figure 4.4: 68aa EntV and 16aa EntV reduce biofilm biomass *in vitro* after 48**

**hours.** The 16aa EntV derivative was hypothesized to have an equal inhibitory effect against *C. albicans* biofilms as the 68aa EntV peptide. A) Biofilms were grown for 48 hours in YNB-AS treated with various concentrations of 68aa EntV and then stained with crystal violet to measure biomass. The 68aa EntV peptide consistently reduced biomass from the 100 nM to 1 nM concentrations. B) Biofilms were treated in the same way as before with 16aa EntV, and the results similarly match the effect of the 68aa EntV peptide. Biomass assays were analyzed by normalizing each experimental technical replicate against the untreated mean. Results represent data collected across three biological replicates, and a two-way ANOVA with a Dunnet's test was used to determine differences between the untreated control and the experimental groups. N=6, \* P < 0.05, \*\* P < 0.01, \*\*\* P < 0.001, \*\*\*\* P < 0.0001.

### **The effect of the 16aa EntV peptide against biofilms is sequence specific**

As before in Chapter 3, two alternative 16aa peptides with rearranged amino acid sequences were used to test the sequence and shape specificity of the inhibitory effect by the 16aa EntV peptide. Briefly, the disordered peptide consists of the same amino acids and has the same overall charge as the 16aa EntV peptide, but this engineered peptide has minimal secondary structure. The helical peptide also has these properties but additionally has been redesigned such that it forms a helix similar to the 16aa EntV peptide but with a distinct amino acid sequence. A more detailed description of these peptides can be found in Figure 3.3.

Neither of the two engineered variant peptides showed any inhibitory effect against *C. albicans* biofilm development (Figure 4.5). While the unaltered 16aa EntV peptide reduced biofilm biomass by approximately 21% at the 100 nM concentration, the disordered and helical engineered peptides at the same concentration only reduced biomass by approximately 1.5% and 4%, respectively (Figure 4.5C). Furthermore, neither engineered peptide at any tested concentration level produced a statistically significant result (Figure 4.5A and B). This demonstrates that the inhibitory effect of the 16aa EntV peptide is sequence specific.



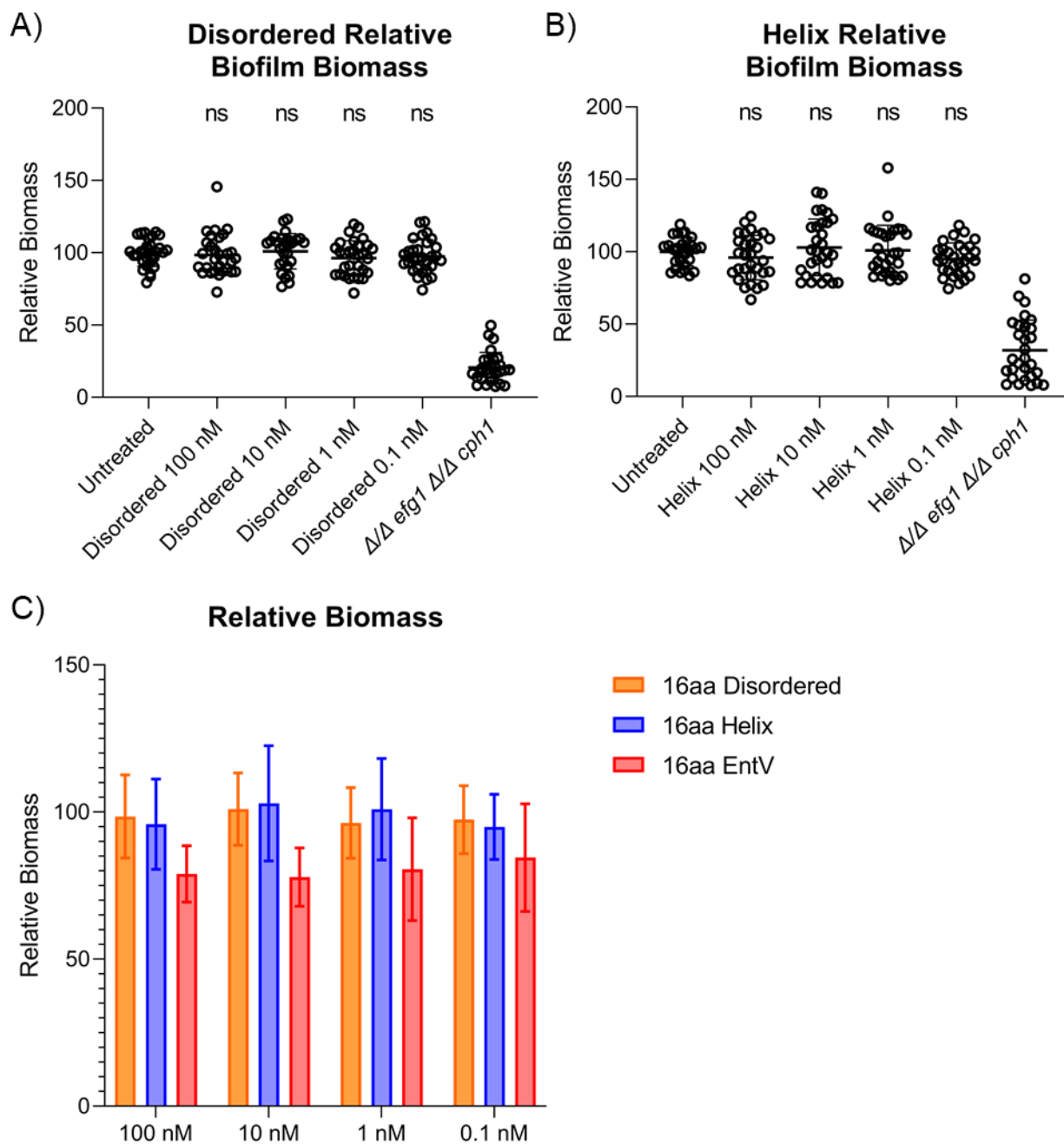


**Figure 4.5: The 16aa EntV peptide has a sequence-specific inhibitory effect on *C. albicans* biofilm development.** To test the sequence specificity of the interaction with the 16aa EntV peptide, two alternative peptides were designed using reordered sequences of the same amino acids as the 16aa EntV peptide. A) Biofilms were grown for 48 hours in YNB-AS treated with various concentrations of an engineered disordered peptide and then stained with crystal violet to measure biomass. This peptide was ineffective in biofilm inhibition. B) Biofilms were treated in the same way as before with an engineered helical peptide, and this peptide had no effect on biofilm development. C) Data from parts A and B were compared against the data presented in 4.4B. Biomass assays were analyzed by normalizing each experimental technical replicate against the untreated mean. Results represent data collected across three biological replicates, and a two-way ANOVA with a Dunnet's test was used to determine differences between the untreated control and the experimental groups. N=6, \*  $P < 0.05$ , \*\*  $P < 0.01$ , \*\*\*  $P < 0.001$ , \*\*\*\*  $P < 0.0001$ .

---

## **EntV biofilm inhibition is unique amongst bacteriocins**

To determine the specificity of the biofilm inhibition interaction with EntV amongst other naturally occurring peptides, I tested two other bacteriocins similar to EntV, Sam57 and YpkK, in the biomass assay. Previous results in this body of work have shown that these peptides do not inhibit *C. albicans* growth and only have minor efficacy in inhibiting adhesion (Figure 3.4).

Figure 4.6 depicts the results of the biomass assays with Sam57 and YpkK. Treatment with the Sam57 bacteriocin at 100 nM produced a slight, although highly statistically significant, reduction in biomass of approximately 10% (Figure 4.6A). This slight effect only present at higher concentrations is consistent with the results from the adhesion assay performed with Sam57 in Figure 3.4A. The biofilms treated with YpkK exhibited a uniform inhibition of approximately 6% across all concentrations tested (Figure 4.6B). Neither of the alternative bacteriocins were as potent as the 68aa EntV peptide (Figure 4.6C). Overall, from these experiments it can be concluded that the alternative bacteriocins Sam57 and YpkK have minimal effect on *C. albicans* biofilm development, and thus the activity of EntV is due to a specific interaction with *C. albicans*.

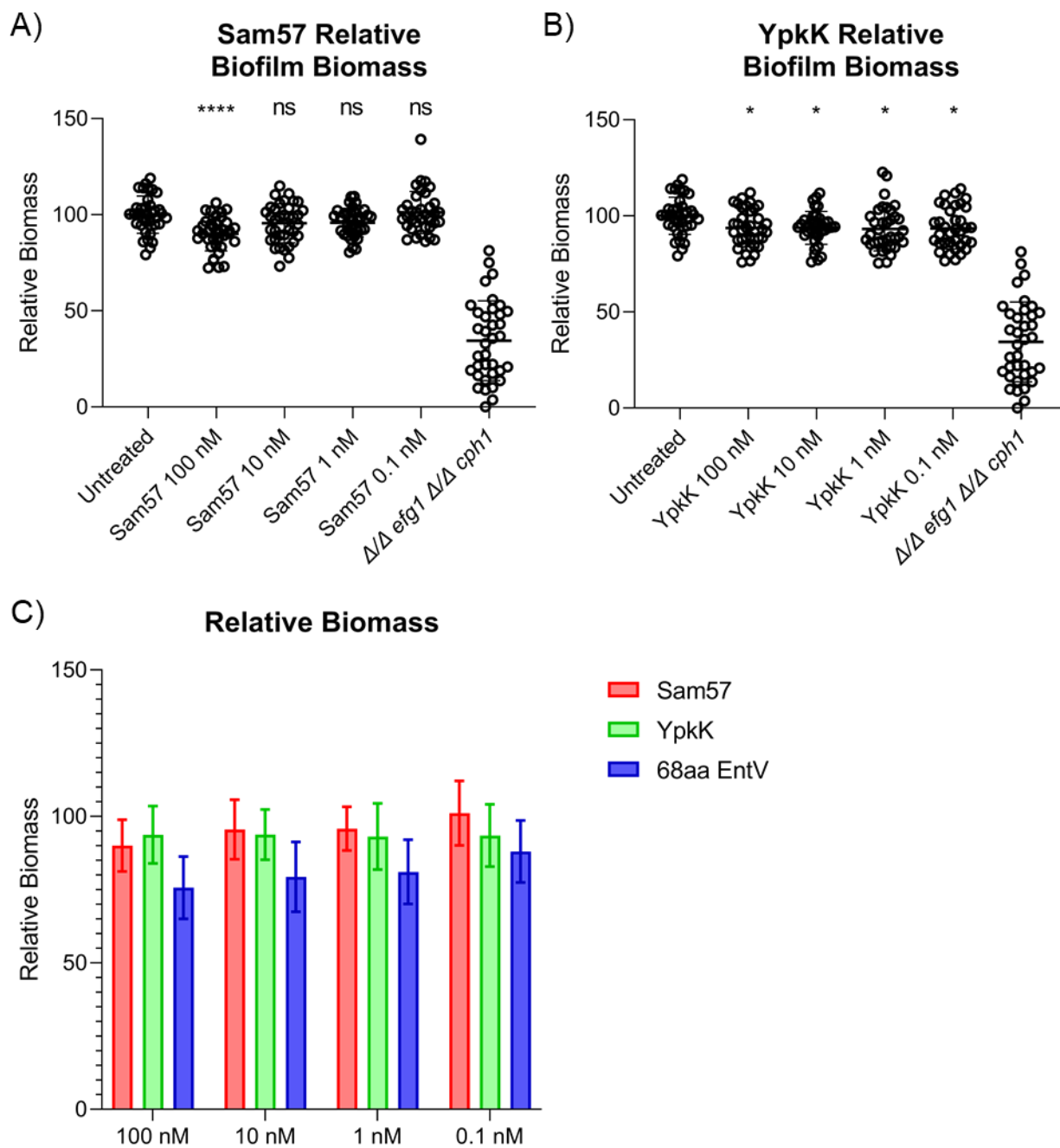


**Figure 4.6: Similar bacteriocins Sam57 and YpkK are less effective than EntV at inhibiting biofilm development.** To determine the specificity of interaction between EntV and *C. albicans*, naturally occurring bacteriocins similar to EntV were tested for activity inhibiting biofilm formation. A) Biofilms were grown for 48 hours in YNB-AS treated with various concentrations of Sam57 and then stained with crystal violet to measure biomass. B) Biofilms were treated in the same way as before with YpkK. C) Data from parts A and B were compared against the data presented in 4.4A. Biomass assays were analyzed by normalizing each experimental technical replicate against the untreated mean. Results represent data collected across three biological replicates, and a two-way ANOVA with a Dunnet's test was used to determine differences between the untreated control and the experimental groups. N=6, \*  $P < 0.05$ , \*\*  $P < 0.01$ , \*\*\*  $P < 0.001$ , \*\*\*\*  $P < 0.0001$ .

---

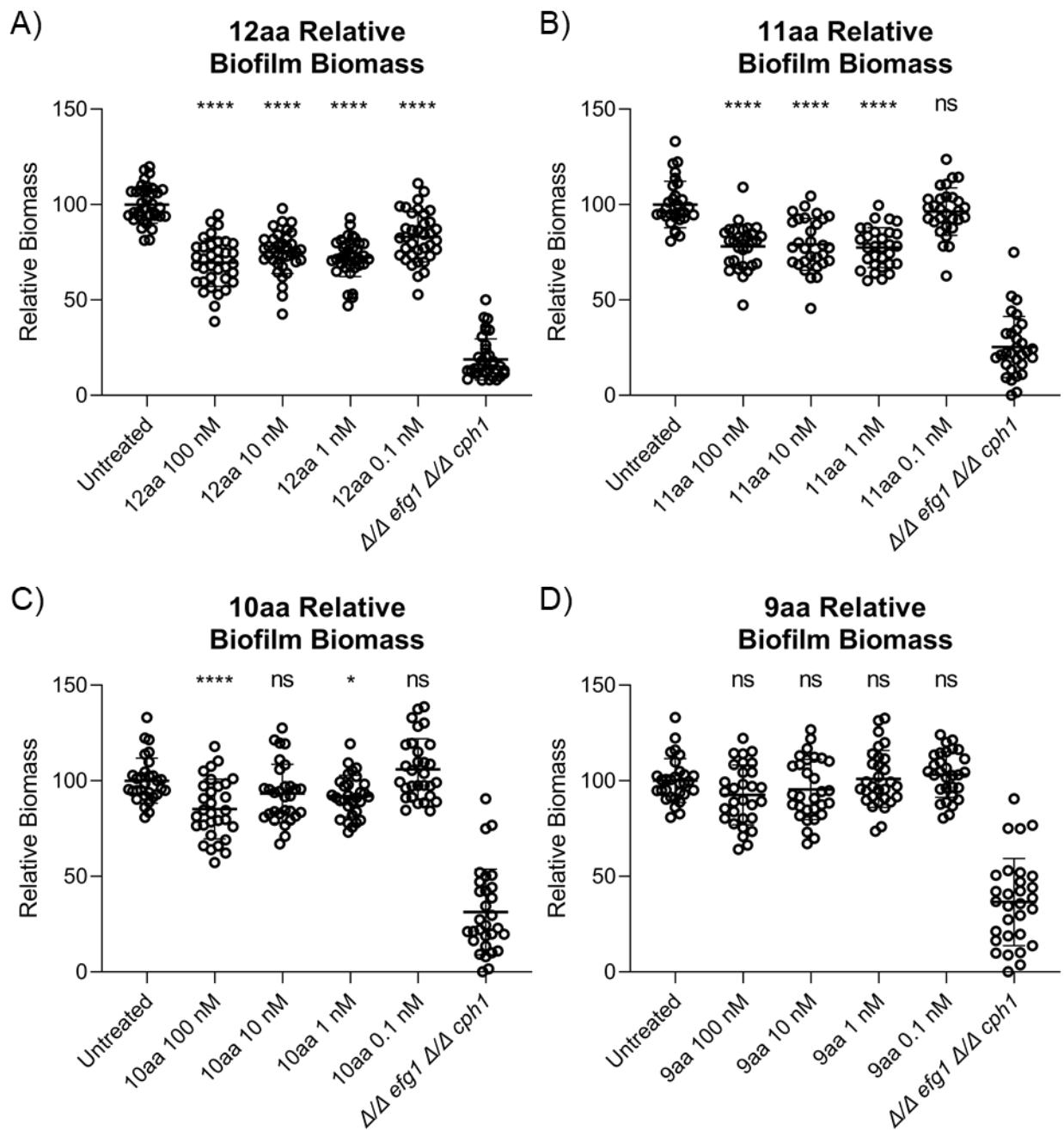
### **Efficacy of smaller EntV peptides**

To further optimize the EntV derived peptides for biofilm inhibition, the 12aa, 11aa, 10aa, and 9aa EntV derived peptides were tested in the biomass assay. A thorough description of the amino acid sequence and secondary structure of these peptides can be found in Figure 3.7. Previous data presented in this body of work showed that the 12aa EntV peptide had an efficacy profile similar to that of the 16aa EntV peptide in reducing adhesion to an abiotic substrate. The 11aa and 10aa peptides were less effective, and inhibition activity was lost upon further trimming to 9aa (Figure 3.7E).

Figure 4.7 depicts the data from the biomass assays with the 12aa – 9aa peptides. These data extend the trend established in the previous chapter. Once again, the 12aa EntV peptide shows potent efficacy, similar to the 16aa EntV peptide. The 100 nM treatment with 12aa EntV showed the best inhibition of any of the peptides tested in this work with a mean difference of approximately 30%. Like the 16aa EntV peptide, the effect was consistent with treatment concentrations of 10 nM and 1 nM, and only at 0.1 nM did the inhibition decrease to approximately 17% (Figures 4.7A and E). The 11aa EntV peptide was less effective than the 12aa EntV peptide with a mean inhibition of only approximately 22% from the 100 nM treatment, but the reduction in efficacy at 0.1 nM was consistent (Figures 4.7B and E)

In the adhesion assay, the 10aa EntV peptide showed similar efficacy to the 12aa EntV peptide at high concentrations (Figure 3.7E), but it was less effective in the biomass assays. The 100 nM treatment with the 10aa EntV peptide produced a mean difference of approximately 15%, with only minimal differences at other concentrations

(Figures 4.7 C and E). The 9aa EntV peptide was ineffective at inhibiting biofilm formation at any tested concentration (Figures 4.7D and E).





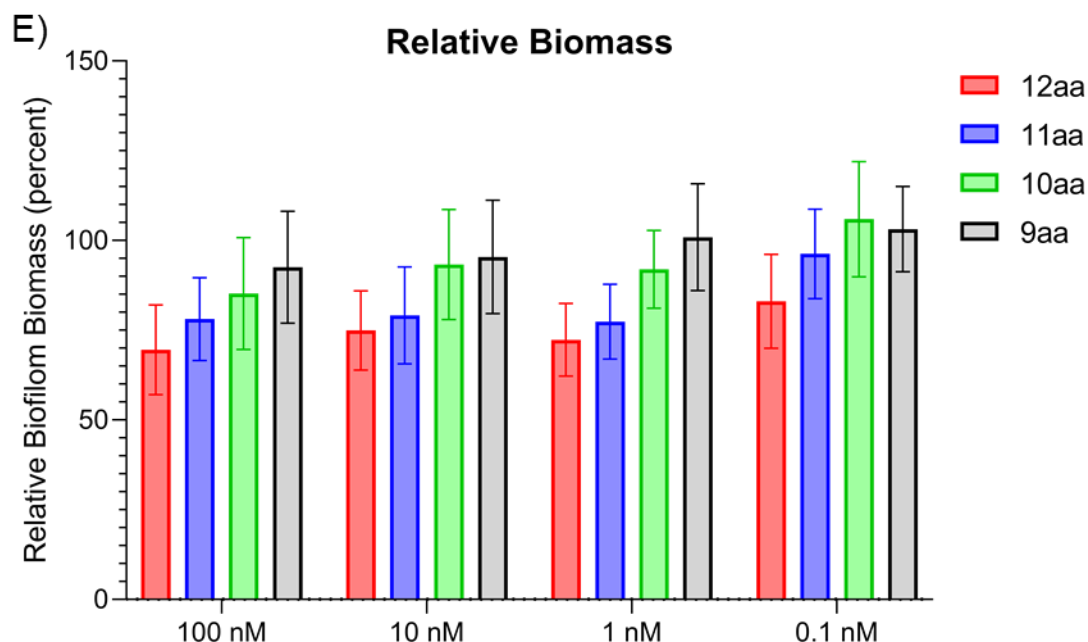


**Figure 4.7: Inhibition of biofilm development by small EntV peptides.** To

determine an optimal size of the EntV peptide for further study, small peptides ranging from 12 to 9 amino acids were tested in the biofilm biomass inhibition assay. Biofilms were grown for 48 hours in YNB-AS with various concentrations of the 12aa EntV peptide (A), 11aa EntV peptide (B), 10aa EntV peptide (C) or 9aa EntV peptide (D). To directly compare the efficacy of these peptides, E) the mean biomass relative to the untreated control is displayed. Biomass assays were analyzed by normalizing each experimental technical replicate against the untreated mean. Results represent data collected across three biological replicates, and a two-way ANOVA with a Dunnet's test was used to determine differences between the untreated control and the experimental groups. N=6 (12aa) or N=5 (11aa, 10aa, 9aa), \*  $P < 0.05$ , \*\*  $P < 0.01$ , \*\*\*  $P < 0.001$ , \*\*\*\*  $P < 0.0001$ .

### **The effect of small EntV peptides on biofilm structure**

The small peptides were examined for their effects on the structure of *C. albicans* biofilms using microscopy as before. These results taken along with the biomass assays provide a more comprehensive understanding of the efficacy of these peptides. The next four figures display the results of this analysis. All the following images were successfully deconvoluted.

Figure 4.8 depicts biofilms treated with the 12aa EntV peptide at a concentration of 300 nM. These biofilms, especially in comparison to the untreated samples in Figure 4.1, are remarkably consistent in their size and structure. The flattening effect that was found as a result of treatment with the 68aa EntV and 16aa EntV peptide is consistently present in all these samples. Figures 4.8C and D depict a biofilm that appears somewhat disorganized and lacking cohesion, a trait consistent with the previously analyzed biofilms, however, this is not true of the other biofilms in this sample.

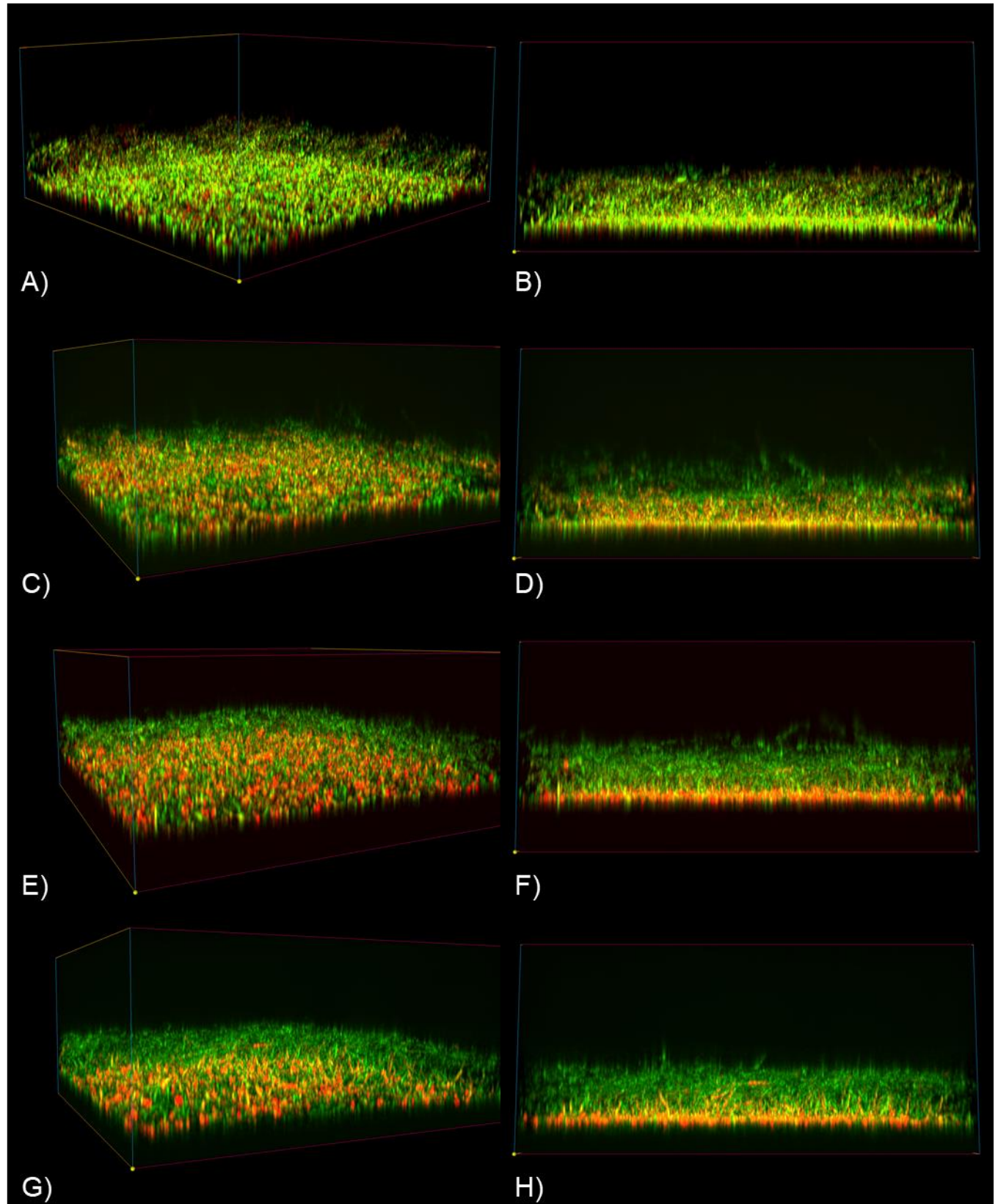
Biofilms treated with the 11aa EntV peptide are depicted in Figure 4.9. Once again, a flattening effect can be observed, but it is less apparent than with treatment from the 12aa EntV peptide. The biofilms in Figures 4.9A-D appear generally regular with some flattening. Notably, previous treated biofilms have displayed a folding over effect, while the hyphae in these images appear to be primarily growing a straight, consistent angle from the yeast bed. The biofilm depicted in Figures 4.9E and F shows characteristic disorder and flattening as has been seen previously. Figures 4.9G and H were included to show a representative image of variation found amongst the samples collected for this study. This biofilm still shows some flattening, but it is close to approximately the same size as some of the smaller untreated biofilms.

Figure 4.10 depicts biofilms treated with the 10aa EntV peptide. These biofilms had a substantial amount of variability in their structures. The biofilm in figure 4.10A and B appears to be significantly flattened with horizontal and disorganized hyphae. Overall, this biofilm looks similar to biofilms treated with the 68aa and 16aa EntV peptides. The biofilm in Figures 4.10C and D also displays characteristic flattening, but the hyphal layer is more cohesive. The biofilms in Figures 4.10E-H are larger with dense hyphae. Figures 4.10 E and F show disorganization while Figures 4.10G and H show a slight flattening effect.

Lastly, Figure 4.11 depicts biofilms treated with the 9aa EntV peptide. These biofilms look most similar to the untreated biofilms in Figure 4.1. The first two biofilms in Figures 4.11A-D display the large size and vertical hyphae of a healthy biofilm. The biofilms in Figures E-H are large and dense. Figures 4.11 G and H shows a small amount of flattening, which is consistent with the finding from the biomass assay that at high concentrations the 9aa EntV peptide has a very slight effect.

Topographical view

y-axis view



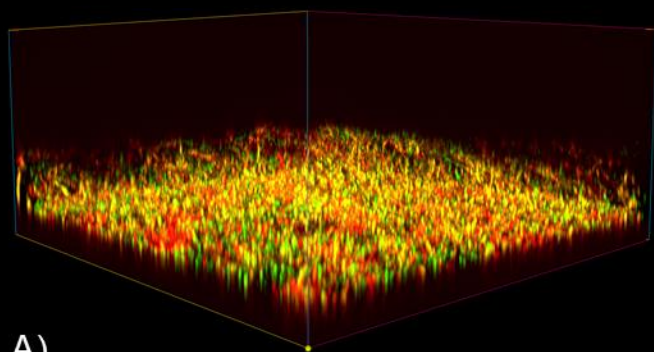
**Figure 4.8: 12aa EntV is a potent inhibitor of biofilm development.**

Representative three-dimensional fluorescence microscopy images of *C. albicans* CEGC1 biofilms treated with 300 nM 12aa EntV. These biofilms were grown statically for 48 hours at 37°C in YNB-AS media with 12aa EntV and then washed. Microscopy was performed using z-stacked images at 20x magnification with 101 frames and 3 µm between each frame, creating a total image 300 µm in depth. Images were deconvoluted using cellSens Dimension 2.3 (Olympus) to increase resolution. Horizontally adjacent figures represent different perspective views of the same image. A and B) This biofilm appears to be flattened with hyphae that grew at an angle out of the yeast bed layer. C and D) This biofilm appears disorganized and lacking cohesion. E and F) This biofilm is flattened. G and H) This biofilm is flattened and appears to have hyphae that initially grew vertically out of the yeast bed layer before laying over horizontally.

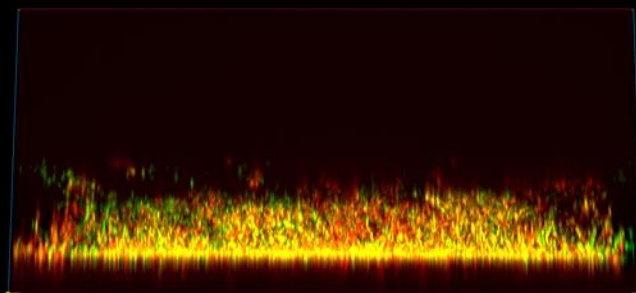
---

Topographical view

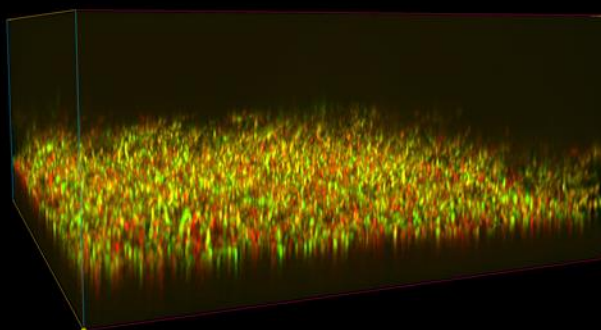
y-axis view



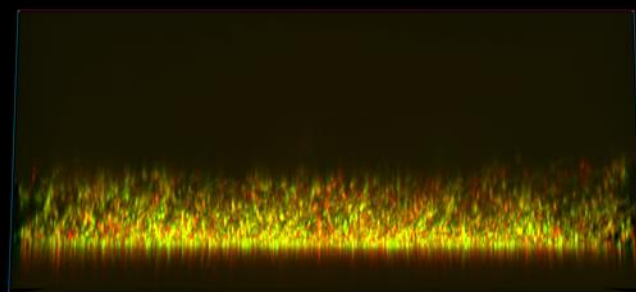
A)



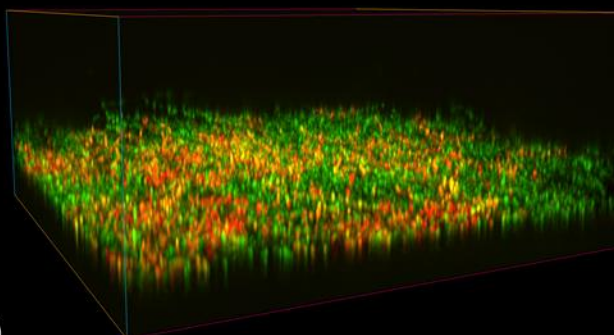
B)



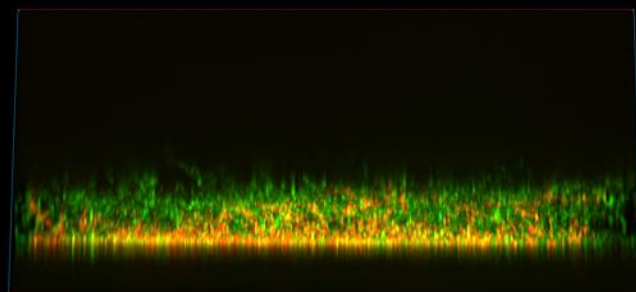
C)



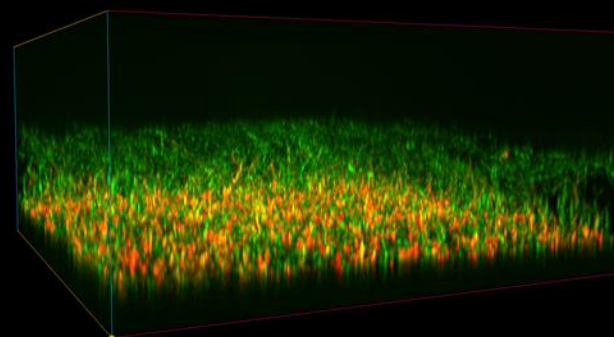
D)



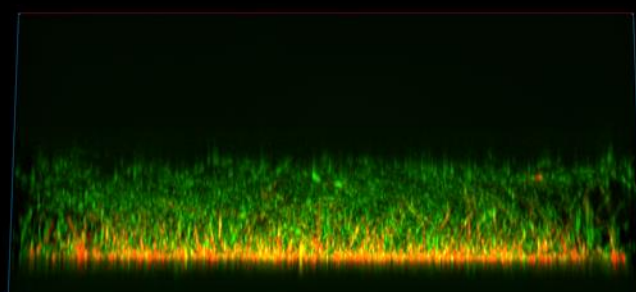
E)



F)



G)



H)

**Figure 4.9: Biofilms treated with 11aa EntV.** Representative three-dimensional fluorescence microscopy images of *C. albicans* CEGC1 biofilms treated with 300 nM 11aa EntV. These biofilms were grown statically for 48 hours at 37°C in YNB-AS media with 11aa EntV and then washed. Microscopy was performed using z-stacked images at 20x magnification with 101 frames and 3 µm between each frame, creating a total image 300 µm in depth. Images were deconvoluted using cellSens Dimension 2.3 (Olympus) to increase resolution. Horizontally adjacent figures represent different perspective views of the same image. A – D) These two biofilms appear to be flattened and have hyphae that grew at a generally consistent angle out from the yeast layer. E and F) This biofilm appears to be disordered and flattened. G and H) This large biofilm was included to show a representative image of the variation in the sample collected in the study. This biofilm shows some flattening with the uppermost hyphae appearing to lay flat over the rest of the structure.

---



Topographical view

y-axis view

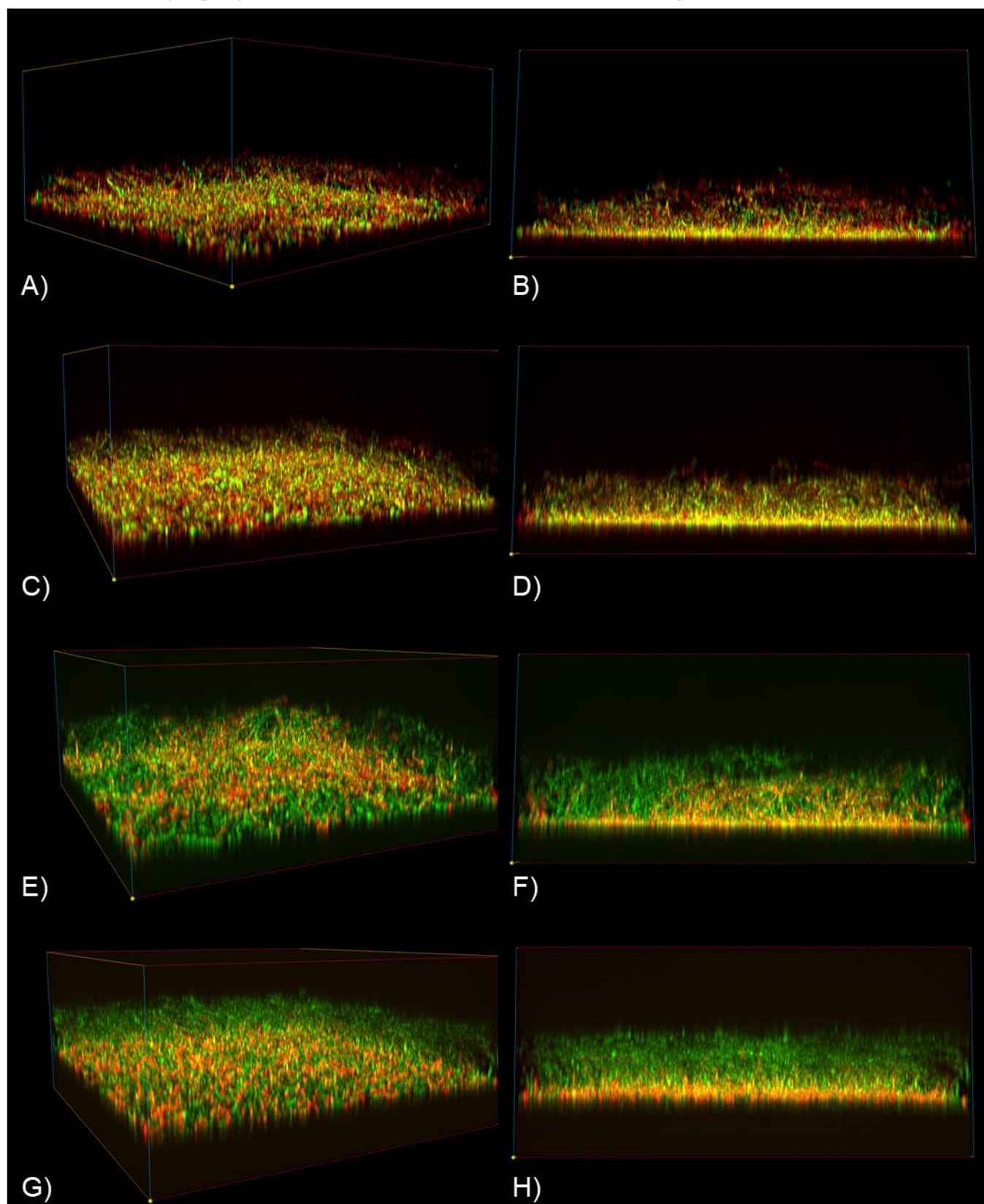




**Figure 4.10: Biofilms treated with the 10aa EntV peptide.** Representative three-dimensional fluorescence microscopy images of *C. albicans* CEGC1 biofilms treated with 300 nM 10aa EntV. These biofilms were grown statically for 48 hours at 37°C in YNB-AS media with 10aa EntV and then washed. Microscopy was performed using z-stacked images at 20x magnification with 101 frames and 3 µm between each frame, creating a total image 300 µm in depth. Images were deconvoluted using cellSens Dimension 2.3 (Olympus) to increase resolution. Horizontally adjacent figures represent different perspective views of the same image. A and B) This biofilm was flattened and showed some disorganization. C and D) This biofilm was flattened but appears to be generally orderly and cohesive. E and F) This biofilm is large and generally disorganized. G and H) This biofilm was slightly flattened.

---

Topographical view

y-axis view

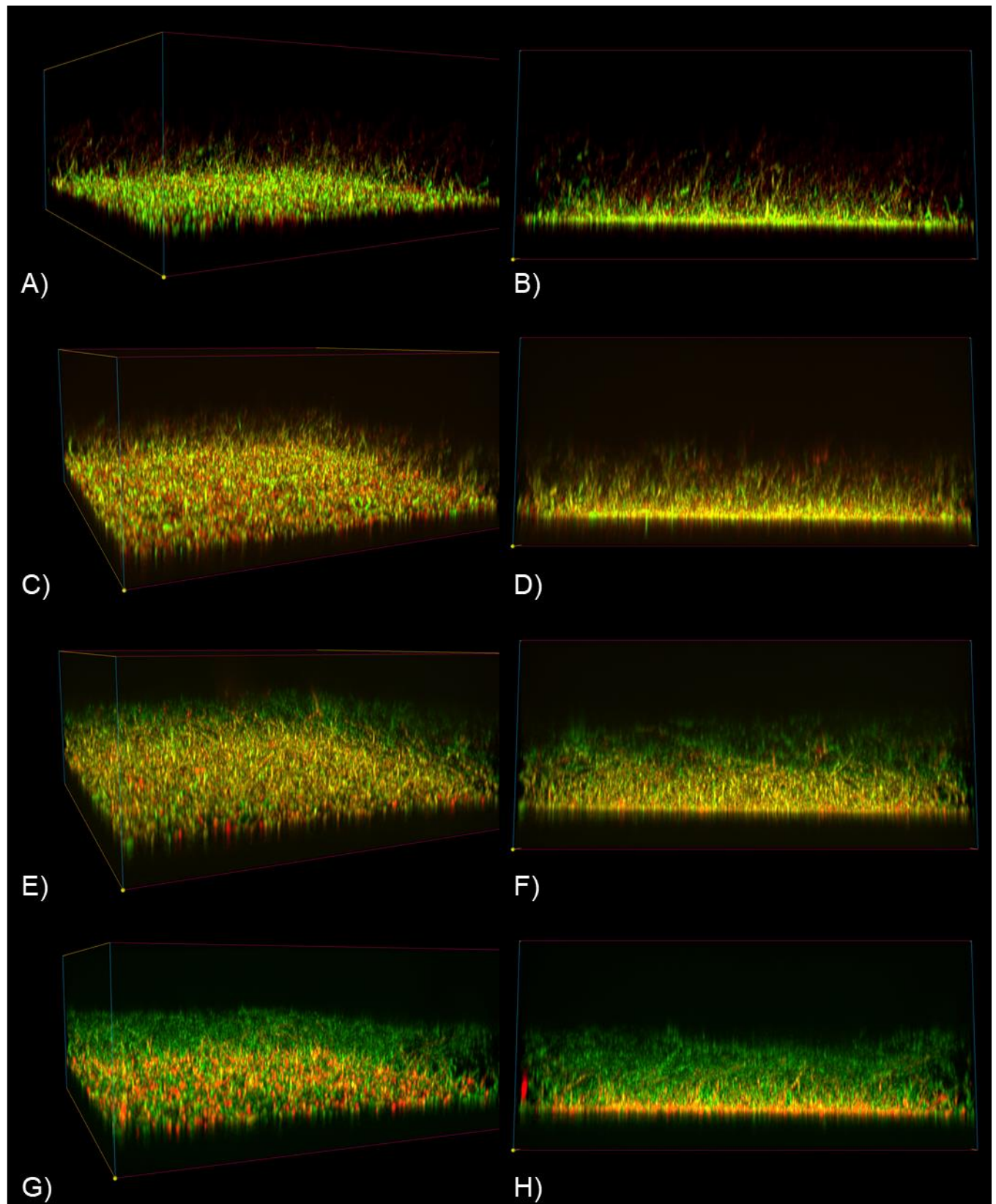


**Figure 4.11: The 9aa EntV peptide does not disrupt biofilm structure.**

Representative three-dimensional fluorescence microscopy images of *C. albicans* CEGC1 biofilms treated with 300 nM 9aa EntV. These biofilms were grown statically for 48 hours at 37°C in YNB-AS media with 9aa EntV and then washed. Microscopy was performed using z-stacked images at 20x magnification with 101 frames and 3 µm between each frame, creating a total image 300 µm in depth. Images were deconvoluted using cellSens Dimension 2.3 (Olympus) to increase resolution. Horizontally adjacent figures represent different perspective views of the same image. A – D) These two biofilms are large with hyphae that grow vertically out of the yeast bed. E and F) This biofilm is large and dense. G and H) This biofilm is large, dense, and generally cohesive. This biofilm appears to be slightly flattened on top.

---

## Discussion

The 68aa EntV peptide has been tested for efficacy in inhibiting the development of *C. albicans* biofilms in prior publications by other members of our lab. The results I have presented in Figures 4.2 and 4.4 use different techniques than what has previously been published, and my results agree with previous findings that the 68aa EntV peptide inhibits biofilm development and reduces biofilm size.

The biomass assay of the biofilms treated with the 16aa EntV peptide provide a verifiable result to show that the 16aa EntV peptide has a comparable effect on biofilm development to the 68aa EntV peptide (Figure 4.4). Both treatments reduced biomass by greater than 20% and only had a decrease in efficacy at the 0.1 nM concentration. Furthermore, biofilms treated with either the 68aa or 16aa EntV peptide showed structural similarities such as a characteristic flattening effect (Figure 4.2 and 4.3). Taken together, these results indicate that the C-terminal helix of EntV is sufficient to elicit the same inhibitory response on *C. albicans* biofilms as the full 68aa peptide.

The inhibitory action is sequence specific to EntV, indicating a specific interaction, as evidenced by the inefficacy of the reordered 16aa peptides in Figure 4.5. Additionally, this interaction is specific to EntV. Sam57 and YpkK, bacteriocins with size and structural similarities to EntV, had minimal to no effect on biofilm biomass (Figure 4.6). In the previous chapter these bacteriocins were shown to have some efficacy in inhibiting *C. albicans* adhesion, although they were less effective than EntV. The inability of these bacteriocins to inhibit biofilm formation provides insight into a) the robustness of *C. albicans* biofilm formation, and b) the high level of specificity of the EntV peptide.

The result that the 12aa EntV peptide was more effective than the shorter peptides is internally consistent with the adhesion assay results in this same work (Figure 3.7), and externally consistent with *in vivo* infection model results from the Garsin and Lorenz labs. However, it was surprising that the 12aa EntV peptide was much more effective than the 16aa EntV peptide in reducing biomass. In the adhesion assays in the previous chapter, these two peptides had virtually identical efficacy profiles for concentrations between 100 nM and 0.1 nM (Figures 3.7E). A potential explanation for the superior efficacy of the 12aa EntV peptide in these assays is the instability predicted in the 16aa EntV peptide as described in Figure 3.1. This instability may also explain the unique spreading characteristic of the data for low concentration treatments of the 16aa EntV peptide in both the adhesion assay (Figure 3.2C) and the biomass assay (4.4B).

In total, the results in this chapter indicate that the 12aa EntV peptide is an optimal choice for further study into biofilm inhibition of *C. albicans*. In this work I chose to grow biofilms under static conditions on level surfaces to maximize reproducibility and the resolution of images I could collect with fluorescence microscopy. However, the most medically relevant biofilms, such as those that occur on central line catheters or dental implants, exist in dynamic environments on uneven surfaces. Future studies with this peptide should include an examination of its efficacy in the central line catheter model with our collaboration with Dr. David Andes. It would also be informative to examine the effect of treatment with the peptide to a biofilm under continuous media flow conditions to measure the structural integrity of the biofilm and the rate of production of disperser cells.

I employed new and innovative technologies to obtain the results in this chapter. Recent publications from our lab and other leaders in the field (15, 72) have compared biofilms using two-dimensional biofilm cross-sections similar to *y-axis* view presented in this work. The three-dimensional high-resolution topographical images in this work provided enlightening additional context to the structures of these biofilms. Additionally, for the biomass assays, an automatic Microplate washer was used to perform the washes. When removing excess dye from a biofilm, the standard across the field is to wash the sample by hand with a pipette (180). By using the automated washer, I at least tripled throughput of the assay and saved plastic waste. The methods and protocols I developed are available for future work that will allow our lab to better understand biofilm structure and conduct large scale screens of biofilms grown under different conditions.

As a final note, it is worth addressing that there is a significant amount of variation in the sizes of some of the biofilms measured by confocal microscopy. This is particularly true of the untreated biofilms presented in Figure 4.1. The biofilms treated with the EntV peptides showed less variation in size, the most consistent of these being the biofilms treated with the 12aa EntV peptide. An explanation for this is that normal biofilm size exhibits a degree of stochastic variation. For biofilms treated with the effective peptides, this variation is reduced by the treatment. This kind of variation and relationship between healthy and unhealthy biofilms has been documented in other previous studies (57, 72, 192, 193). In this study I used a measure of biomass to compensate for the immutable variation of visual measurements, but another alternative measurement used for the same reason is dry mass of a biofilm (193).

**Chapter 5: Hyphal invasion of epithelial cells is inhibited by EntV in an *ex vivo* co-culture assay**

## Introduction

Commensal colonization by *C. albicans* becomes invasive disease when the fungal cells cross a tissue surface. One method by which *C. albicans* can invade host epithelial tissue is endocytosis, whereby the host epithelial cell initiates internalization of the fungal cell (194–196). Hyphae are more potent at causing this response, as a non-filamentous  $\Delta/\Delta$  *efg1/efg1* mutant has been found to be less efficient at inducing endocytosis than wild-type cells (197). A potential explanation for this is that Als3, a hyphal cell wall protein and adhesin, can induce endocytosis by binding to E-cadherin and N-cadherin on host cells (5). *C. albicans* can also directly penetrate epithelial cells (196, 198). Hyphae puncture host cells using physical force and several secreted hydrolases including aspartyl proteinases, phospholipases, and lipases (199–201).

In this chapter I examine the activity of 68aa EntV and the C-terminal derived 16aa EntV peptides in inhibiting *C. albicans* virulence in an *ex vivo* tissue culture model. In this model, *C. albicans* cells were cocultured with a confluent single layer of human pharyngeal carcinoma cells (FaDu). Invasion of the host cell layer by *C. albicans* hyphal cells was measured as a proxy for virulence. I hypothesized that the C-terminal derived 16aa EntV peptide would be equally or more potent at inhibiting *C. albicans* invasion into the FaDu cell layer.

The FaDu cell line originated from a 56-year-old male patient who presented to a hospital in Calcutta in 1968 with a pharyngeal squamous cell carcinoma. This was only the third established oral or pharyngeal epidermal cell line, the other two being KB and Hep-2. When first described, FaDu cells were notable for their ability to grow into even and confluent monolayers (202). Infection assays with FaDu cells have been



previously done with *C. albicans* (203) and a wide range of other pathogens including adenoviruses (204) and *Neisseria meningitidis* (205).

The data presented in this section remain preliminary. This model contains a complex system of interactions between host cells, fungal cells, and media conditions, and some of the variables were difficult to control. Thus, replication of the results presented was inconsistent. Further research will be necessary to modify the technical aspects of the assay to improve reproducibility. Nevertheless, the results presented indicate potential for future success with this virulence model.

## Results

To test the activity of the 68aa EntV and 16aa EntV peptides in inhibiting *ex vivo* tissue invasion, I developed a FaDu invasion assay. A confluent layer of FaDu cells was grown in 8-well chamber slides (Ibidi), treated with EntV peptides at a concentration of 300 nM, and co-incubated with *C. albicans* strain JRC58B. This fungal strain constitutively transcribes the gene for the fluorescent protein mCherry from the *ACT1* promoter (*ACT1p-mCherry*). After a 2-hour co-incubation at 37°C in a 5% CO<sub>2</sub> humidified incubator, the cells were fixed with paraformaldehyde and stained with NucBlue and a polyclonal anti-*Candida*-FITC antibody. Fluorescence microscopy images were taken and analyzed manually.

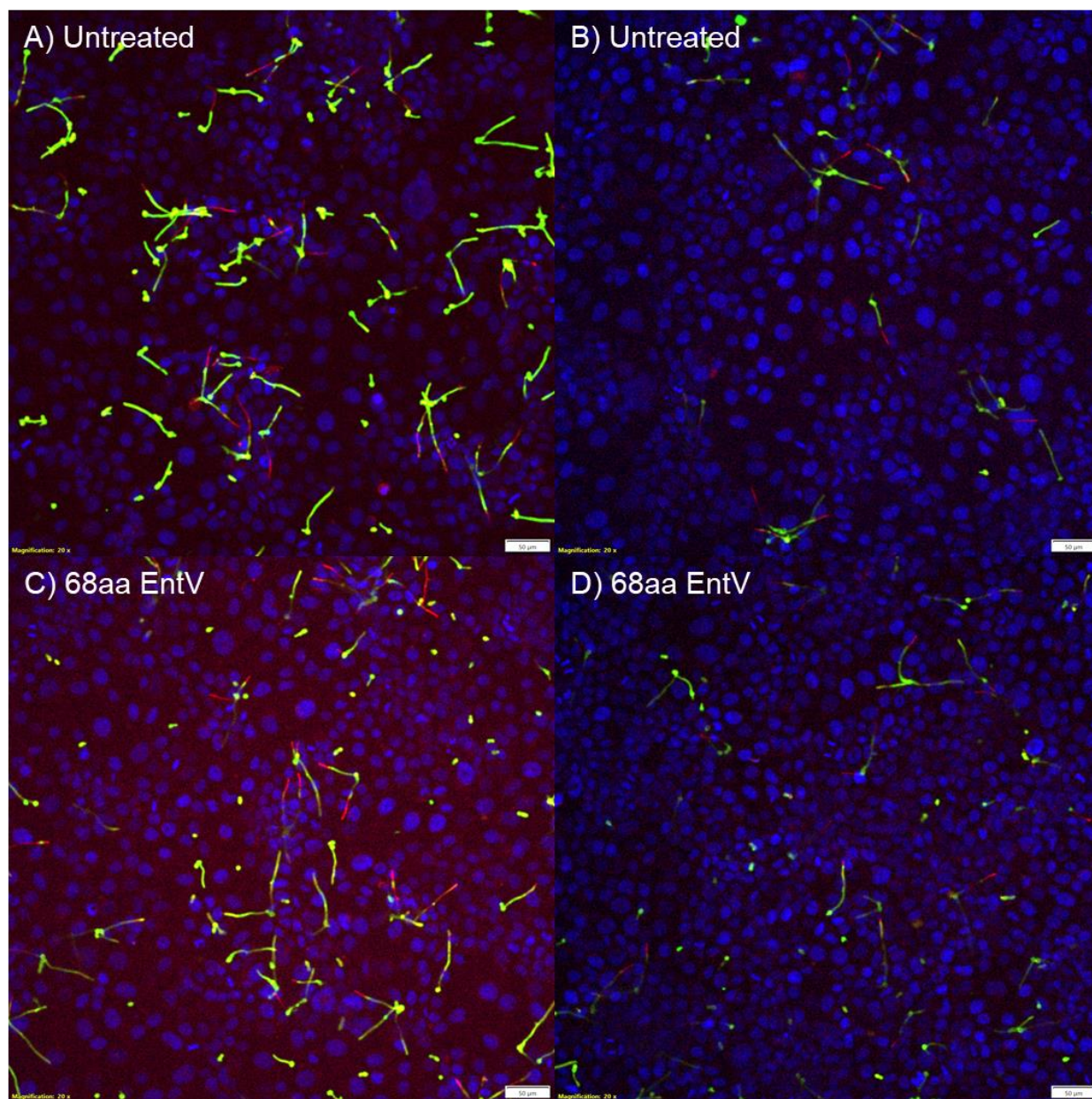
To interpret the final presentation of this data, green fluorescent signal depicts *C. albicans* cells that were on the surface of the epithelial cell layer and were accessible to the antibody stain. While all the *ACT1p-mCherry C. albicans* cells produce mCherry and are visible in the red fluorescent signal, cells that are exclusively visible with the red fluorescent signal are those that have invaded the host cell layer. Lastly, the blue fluorescent signal depicts the nuclei of the FaDu cells.

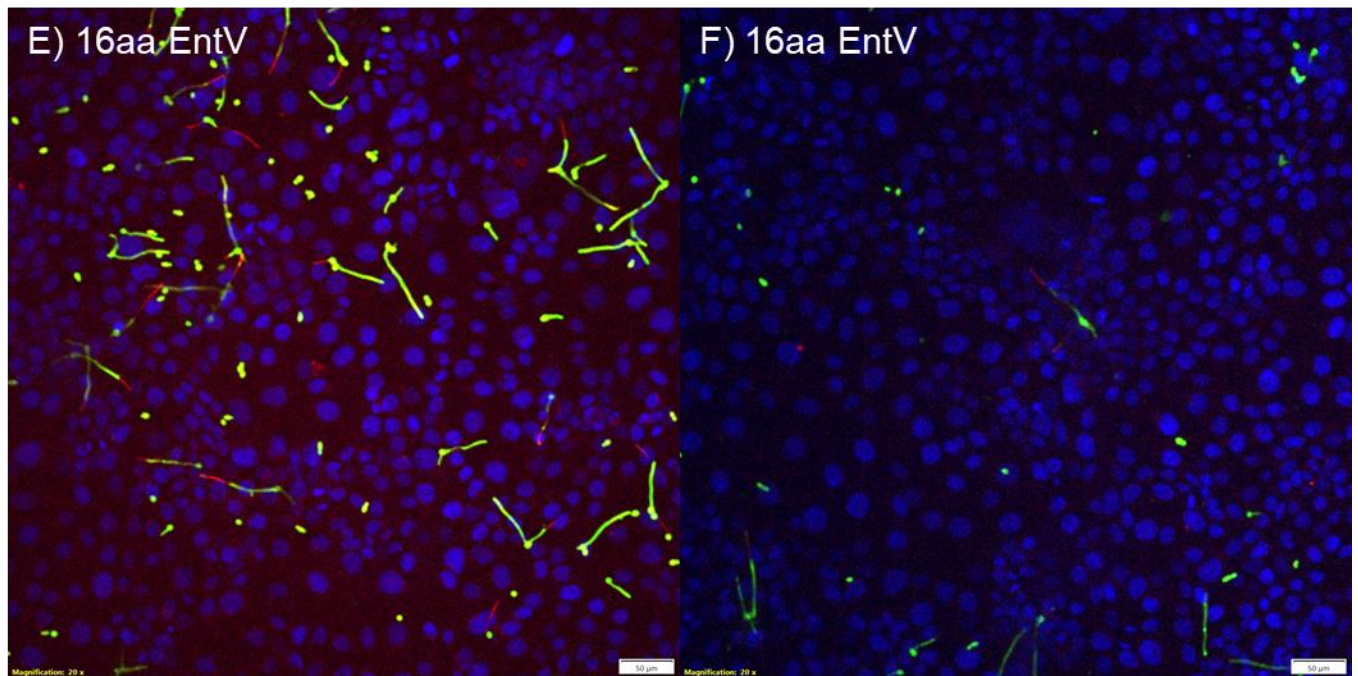
Figure 5.1 depicts representative images of FaDu cell layers infected with the *ACT1p-mCherry C. albicans* strain and a numerical comparison of hyphal and invasion frequency between treatment conditions. In the untreated co-cultures (Figures 5.1A and B), more than 80% of all the *C. albicans* cells formed hyphae (Figure 5.1G), and subsequently many of those hyphae invaded into the cell layer. Figure 5.1A depicts a region of the cell layer more densely populated with *C. albicans* cells than Figure 5.1B, but the trend of near universal hyphal formation is consistent. For these two figures,

approximately half of the total *C. albicans* cells formed hyphae that invaded into the host cell layer (Figure 5.1H).

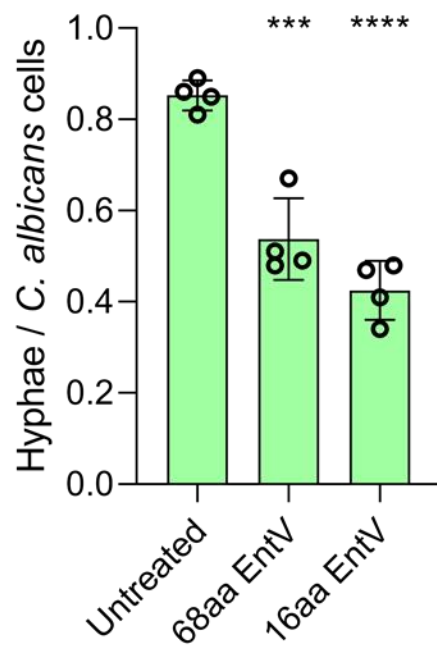
Figures 5.1C and D depict co-cultures treated with 300 nM 68aa EntV peptide. Approximately half of the *C. albicans* cells treated with the 68aa EntV peptide formed hyphae (5.1G), which is significantly fewer than in the untreated sample, but this did not translate to a significant reduction in invasion (5.1H). The 16aa EntV peptide was also effective in reducing hyphae in these cocultures (Figures 5.1E, F, and G). Additionally, the 16aa EntV peptide treatment significantly reduced invasion by approximately 27% from the untreated control (p-value = 0.0030, \*\*) and 20% from the 68aa EntV treated samples (p-value = 0.0176, \*) (Figure 5.1H).

These results remain incomplete and in need of replication and further study, however they do indicate that EntV and the C-terminal helix thereof are potentially capable of inhibiting invasion and virulence in this *ex vivo* model. Furthermore, these data indicate the potential that the 16aa EntV peptide is superior in activity to the 68aa EntV peptide.





G) **Hyphae Frequency**



H) **Invasion Frequency**

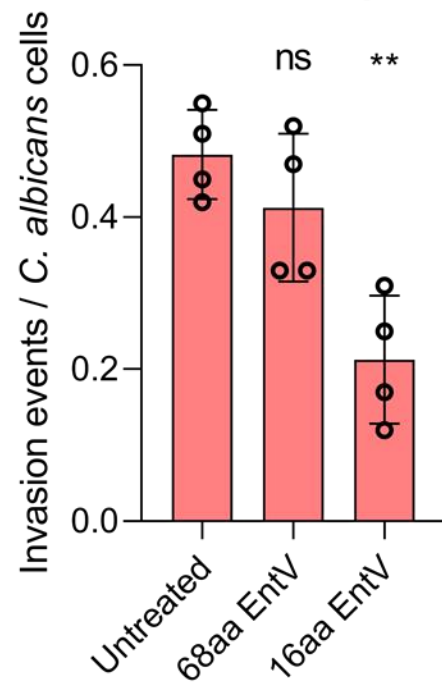


**Figure 5.1: The C-terminal helix of EntV inhibits hyphal formation and epithelial invasion in an *ex vivo* co-culture assay.** The 68aa EntV and C-terminus derived 16aa EntV peptides were tested in an epithelial co-culture model for inhibition of invasion and virulence. In this model, co-cultures of *ACT1p-mCherry* and a confluent layer of pharyngeal epithelial cells (FaDu cells) were fixed and stained with NucBlue and an anti-*Candida*-FITC antibody. Hyphae that invaded into the FaDu cell layer were unstained by the antibody (red fluorescent signal) while yeast and hyphae resting on the cell surface were exposed to the antibody (green fluorescent signal). A and B) In untreated co-cultures, *C. albicans* readily formed hyphae and invaded the FaDu cell layer. C and D) Co-cultures treated with 300 nM 68aa EntV had fewer hyphal cells than untreated co-cultures. E and F) Treatment with 300 nM 16aa EntV reduced both hyphal development and invasion into the epithelial layer. G) *C. albicans* cells were counted manually, and the number of hyphal cells was divided by the number of total cells. H) The number of hyphal invasion events was divided by the number of total *C. albicans* cells. Numerical results represent data collected from two separate biological replicates, each with two technical replicates. Statistics were determined using a one-way ANOVA with a Tukey's test with a single pooled variance to compare the mean values of each group. N=3, \* P < 0.05, \*\* P < 0.01, \*\*\* P < 0.001, \*\*\*\* P < 0.0001.

---



## Discussion

The results in this chapter remain preliminary due to technical difficulties. Therefore, these results are best interpreted as potential trends. From the data presented in this chapter, 68aa EntV has the potential to inhibit *C. albicans* hyphal formation in the FaDu co-culture model. The 16aa EntV peptide also has the potential to inhibit hyphal formation and additionally reduce *C. albicans* invasion into the epithelial cell layer. Further work is necessary to improve the technical aspects of this assay, and future studies should include analyses of other peptides previously discussed in this work (Chapter 3), particularly the small 12aa – 9aa EntV peptides.

The technical difficulties in replicating this data produced both over- and under-stimulation of hyphal development in the assay. This creates confounding factors if hyphae never form in the co-culture or form too rapidly such that the *C. albicans* cells germinate before coming in contact with the FaDu cell layer. Despite these issues, the data and model presented here remain important for this work because the interaction of *C. albicans* cells with a confluent epithelial cell layer substrate most closely simulates the conditions that exist in the human or murine host with oropharyngeal candidiasis. To further improve the assay and potentially increase reproducibility, the co-culture media could include mucin and co-culture could be performed under continuous flow conditions to simulate the dynamic oral environment. This would better elucidate differences between adhered and unadhered *C. albicans* cells than is possible under static co-culture conditions.

## Chapter 6: Discussion



## Efficacy of C-terminal derived peptides

The central hypothesis of this work was that small peptides derived from the C-terminal central helix of EntV would have equal to improved efficacy in inhibiting *C. albicans* *in vitro* biofilm formation and *ex vivo* virulence. In Chapter 3, these peptides were tested for efficacy in inhibiting adhesion to an abiotic substrate, the first step in *in vitro* biofilm formation. C-terminal derived 16aa and 12aa EntV peptides were found to have increased potency in inhibiting adhesion compared to the 68aa EntV peptide (Figure 3.7E).

In Chapter 4, the biomass and architecture of mature biofilms treated with the peptides were analyzed. Biofilms treated with the C-terminal derived 16aa and 12aa EntV peptides showed characteristic structural alterations consistent with biofilms treated with the 68aa EntV peptide (Figures 4.2, 4.3, and 4.8). These structural alterations included a general flattening effect and disorganization of the upper layers of the biofilm. Additionally, the mature biofilms grown in media containing either the 68aa EntV or 16aa EntV peptides had similarly reduced biomasses (Figure 4.4). The 12aa EntV peptide outperformed either of these other two in reducing mature biofilm biomass (Figure 4.7A). Lastly, the preliminary results presented in Chapter 5 indicate that the 68aa EntV and 16aa EntV peptides have the potential to inhibit *C. albicans* hyphal formation in an *ex vivo* epithelial cell invasion model. Furthermore, the 16aa EntV peptide was found to have the potential to inhibit invasion into the epithelial cell layer in this model (Figure 5.1).

Taken together, the results from the three previous chapters strongly indicate that the C-terminal helix of EntV is a potent inhibitor of *C. albicans* biofilm formation and

virulence with overall superior efficacy in these assays compared to the 68aa EntV peptide. The peptide of optimal efficacy and minimal size in these assays was determined to be the 12aa EntV peptide. Determining an optimal peptide of minimum size is important for development for potential future applications. The 68aa EntV peptide is too large to become a viable pharmaceutical product, but the size of the 12aa EntV peptide is more in accordance with other antimicrobial peptides currently in clinical use or under investigation (101). An additional advantage of identifying the minimal size effective peptide is that because the 12aa EntV peptide omits the amino acid residues that are predicted to form the N-terminal tail of the 16aa EntV peptide, the 12aa EntV peptide is predicted to have a more stable helical structure (Figure 3.6).

### **Translating to *in vivo* work**

Prior to the results presented in this work, *in vivo* *C. elegans* infection assays were performed with the small 12aa – 9aa EntV peptides. These assays (unpublished) found that the 12aa EntV peptide inhibited *C. albicans* virulence with the same potency as the 16aa and 68aa EntV peptides. The 11aa and 10aa EntV peptides showed less efficacy, and the 9aa EntV peptide was ineffective in inhibiting virulence (M. Cruz and D. Garsin, personal communication). The general trend of these results concurs with the results presented in this work summarized in Figures 3.7E and 4.7E.

These data informed further *in vivo* experiments in a murine oropharyngeal candidiasis (OPC) model. In this infection model, mice are given a sublingual inoculation of *C. albicans* and allowed to drink freely from a 100 nM peptide solution in water. The mice are later euthanized, and the tongues are excised and analyzed for fungal burden and histology. In this model the 12aa EntV peptide virtually eliminated

fungal burden and performed as well as the 68aa EntV and 16aa EntV peptides. Additionally, in agreement with my *in vitro* experiments and the previous *in vivo* *C. elegans* infection assays, the 11aa and 10aa EntV peptides were less effective at inhibiting virulence in the murine OPC model, and the 9aa EntV peptide was ineffective at inhibiting virulence (G. Buda de Cesare, M. Cruz, and S. Guha, personal communication).

### **An examination of important residues**

Prior to the start of this work, *C. elegans* infection assays performed in the Garsin lab showed that the cysteine residue at position 15 of the 16aa EntV peptide is necessary for activity (M. Cruz and D. Garsin, personal communication). I hypothesized that the only other two polar amino acid residues in the 16aa EntV peptide, the glutamine residues at positions 7 and 14, were necessary for activity. Contrary to my hypothesis, the results summarized in Figure 3.5E indicate that these glutamine residues are not strictly necessary for activity. The Q – I peptide replaced these with isoleucine residues, and the activity was mostly unchanged. Only when the glutamine residues were altered to oppositely charged glutamate residues (Q – E peptide) was activity lost. This finding is consistent with results from the testing these peptides in the *C. elegans* infection model (M. Cruz and D. Garsin, personal communication).

The residues of the EntV peptide essential for activity remain unknown. To address this question in a follow up study, an alanine scan will be performed on the 12aa EntV peptide. An alanine scan is a well-established technique to identify important residues whereby each amino acid of a peptide is mutated to an alanine and

the peptide is tested for a change in activity. Alanine is used as the replacement because it has a small, nonpolar sidechain and typically does not alter secondary structure (206–208). Activity will be measured by multiple methods including the *C. elegans* infection assay and the *in vitro* biofilm assays described in this work.

### **Determination of mechanism of action**

An understanding of the important residues of the EntV peptide may provide some insight into the identity of the fungal binding partner EntV interacts with. However, determining the mechanism of action will likely require the use of multiple techniques including the identification of resistant mutants and determining the localization of EntV in interaction with *C. albicans*.

A previous graduate student in our lab, Carrie Graham, Ph.D., tested a library of *C. albicans* homozygous mutants for biofilm formation when treated with supernatant collected from overnight cultures of *E. faecalis*. 24 transcription factor mutants and 15 cell wall protein mutants were identified that showed resistance to the supernatant treatment (209). *E. faecalis* supernatant, while a potent inhibitor of *C. albicans* biofilm formation, contains numerous factors that could interact with *C. albicans*, many of which are unknown. To refine this assay, it should be repeated with the 12aa EntV peptide. Additionally, many more mutants can be tested with the high-throughput biofilm assay I developed. Once resistant mutants are identified, precise protein-protein interaction experiments can be performed to determine the exact binding partner and kinetics of the interaction (210).

Localization experiments of the 68aa EntV peptide interacting with *C. albicans* have previously been performed using a variant of the 68aa EntV peptide with a C-

terminal FITC tag. Currently unpublished results have shown localization of EntV to the cell surface of *C. albicans* (Y. Chebaro and M. Lorenz, personal communication). I performed this same experiment using live *C. albicans* cells incubated at 37°C in various media. I replicated these results with the additional finding that the 68aa EntV-FITC peptide preferentially localizes to hyphae and appears to exhibit some cooperativity when binding (results unpublished). These results have been replicated by other members of the lab using fixed *C. albicans* cells (G. Buda de Cesare and M. Lorenz, personal communication). The findings suggest that EntV interacts with a factor on the surface of *C. albicans* cells that is either more abundant or more exposed on the surface of hyphae than of yeast.

Further localization experiments could examine aberrant localization of the 68aa EntV-FITC peptide with mutants identified by an *in vitro* biofilm screen performed with the 12aa EntV peptide. Additionally, larger biofilm structures could be analyzed for EntV localization using the microscopy techniques I employed to examine biofilms in Chapter 4. Addition of the 68aa EntV peptide to biofilms already grown for 24 hours has previously been shown to reduce final biofilm biomass after 48 total hours of incubation (15). Determining EntV localization in these biofilms would investigate the permeability of *C. albicans* biofilms to EntV and the distribution of the EntV peptide across the heterogeneous biofilm structure.

### **Future Development**

The broad goal of the EntV project is to determine if EntV can be turned into something suitable for pharmaceutical use to treat or prevent *C. albicans* infections. Future research into the pharmaceutical potential of EntV will involve chemically

modifying the 12aa EntV peptide to balance three important factors: potency, stability, and toxicity.

EntV has proven to be highly potent in our *in vivo* experiments thus far. Sub-nanomolar concentrations of the 68aa EntV peptide have been protective in the *C. elegans* infection assay (15). However, this may not necessarily translate to potency in humans, so improving the activity of the peptide should be a priority. Current work in our lab is underway to produce a library of amino acid variants on the pattern of the 11aa and 10aa EntV peptides. These peptides have shown suboptimal efficacy in the *in vitro* biofilm assays in this work (Figures 3.7 and 4.7), the *in vivo C. elegans* infection assay (unpublished data), and the murine oropharyngeal candidiasis model (unpublished data). If the activity of these peptides can be improved by modifying the peptide, then translating these modifications to the 12aa EntV peptide may further improve potency.

Solid Phase Peptide Synthesis is being used to create a library of variant peptides. An advantage of this technique is that because the peptides are attached to a solid substrate, it is easy to collect, separate, and mix batches of peptides. After each amino acid addition step, the substrate beads can be collected, separated out, and mixed with beads from different groups for the next amino acid addition. This technique allows for the feasible production of several hundred variant peptides and the inclusion of unnatural amino acids (211, 212). These peptide variants will be tested in the high throughput *in vitro* biofilm assay developed for this work (Chapter 4) and a high throughput *C. elegans* infection assay (213).

Research will need to be conducted into the pharmacokinetics of the 12aa EntV peptide. Peptide drugs, especially those administered into the bloodstream, typically have short half-lives in the body due to the action of proteases and peptidases (214). Exopeptidases, enzymes that cleave the terminal peptide bond, are likely a significant threat to the 12aa EntV peptide's stability in the body because the cysteine at the C-terminus of this peptide is essential and the N-terminus cannot be reduced without a decrease in activity. One way to mitigate this effect is to modify the N- and C- termini (215). Another method to increase stability is to synthesize the peptide using D-amino acids, the stereoisomers of the naturally occurring amino acids (216, 217). Lastly, for administration into the bloodstream, it may be possible to fuse the 12aa EntV peptide to a host protein such as albumin (218).

A correct balance between potency and stability will have to be determined while developing this potential drug. Alterations to the amino acid sequence of the 12aa EntV peptide could increase potency but may introduce some instability into the remarkably stable helix. Modifications to the N- and C-termini or fusion to albumin could significantly increase the half-life of the peptide in the body but may decrease the peptide's affinity for the binding site and thus its potency. The third factor to balance is toxicity. Inclusion of unnatural amino acids, such as the D-amino acids, could make the peptide toxic, and there are concerns about these unnatural amino acids accumulating in the liver and other organs (219, 220).

### **Future applications**

As a non-fungicidal attenuator of virulence, EntV is likely suitable as an additive to existing antifungal therapy or as a preventative against infection. The potent activity

of EntV in inhibiting adhesion and biofilm formation as demonstrated in this work indicate this peptide may have potential in treating mucosal oropharyngeal and esophageal infections, preventing biofilm formation on central venous catheters, and treating disseminated infections.

#### Oropharyngeal / esophageal candidiasis

Oropharyngeal and esophageal candidiasis are mucocutaneous infections with generally good prognoses. Mild oropharyngeal infections are typically treated with topical clotrimazole in the form of a troche (throat lozenge). Moderate-to-severe cases of oropharyngeal infection and esophageal infections are typically treated with oral fluconazole (89). The addition of EntV to treatment of moderate-to-severe oropharyngeal and esophageal candidiasis could clear the infection more quickly. This could potentially be administered as a troche, mouthwash, or ingestible solution. To test the potential for synergy between these treatments, the murine oropharyngeal candidiasis model established in our lab could be modified. Treatment could be withheld for 1 – 2 days to allow the infection to establish itself. Then we could treat the infection with various combinations of EntV and fluconazole, clotrimazole, or nystatin.

#### Catheter-related blood-stream infections

For critically ill nonneutropenic immunocompetent patients, the use of central venous catheters is common and is the greatest risk factor for developing candidemia (11–13). Biofilm production by *C. albicans* and *C. parapsilosis* in these catheters correlates with a significant increase in mortality (49). To prevent the development of microbial colonization and biofilm formation, some central venous catheters are now



coated with antimicrobial agents. Unfortunately, fungal pathogens are often overlooked in studies of the effectiveness of different coatings (221).

Of the different coatings currently available, there is not one that is perfect for every application. Chlorhexidine/silver sulfadiazine coated catheters have been studied for several years with conflicting results regarding their efficacy (221, 222), but a recent meta-analysis found overall positive results indicating they decrease colonization and blood-stream infections, including against *C. albicans*. The disadvantage of these catheters is that they have a short shelf life (223). Other coatings include silver ions, benzalkonium chloride, and minocycline/rifampicin, which is potent against bacterial species but inadvertently increases the risk of fungal colonization (223).

EntV could be a potential catheter coating agent that may work in concert with some of these other catheter coatings. Our lab has established a collaboration with a leader in the field of catheter associated *C. albicans* biofilm formation, David Andes, M.D. Unpublished work examining the effectiveness of the 68aa EntV peptide in inhibiting biofilm formation when added to the lumen of venous catheters in rats has shown promising results. Future work with this model should include studies with the 12aa EntV peptide and coated catheters currently available on the market. The ultimate goal of this work would be to create a shelf stable catheter that inhibits colonization and biofilm formation from the broadest possible range of microbial species.

## Disseminated infections

There is critical need to develop new treatments for disseminated and invasive candidiasis. There is a paucity of drugs approved to treat these infections. Of the drugs that have been approved, there are only three chemical classes (89), and one these, the polyenes, carry the risk of severe adverse effects (82, 83, 87).

EntV, as an inhibitor of virulence, could be used in combination with currently approved drugs to increase the efficacy of the treatment. This type of drug strategy has become more prominent in recent years as the threat of antimicrobial resistance in many different pathogenic species becomes more urgent (224–228). To investigate this potential, our lab conducted an experiment with a murine disseminated candidiasis model. For this experiment, *C. albicans* cells were grown to log phase, soaked in PBS for one hour with either the 12aa EntV peptide or a DMSO vector control, and administered to mice via a tail vein injection. The results of this experiment remain preliminary, but the 12aa EntV peptide had a potent effect in reducing mortality in the treated mice compared to the untreated control group (P. Miramon Martinez and M. Lorenz, personal communication). Future research on this topic should include *in vitro* and *in vivo* examinations of synergy between EntV and the approved antifungal drugs.

## **Evolution of EntV**

The specificity of the 16aa C-terminal derived EntV peptide was tested in the *in vitro* adhesion and biomass assays in Figures 3.3 and 4.5. These experiments confirmed that the effect of the 16aa EntV peptide is specific to its helical shape and amino acid sequence. Additionally, two bacteriocins produced by *Streptococcus pyogenes* and *Corynebacterium jeikeium* that share similarities in size and structural

motifs with EntV (174) were tested for efficacy in the *in vitro* adhesion and biomass assays (Figures 3.4 and 4.6). These peptides were ineffective in inhibiting *C. albicans* biofilm formation in these assays, indicating that attenuation of *C. albicans* virulence is specific to EntV. Taken together, these results suggest that the *C. albicans* virulence attenuation activity of EntV may provide some evolutionary advantage to *E. faecalis*.

One potential explanation for this is that *E. faecalis* is well adapted to live as a commensal in the host environment. In addition to humans and other mammals, *E. faecalis* colonizes distantly related animals such as insects and birds (229, 230). This would suggest that *E. faecalis* was an early member of host microbiota and has had adequate time to evolve specific adaptations to its environment (231). One such adaptation could be to promote healthy commensal growth by inhibiting an immunostimulatory effect from other gut commensals, such as *C. albicans*. Producing a secreted factor, such as EntV, that inhibits *C. albicans* adhesion and hyphal formation could reduce host inflammation by reducing fungal interaction with and recognition by host cell pattern-recognition receptors (PRRs) (232). Therefore, the evolutionary advantage of producing EntV for *E. faecalis* is protection from the host immune system.

*C. albicans* has many complex interactions with other microbial species including *E. faecalis*, *P. aeruginosa*, and *Streptococci* (6, 7). The impetus for this project was the observation that *E. faecalis* has the ability to influence *C. albicans* virulence (173). However, *C. albicans* also influences the virulence of these bacterial species (155, 173). Further investigation into these interactions and other polymicrobial communities may provide useful insights into the natural world and lead to the development of new drugs and technologies.

## Appendix

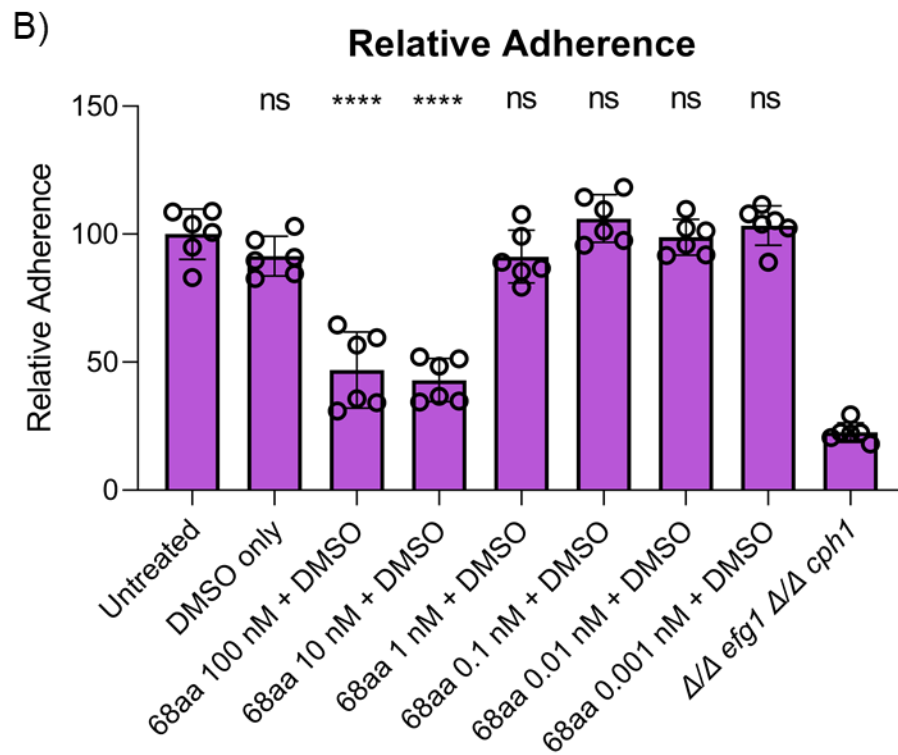
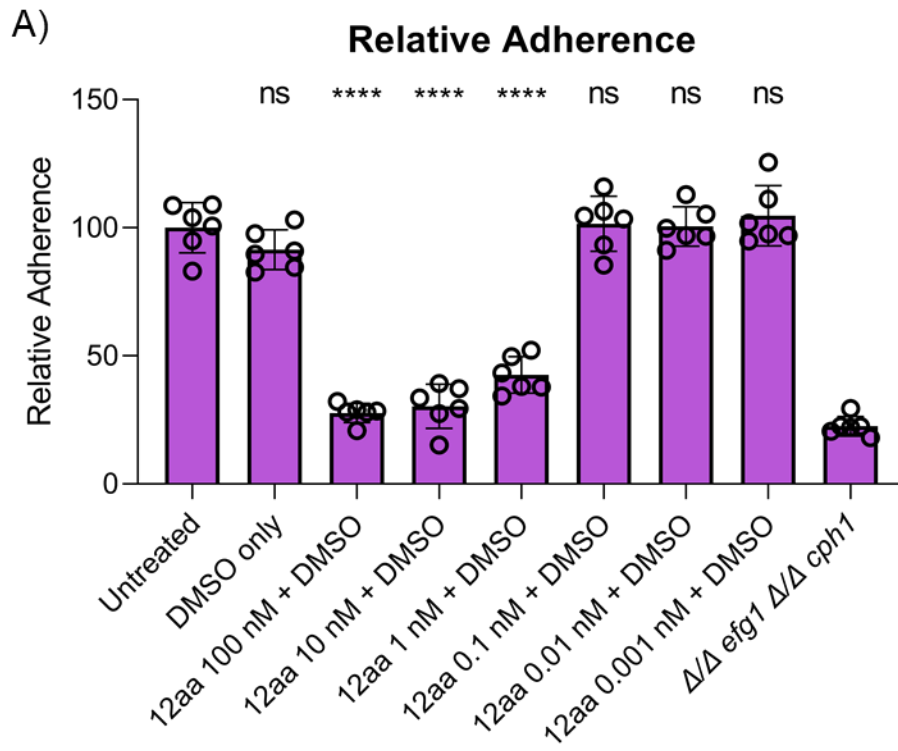


**Figure A.1: DMSO does not inhibit adhesion at relevant concentrations.** To rigorously ensure the DMSO vector could not be causing the inhibition effect, I tested the 12aa EntV and 68aa EntV with extra DMSO at each concentration. In addition to a DMSO control, I added 0.5  $\mu$ l of DMSO to each peptide solution of both the PBS pre-soak and the YNB-AS media. This amount of DMSO is greater than what is normally in the media but still is only at a concentration of 0.03% (v/v). The DMSO only control had no significant inhibitory effect on adhesion, and all other peptide concentrations match the results from Chapter 3 (Figures 3.2 and 3.7). Therefore, the DMSO vector does not have an effect on adhesion.

---

## Bibliography

1. Akpan A, Morgan R. 2002. Oral candidiasis. *Postgraduate Medical Journal* 78:455–459.
2. Peters BM, Yano J, Noverr MC, Fidel PL. 2014. Candida Vaginitis: When Opportunism Knocks, the Host Responds. *PLoS Pathogens* 10.
3. Soll DR, Galask R, Schmid J, Hanna C, Mac K, Morrow B. 1991. Genetic Dissimilarity of Commensal Strains of *Candida* spp. Carried in Different Anatomical Locations of the Same Healthy Women. *Journal of Clinical Microbiology* 29:1702–1710.
4. Perlroth J, Choi B, Spellberg B. 2007. Nosocomial fungal infections: Epidemiology, diagnosis, and treatment. *Medical Mycology* 45:321–346.
5. Liu Y, Filler SG. 2011. *Candida albicans* Als3, a multifunctional adhesin and invasin. *Eukaryotic Cell* 10:168–173.
6. Peleg AY, Hogan DA, Mylonakis E. 2010. Medically important bacterial–fungal interactions. *Nature Reviews Microbiology* 8.
7. Harriott MM, Noverr MC. 2011. Importance of *Candida*–bacterial polymicrobial biofilms in disease. *Trends in Microbiology* 19.
8. Lionakis MS. 2014. New insights into innate immune control of systemic candidiasis. *Medical Mycology* 52:555–564.
9. Jacobsen ID, Wilson D, Wächtler B, Brunke S, Naglik JR, Hube B. 2012. *Candida albicans* dimorphism as a therapeutic target. *Expert Review of Anti-Infective Therapy* 10:85–93.

10. Sardi JCO, Scorzoni L, Bernardi T, Fusco-Almeida AM, Mendes Giannini MJS. 2013. *Candida* species: Current epidemiology, pathogenicity, biofilm formation, natural antifungal products and new therapeutic options. *Journal of Medical Microbiology* 62:10–24.
11. Kojic EM, Darouiche RO. 2004. *Candida* Infections of Medical Devices. *Clinical Microbiology Reviews* 17:255–267.
12. Pfaller MA, Diekema DJ. 2007. Epidemiology of invasive candidiasis: A persistent public health problem. *Clinical Microbiology Reviews* 20:133–163.
13. Cauda R. 2009. *Candidaemia* in Patients with an Inserted Medical Device. *Drugs* 69:33–38.
14. Pierce CG, Chaturvedi AK, Lazzell AL, Powell AT, Saville SP, Mchardy SF, Lopez-Ribot JL. 2015. A novel small molecule inhibitor of *Candida albicans* biofilm formation, filamentation and virulence with low potential for the development of resistance. *npj Biofilms and Microbiomes* 1.
15. Graham CE, Cruz MR, Garsin DA, Lorenz MC. 2017. Enterococcus faecalis bacteriocin EntV inhibits hyphal morphogenesis, biofilm formation, and virulence of *Candida albicans*. *Proceedings of the National Academy of Sciences of the United States of America* 114:4507–4512.
16. Janniger CK, Schwartz RA, Szepietowski JC, Reich A. 2005. Intertrigo and common secondary skin infections. *American Family Physician* 72:833–838.
17. Klotz SA, Penn CC, Negvesky GJ, Butrus SI. 2000. Fungal and Parasitic Infections of the Eye. *Clinical Microbiology Reviews* 13.



18. Kirkpatrick CH. 2001. Chronic mucocutaneous candidiasis. *The Pediatric Infectious Disease Journal* 20.
19. Endrigo Tinoco-Araujo J, Ferreira D, Araújo G, Gomes Barbosa P, Sérgio P, Santos S, Myriam Costa De Medeiros A. 2013. Invasive candidiasis and oral manifestations in premature newborns Candidíase invasiva e alterações bucais em recém-nascidos prematuros. *einstein* 11:71–75.
20. Millsop JW, Fazel N. 2016. Oral candidiasis. *Clinics in Dermatology* 34:487–494.
21. Nielsen H, Bentsen KD, Hojtvéd L, Willemoes EH, Scheutz F, Schiodt M, Stoltze K, Pindborg JJ. 1994. Oral candidiasis and immune status of HIV-infected patients. *Journal of Oral Pathology and Medicine* 23.
22. Sobel JD. 1997. Vaginitis. *New England Journal of Medicine* 337:1896–1903.
23. Maccato M, Kaufman RH. 1991. Fungal vulvovaginitis. *Curr Opin Obstet Gynecol* 3:849–852.
24. Hurley R, de Louvois MDJ. 1979. Candida vaginitis. *Postgraduate Medical Journal* 55:645–647.
25. Zaoutis TE, Argon J, Chu J, Berlin JA, Walsh TJ, Feudtner C. 2005. The Epidemiology and Attributable Outcomes of Candidemia in Adults and Children Hospitalized in the United States: A Propensity Analysis. *Clinical Infectious Diseases* 41:1232–1239.
26. Wisplinghoff H, Ebbers J, Geurtz L, Stefanik D, Major Y, Edmond MB, Wenzel RP, Seifert H. 2014. Nosocomial bloodstream infections due to *Candida* spp. in the USA: Species distribution, clinical features and antifungal susceptibilities. *International Journal of Antimicrobial Agents* 43:78–81.

27. Preisler HD, Hasenclever HF, Levitan AA, Henderson ES. 1969. Serologic Diagnosis of Disseminated Candidiasis in Patients with Acute Leukemia. *Annals of Internal Medicine* 70:19–30.
28. Bodey GP, Nies BA, Freireich EJ. 1965. Multiple Organism Septicemia in Acute Leukemia Analysis of 54 Episodes. *Arch Intern Med* 116:266–72.
29. Koh AY, Köhler JR, Coggshall KT, van Rooijen N, Pier GB. 2008. Mucosal damage and neutropenia are required for *Candida albicans* dissemination. *PLoS Pathogens* 4.
30. Abe F, Tateyama M, Shibuya H, Azumi N, Ommura Y. 1984. Disseminated fungal infection. A Review of 20 Autopsy Cases. *Acta Pathologica Japonica* 34:1201–1208.
31. Giuliano S, Guastalegname M, Russo A, Falcone M, Ravasio V, Rizzi M, Bassetti M, Viale P, Pasticci MB, Durante-Mangoni E, Venditti M. 2017. *Candida* endocarditis: systematic literature review from 1997 to 2014 and analysis of 29 cases from the Italian Study of Endocarditis. *Expert Review of Anti-Infective Therapy* 15:807–818.
32. Liu Y, Mittal R, Solis N v., Prasadaraao N v., Filler SG. 2011. Mechanisms of *candida albicans* trafficking to the brain. *PLoS Pathogens* 7:e1002305-.
33. Spellberg B, Ibrahim AS, Edwards Jr JE, Filler SG. 2005. Mice with Disseminated Candidiasis Die of Progressive Sepsis. *Journal of Infectious Diseases* 192:336–343.

34. Das I, Nightingale P, Patel M, Jumaa P. 2011. Epidemiology, clinical characteristics, and outcome of candidemia: Experience in a tertiary referral center in the UK. *International Journal of Infectious Diseases* 15:e759–e763.
35. Saville SP, Lazzell AL, Monteagudo C, Lopez-Ribot JL. 2003. Engineered control of cell morphology in vivo reveals distinct roles for yeast and filamentous forms of *Candida albicans* during infection. *Eukaryotic Cell* 2:1053–1060.
36. Lo HJ, Köhler JR, DiDomenico B, Loebenberg D, Cacciapuoti A, Fink GR. 1997. Nonfilamentous *C. albicans* Mutants Are Avirulent. *Cell* 90:939–949.
37. Murad AM, Leng P, Straffon M, Wishart J, Macaskill S, MacCallum D, Schnell N, Talibi D, Marechal D, Tekaiia F, d'Enfert C, Gaillardin C, Odds FC, Brown AJP. 2001. NRG1 represses yeast-hypha morphogenesis and hypha-specific gene expression in *Candida albicans*. *EMBO Journal* 20:4742–4752.
38. Garcia-Tamayo J, Castillo G, Martinez AJ. 1982. Human genital candidiasis: histochemistry, scanning and transmission electron microscopy. *Acta Cytologica* 26:7–14.
39. Lossinsky AS, Jong A, Fiala M, Mukhtar M, Buttle KF, Ingram M. 2006. The histopathology of *Candida albicans* invasion in neonatal rat tissues and in the human blood-brain barrier in culture revealed by light, scanning transmission and immunoelectron microscopy. *Histology and Histopathology* 21:1029–1041.
40. Bernhardt J, Herman D, Sheridan M, Calderone R. 2001. Adherence and Invasion Studies of *Candida albicans* Strains, Using In Vitro Models of Esophageal Candidiasis. *Journal of Infectious Diseases* 184:1170–1175.

41. Allert S, Förster TM, Svensson C-M, Richardson JP, Pawlik T, Hebecker B, Rudolphi S, Juraschitz M, Schaller M, Blagojevic M, Morschhäuser J, Thilo Figge M, Jacobsen ID, Naglik JR, Kasper L, Mogavero S, Hube B. 2018. *Candida albicans*-Induced Epithelial Damage Mediates Translocation through Intestinal Barriers Downloaded from. *mBio* 9:e00915-18.
42. Lorenz MC, Bender JA, Fink GR. 2004. Transcriptional response of *Candida albicans* upon internalization by macrophages. *Eukaryotic Cell* 3:1076–1087.
43. Rubin-Bejerano I, Fraser I, Grisafi P, Fink GR. 2003. Phagocytosis by neutrophils induces an amino acid deprivation response in *Saccharomyces cerevisiae* and *Candida albicans*. *Proceedings of the National Academy of Sciences of the United States of America* 100:11007–11012.
44. Feng Q, Summers E, Guo B, Fink G. 1999. Ras Signaling Is Required for Serum-Induced Hyphal Differentiation in *Candida albicans*. *Journal of Bacteriology* 181:6339–6346.
45. White SJ, Rosenbach A, Lephart P, Nguyen D, Benjamin A, Tzipori S, Whiteway M, Meccas J, Kumamoto CA. 2007. Self-regulation of *Candida albicans* population size during GI colonization. *PLoS Pathogens* 3:1866–1878.
46. Lachke SA, Lockhart SR, Daniels KJ, Soll DR. 2003. Skin facilitates *Candida albicans* mating. *Infection and Immunity* 71:4970–4976.
47. Yano J, Yu A, Jr PLF, Noverr MC. 2016. Transcription Factors Efg1 and Bcr1 Regulate Biofilm Formation and Virulence during *Candida albicans*-Associated Denture Stomatitis. *PLoS ONE* 11.

48. Cornely OA, Bassetti M, Calandra T, Garbino J, Kullberg BJ, Lortholary O, Meersseman W, Akova M, Arendrup MC, Arian-Akdogan S, Bille J, Castagnola E, Cuenca-Estrella M, Donnelly JP, Groll AH, Herbrecht R, Hope WW, Jensen HE, Lass-Flörl C, Petrikos G, Richardson MD, Roilides E, Verweij PE, Viscoli C, Ullmann AJ. 2012. ESCMID guideline for the diagnosis and management of Candida diseases 2012: Non-neutropenic adult patients. *Clinical Microbiology and Infection* 18:19–37.
49. Tumbarello M, Posteraro B, Trecarichi EM, Fiori B, Rossi M, Porta R, Donati KDG, la Sorda M, Spanu T, Fadda G, Cauda R, Sanguinetti M. 2007. Biofilm production by *Candida* species and inadequate antifungal therapy as predictors of mortality for patients with candidemia. *Journal of Clinical Microbiology* 45:1843–1850.
50. Chandra J, Kuhn DM, Mukherjee PK, Hoyer LL, McCormick T, Ghannoum MA. 2001. Biofilm formation by the fungal pathogen *Candida albicans*: Development, architecture, and drug resistance. *Journal of Bacteriology* 183:5385–5394.
51. Fox EP, Nobile CJ. 2012. A sticky situation: Untangling the transcriptional network controlling biofilm development in *Candida albicans*. *Transcription* 3:315–322.
52. Ramage G, Mowat E, Jones B, Williams C, Lopez-Ribot J. 2009. Our Current Understanding of Fungal Biofilms. *Critical Reviews in Microbiology* 35:340–355.
53. Ramage G, Saville SP, Thomas DP, López-Ribot JL. 2005. *Candida* Biofilms: an Update. *Eukaryotic Cell* 4:633–638.

54. Nobile CJ, Johnson AD. 2015. *Candida albicans* Biofilms and Human Disease. *Annual Review of Microbiology* 69:71–92.
55. Finkel JS, Mitchell AP. 2011. Genetic control of *Candida albicans* biofilm development. *Nature Reviews Microbiology* 9:109–118.
56. Li F, Palecek SP. 2008. Distinct domains of the *Candida albicans* adhesin EAP1 p mediate cell-cell and cell-substrate interactions. *Microbiology* 154:1193–1203.
57. Nobile CJ, Schneider HA, Nett JE, Sheppard DC, Filler SG, Andes DR, Mitchell AP. 2008. Complementary adhesin function in *C. albicans* biofilm formation. *Current Biology* 18:1017–1024.
58. Sundstrom P, Balish E, Allen CM. 2002. Essential Role of the *Candida albicans* Transglutaminase Substrate, Hyphal Wall Protein 1, in Lethal Oroesophageal Candidiasis in Immunodeficient Mice. *The Journal of Infectious Diseases* 185.
59. Kempf M, Cottin J, Licznar P, Lefrançois C, Robert R, Apaire-Marchais V. 2009. Disruption of the GPI protein-encoding gene IFF4 of *Candida albicans* results in decreased adherence and virulence. *Mycopathologia* 168:73–77.
60. McCall AD, Pathirana RU, Prabhakar A, Cullen PJ, Edgerton M. 2019. *Candida albicans* biofilm development is governed by cooperative attachment and adhesion maintenance proteins. *npj Biofilms and Microbiomes* 5.
61. Bailey DA, Feldmann PJ, Bovey M, Gow NA, Brown AJ. 1996. The *Candida albicans* HYR1 gene, which is activated in response to hyphal development, belongs to a gene family encoding yeast cell wall proteins. *Journal of Bacteriology* 178.

62. Nobile CJ, Nett JE, Andes DR, Mitchell AP. 2006. Function of *Candida albicans* Adhesin Hwp1 in Biofilm Formation. *Eukaryotic Cell* 5:1604–1610.
63. Qin Y, Zhang L, Xu Z, Zhang J, Jiang YY, Cao Y, Yan T. 2016. Innate immune cell response upon *Candida albicans* infection. *Virulence* 7:512–526.
64. Biswas S, van Dijck P, Datta A. 2007. Environmental Sensing and Signal Transduction Pathways Regulating Morphopathogenic Determinants of *Candida albicans*. *Microbiology and Molecular Biology Reviews* 71:348–376.
65. Brown AJP, Gow NAR. 1999. Regulatory networks controlling *Candida albicans* morphogenesis. *Trends in Microbiology* 7:333–338.
66. Kumamoto CA. 2005. A contact-activated kinase signals *Candida albicans* invasive growth and biofilm development. *Proceedings of the National Academy of Sciences of the United States of America* 102:5576–5581.
67. Diez-Orejas R, Molero G, Navarro-Garcia F, Pla J, Nombela C, Sanchez-Perez M. 1997. Reduced Virulence of *Candida albicans* MKC1 Mutants: a Role for Mitogen-Activated Protein Kinase in Pathogenesis. *Infection and Immunity* 65:833–837.
68. Berman J, Sudbery PE. 2002. *Candida albicans*: A molecular revolution built on lessons from budding yeast. *Nature Reviews Genetics* 3:918–930.
69. Yi S, Sahni N, Daniels KJ, Lu KL, Srikantha T, Huang G, Garnaas AM, Soll DR. 2011. Alternative mating type configurations ( $a/\alpha$  versus  $a/a$  or  $\alpha/\alpha$ ) of *Candida albicans* result in alternative biofilms regulated by different pathways. *PLoS Biology* 9.

70. Hall RA, de Sordi L, MacCallum DM, Topal H, Eaton R, Bloor JW, Robinson GK, Levin LR, Buck J, Wang Y, Gow NAR, Steegborn C, Mühlischlegel FA. 2010. CO<sub>2</sub> acts as a signalling molecule in populations of the fungal pathogen *Candida albicans*. *PLoS Pathogens* 6.
71. Bockmühl DP, Ernst JF. 2001. A Potential Phosphorylation Site for an A-Type Kinase in the Efg1 Regulator Protein Contributes to Hyphal Morphogenesis of *Candida albicans*. *Genetics* 157:1523–1530.
72. Fox EP, Bui CK, Nett JE, Hartooni N, Mui MC, Andes DR, Nobile CJ, Johnson AD. 2015. An expanded regulatory network temporally controls *Candida albicans* biofilm formation. *Molecular Microbiology* 96:1226–1239.
73. Noffz CS, Liedschulte V, Lengeler K, Ernst JF. 2008. Functional mapping of the *Candida albicans* Efg1 regulator. *Eukaryotic Cell* 7:881–893.
74. Banerjee M, Thompson DS, Lazzell A, Carlisle PL, Pierce C, Monteagudo C, López-Ribot JL, Kadosh D. 2008. UME6, a novel filament-specific regulator of *Candida albicans* hyphal extension and virulence. *Molecular Biology of the Cell* 19:1354–1365.
75. Zeidler U, Lettner T, Lassnig C, Müller M, Lajko R, Hintner H, Breitenbach M, Bito A. 2009. UME6 is a crucial downstream target of other transcriptional regulators of true hyphal development in *Candida albicans*. *FEMS Yeast Research* 9:126–142.
76. Banerjee M, Uppuluri P, Zhao XR, Carlisle PL, Vipulanandan G, Villar CC, López-Ribot JL, Kadosh D. 2013. Expression of UME6, a key regulator of



- Candida albicans* hyphal development, enhances biofilm formation via Hgc1- and Sun41- dependent mechanisms. *Eukaryotic Cell* 12:224–232.
77. Kadosh D, Johnson AD. 2005. Induction of the *Candida albicans* filamentous growth program by relief of transcriptional repression: A genome-wide analysis. *Molecular Biology of the Cell* 16:2903–2912.
  78. Nett J, Lincoln L, Marchillo K, Massey R, Holoyda K, Hoff B, VanHandel M, Andes D. 2007. Putative role of  $\beta$ -1,3 glucans in *Candida albicans* biofilm resistance. *Antimicrobial Agents and Chemotherapy* 51:510–520.
  79. Nett JE, Sanchez H, Cain MT, Andes DR. 2010. Genetic basis of *Candida* Biofilm resistance due to drug-sequestering matrix glucan. *Journal of Infectious Diseases* 202:171–175.
  80. Nett JE, Crawford K, Marchillo K, Andes DR. 2010. Role of Fks1p and matrix glucan in *Candida albicans* biofilm resistance to an echinocandin, pyrimidine, and polyene. *Antimicrobial Agents and Chemotherapy* 54:3505–3508.
  81. Uppuluri P, Chaturvedi AK, Srinivasan A, Banerjee M, Ramasubramaniam AK, Köhler JR, Kadosh D, Lopez-Ribot JL. 2010. Dispersion as an important step in the *Candida albicans* biofilm developmental cycle. *PLoS Pathogens* 6.
  82. Lepak A, Andes D. 2011. Fungal Sepsis: Optimizing Antifungal Therapy in the Critical Care Setting. *Critical Care Clinics* 27:123–147.
  83. Moudgal V, Sobel J. 2010. Antifungals to treat *Candida albicans*. *Expert Opinion on Pharmacotherapy* 11:2037–2048.
  84. Denning DW, Hope WW. 2010. Therapy for fungal diseases: Opportunities and priorities. *Trends in Microbiology* 18:195–204.

85. Ghannoum MA, Rice LB. 1999. Antifungal Agents: Mode of Action, Mechanisms of Resistance, and Correlation of These Mechanisms with Bacterial Resistance. *Clinical Microbiology Reviews* 12:501–517.
86. Yamamoto T, Umegawa Y, Yamagami M, Suzuki T, Tsuchikawa H, Hanashima S, Matsumori N, Murata M. 2019. The Perpendicular Orientation of Amphotericin B Methyl Ester in Hydrated Lipid Bilayers Supports the Barrel-Stave Model. *Biochemistry* 58:2282–2291.
87. Deray G. 2002. Amphotericin B nephrotoxicity. *Journal of Antimicrobial Chemotherapy* 49:37–41.
88. Sheehan DJ, Hitchcock CA, Sibley CM. 1999. Current and Emerging Azole Antifungal Agents. *Clinical Microbiology Reviews* 12:40–79.
89. Pappas PG, Kauffman CA, Andes D, Benjamin DK, Calandra TF, Edwards JE, Filler SG, Fisher JF, Kullberg BJ, Ostrosky-Zeichner L, Reboli AC, Rex JH, Walsh TJ, Sobel JD. 2009. Clinical practice guidelines for the management of candidiasis: 2009 Update by the Infectious Diseases Society of America. *Clinical Infectious Diseases*.
90. Canuto MM, Rodero FG. 2002. Antifungal drug resistance to azoles and polyenes. *Lancet Infectious Diseases* 2:550–563.
91. Denning DW. 2003. Echinocandin antifungal drugs. *Lancet* 362:1142–1151.
92. Holt SL, Drew RH. 2011. Echinocandins: Addressing outstanding questions surrounding treatment of invasive fungal infections. *American Journal of Health-System Pharmacy*. American Society of Health-Systems Pharmacy.

93. Rex JH, Pappas PG, Karchmer AW, Sobel J, Edwards JE, Hadley S, Brass C, Vazquez JA, Chapman SW, Horowitz HW, Zervos M, McKinsey D, Lee J, Babinchak T, Bradsher RW, Cleary JD, Cohen DM, Danziger L, Goldman M, Goodman J, Hilton E, Hyslop NE, Kett DH, Lutz J, Rubin RH, Scheld WM, Schuster M, Simmons B, Stein DK, Washburn RG, Mautner L, Chu T, Panzer H, Rosenstein RB, Booth J. 2003. A Randomized and Blinded Multicenter Trial of High-Dose Fluconazole plus Placebo versus Fluconazole plus Amphotericin B as Therapy for Candidemia and Its Consequences in Nonneutropenic Subjects. *Clinical Infectious Diseases* 36.
94. Belanger ES, Yang E, Forrest GN. 2015. Combination Antifungal Therapy: When, Where, and Why. *Current Clinical Microbiology Reports* 2:67–75.
95. Johnson MD, Perfect JR. 2010. Use of antifungal combination therapy: Agents, order, and timing. *Current Fungal Infection Reports* 4:87–95.
96. Campitelli M, Zeineddine N, Samaha G, Maslak S. 2017. Combination Antifungal Therapy: A Review of Current Data. *Journal of Clinical Medicine Research* 9:451–456.
97. Stiller RL, Bennett JE, Scholer HJ, Wall M, Polak A, Stevens DA. 1982. Susceptibility to 5-Fluorocytosine and Prevalence of Serotype in 402 *Candida albicans* Isolates from the United States. *Antimicrobial Agents and Chemotherapy* 22:482–487.
98. Pennington KM, Dykhoff HJ, Yao X, Sangaralingham LR, Shah ND, Peters SG, Barreto JN, Razonable RR, Kennedy CC. 2021. The Impact of Antifungal

Prophylaxis in Lung Transplant Recipients. *Annals of the American Thoracic Society* 18.

99. Wang J, Zhou M, Xu JY, Zhou RF, Chen B, Wan Y. 2020. Comparison of Antifungal Prophylaxis Drugs in Patients with Hematological Disease or Undergoing Hematopoietic Stem Cell Transplantation: A Systematic Review and Network Meta-analysis. *JAMA Network Open* 3:e2017652.
100. Brion LP, Uko SE, Goldman DL. 2007. Risk of resistance associated with fluconazole prophylaxis: Systematic review. *Journal of Infection* 54:521–529.
101. Buda De Cesare G, Cristy SA, Garsin DA, Lorenz MC. 2020. Antimicrobial Peptides: a New Frontier in Antifungal Therapy. *mBio* 11:e02123-20.
102. Fernández de Ullivarri M, Arbulu S, Garcia-Gutierrez E, Cotter PD. 2020. Antifungal Peptides as Therapeutic Agents. *Frontiers in Cellular and Infection Microbiology* 10.
103. Mücke PA, Maaß S, Kohler TP, Hammerschmidt S, Becher D. 2020. Proteomic adaptation of streptococcus pneumoniae to the human antimicrobial peptide LL-37. *Microorganisms* 8.
104. Nguyen LT, Haney EF, Vogel HJ. 2011. The expanding scope of antimicrobial peptide structures and their modes of action. *Trends in Biotechnology* 29:464–472.
105. Tsai PW, Yang CY, Chang HT, Lan CY. 2011. Human antimicrobial peptide LL-37 inhibits adhesion of *Candida albicans* by interacting with yeast cell-wall carbohydrates. *PLoS ONE* 6:e17755.

106. Mathews M, Jia HP, Guthmiller JM, Losh G, Graham S, Johnson GK, Tack BF, McCray PB. 1999. Production of  $\beta$ -Defensin Antimicrobial Peptides by the Oral Mucosa and Salivary Glands. *Infection and Immunity* 67.
107. Krishnakumari V, Rangaraj N, Nagaraj R. 2009. Antifungal Activities of Human Beta-Defensins HBD-1 to HBD-3 and Their C-Terminal Analogs Phd1 to Phd3. *Antimicrobial Agents and Chemotherapy* 53.
108. Takesako K, Kuroda H, Inoue T, Haruna F, Yoshikawa Y, Kato I, Uchida K, Hiratani T, Yamaguchi H. 1993. Biological properties of aureobasidin A, a cyclic depsipeptide antifungal antibiotic. *Journal of Antibiotics (Tokyo)* 46:1414–1420.
109. Aeed PA, Young CL, Nagiec MM, Elhammer ÅP. 2009. Inhibition of inositol phosphorylceramide synthase by the cyclic peptide aureobasidin A. *Antimicrobial Agents and Chemotherapy* 53:496–504.
110. Zhong W, Jeffries MW, Georgopapadakou NH. 2000. Inhibition of Inositol Phosphorylceramide Synthase by Aureobasidin A in *Candida* and *Aspergillus* Species. *Antimicrobial Agents and Chemotherapy* 44:651–653.
111. Heidler SA, Radding JA. 2000. Inositol phosphoryl transferases from human pathogenic fungi. *Biochimica Biophysica Acta* 1500:147–152.
112. Katsuki Y, Yamaguchi Y, Tani M. 2018. Overexpression of PDR16 confers resistance to complex sphingolipid biosynthesis inhibitor aureobasidin A in yeast *Saccharomyces cerevisiae*. *FEMS Microbiology Letters* 365:fnx255.
113. Bills G, Li Y, Chen L, Yue Q, Niu X-M, An Z. 2014. New insights into the echinocandins and other fungal non-ribosomal peptides and peptaibiotics. *Nat Prod Rep* 31.

114. Patil A, Majumdar S. 2017. Echinocandins in antifungal pharmacotherapy. *Journal of Pharmacy and Pharmacology* 69:1635–1660.
115. Perlin DS. 2007. Resistance to echinocandin-class antifungal drugs. *Drug Resistance Updates* 10:121–130.
116. Stenland CJ, Lis LG, Schendel FJ, Hahn NJ, Smart MA, Miller AL, von Keitz MG, Gurvich VJ. 2013. A practical and scalable manufacturing process for an antifungal agent, nikkomycin Z. *Organic Process Research and Development* 17:265–272.
117. Gow NAR, Latge J-P, Munro CA. 2017. The fungal cell wall: structure, biosynthesis, and function, p. 267–292. *In* Hetiman, J, Howlett, BJ, Crous, PW, Stukenbrock, EH, James, TY, Gow, NAR (eds.), *The fungal kingdom*. ASM Press, Washington, DC.
118. Chattaway FW, Holmes MR, Barlow AJE. 1968. Cell Wall Composition of the Mycelial and Blastospore Forms of *Candida albicans*. *J gen Microbiol* 51:367–376.
119. Li RK, Rinaldi MG. 1999. In Vitro Antifungal Activity of Nikkomycin Z in Combination with Fluconazole or Itraconazole. *Antimicrobial Agents and Chemotherapy* 43:1401–1405.
120. Kovács R, Nagy F, Tóth Z, Bozó A, Balázs B, Majoros L. 2019. Synergistic effect of nikkomycin Z with caspofungin and micafungin against *Candida albicans* and *Candida parapsilosis* biofilms. *Letters in Applied Microbiology* 69.
121. Subbalakshmi C, Sitaram N. 1998. Mechanism of antimicrobial action of indolicidin. *FEMS Microbiology Letters* 160.

122. Marchand C, Krajewski K, Lee H-F, Antony S, Johnson AA, Amin R, Roller P, Kvaratskhelia M, Pommier Y. 2006. Covalent binding of the natural antimicrobial peptide indolicidin to DNA abasic sites. *Nucleic Acids Research* 34.
123. Farzanegan A, Roudbary M, Falahati M, Khoobi M, Gholibegloo E, Farahyar S, Karimi P, Khanmohammadi M. 2018. Synthesis, characterization and antifungal activity of a novel formulated nanocomposite containing Indolicidin and Graphene oxide against disseminated candidiasis. *Journal de Mycologie Médicale* 28.
124. Rahimi H, Roudbarmohammadi S, Delavari H H, Roudbary M. 2019. Antifungal effects of indolicidin-conjugated gold nanoparticles against fluconazole-resistant strains of *Candida albicans* isolated from patients with burn infection. *International Journal of Nanomedicine* Volume 14.
125. Nikawa H, Jin C, Fukushima H, Makihiro S, Hamada T. 2001. Antifungal activity of histatin-5 against non-*albicans* *Candida* species. *Oral Microbiology and Immunology* 16.
126. Helmerhorst EJ, Troxler RF, Oppenheim FG. 2001. The human salivary peptide histatin 5 exerts its antifungal activity through the formation of reactive oxygen species. *Proceedings of the National Academy of Sciences* 98.
127. Jang WS, Bajwa JS, Sun JN, Edgerton M. 2010. Salivary histatin 5 internalization by translocation, but not endocytosis, is required for fungicidal activity in *Candida albicans*. *Molecular Microbiology* 77.
128. Li XS, Reddy MS, Baev D, Edgerton M. 2003. *Candida albicans* Ssa1/2p Is the Cell Envelope Binding Protein for Human Salivary Histatin 5. *Journal of Biological Chemistry* 278.

129. Baev D, Rivetta A, Vylkova S, Sun JN, Zeng G-F, Slayman CL, Edgerton M. 2004. The TRK1 Potassium Transporter Is the Critical Effector for Killing of *Candida albicans* by the Cationic Protein, Histatin 5. *Journal of Biological Chemistry* 279.
130. Norris HL, Kumar R, Ong CY, Xu D, Edgerton M. 2020. Zinc Binding by Histatin 5 Promotes Fungicidal Membrane Disruption in *C. albicans* and *C. glabrata*. *Journal of Fungi* 6.
131. Vylkova S, Jang WS, Li W, Nayyar N, Edgerton M. 2007. Histatin 5 Initiates Osmotic Stress Response in *Candida albicans* via Activation of the Hog1 Mitogen-Activated Protein Kinase Pathway. *Eukaryotic Cell* 6.
132. Rauseo AM, Coler-Reilly A, Larson L, Spec A. 2020. Hope on the horizon: Novel fungal treatments in development. *Open Forum Infectious Diseases* 7:ofaa016.
133. Yeung ATY, Gellatly SL, Hancock REW. 2011. Multifunctional cationic host defence peptides and their clinical applications. *Cellular and Molecular Life Sciences* 68:2161–2176.
134. Drlica K, Zhao X. 2007. Mutant selection window hypothesis updated. *Clinical Infectious Diseases*.
135. Yu G, Baeder DY, Regoes RR, Rolff J. 2018. Predicting drug resistance evolution: Insights from antimicrobial peptides and antibiotics. *Proceedings of the Royal Society B: Biological Sciences* 285.
136. el Shazely B, Yu G, Johnston PR, Rolff J. 2020. Resistance Evolution Against Antimicrobial Peptides in *Staphylococcus aureus* Alters Pharmacodynamics Beyond the MIC. *Frontiers in Microbiology* 11.



137. Yin J, Meng Q, Cheng D, Fu J, Luo Q, Liu Y, Yu Z. 2020. Mechanisms of bactericidal action and resistance of polymyxins for Gram-positive bacteria. *Applied Microbiology and Biotechnology* 104:3771–3780.
138. Swidergall M, Ernst JF. 2014. Interplay between *Candida albicans* and the antimicrobial peptide armory. *Eukaryotic Cell* 13:950–957.
139. Lazzaro BP, Zasloff M, Rolff J. 2020. Antimicrobial peptides: Application informed by evolution. *Science* 368.
140. Cullen TW, Schofield WB, Barry NA, Putnam EE, Rundell EA, Trent MS, Degnan PH, Booth CJ, Yu H, Goodman AL. 2015. Antimicrobial peptide resistance mediates resilience of prominent gut commensals during inflammation. *Science* 347.
141. Arnold MFF, Shabab M, Penterman J, Boehme KL, Griffiths JS, Walker GC. 2017. Genome-Wide Sensitivity Analysis of the Microsymbiont *Sinorhizobium meliloti* to Symbiotically Important, Defensin-Like Host Peptides. *mBio* 8:e01060-17.
142. Mallick EM, Bennett RJ. 2013. Sensing of the Microbial Neighborhood by *Candida albicans*. *PLoS Pathogens* 9.
143. Fourie R, Ells R, Swart CW, Sebolai OM, Albertyn J, Pohl CH. 2016. *Candida albicans* and *Pseudomonas aeruginosa* Interaction, with Focus on the Role of Eicosanoids. *Frontiers in Physiology* 7.
144. Déziel E, Comeau Y, Villemur R. 2001. Initiation of Biofilm Formation by *Pseudomonas aeruginosa* 57RP Correlates with Emergence of Hyperpiliated and Highly Adherent Phenotypic Variants Deficient in Swimming, Swarming, and Twitching Motilities. *Journal of Bacteriology* 183.

145. El-Azizi MA, Starks SE, Khardori N. 2004. Interactions of *Candida albicans* with other *Candida* spp. and bacteria in the biofilms. *Journal of Applied Microbiology* 96.
146. McAlester G, O'Gara F, Morrissey JP. 2008. Signal-mediated interactions between *Pseudomonas aeruginosa* and *Candida albicans*. *Journal of Medical Microbiology* 57.
147. Leclair LW, Hogan DA. 2010. Mixed bacterial-fungal infections in the CF respiratory tract. *Medical Mycology* 48.
148. Gibson J, Sood A, Hogan DA. 2009. *Pseudomonas aeruginosa* *Candida albicans* Interactions: Localization and Fungal Toxicity of a Phenazine Derivative. *Applied and Environmental Microbiology* 75.
149. Hogan DA. 2002. *Pseudomonas*-*Candida* Interactions: An Ecological Role for Virulence Factors. *Science* 296.
150. Morales DK, Hogan DA. 2010. *Candida albicans* Interactions with Bacteria in the Context of Human Health and Disease. *PLoS Pathogens* 6.
151. Davis-Hanna A, Piispanen AE, Stateva LI, Hogan DA. 2007. Farnesol and dodecanol effects on the *Candida albicans* Ras1-cAMP signalling pathway and the regulation of morphogenesis. *Molecular Microbiology* 67.
152. Kebaara BW, Langford ML, Navarathna DHMLP, Dumitru R, Nickerson KW, Atkin AL. 2008. *Candida albicans* Tup1 Is Involved in Farnesol-Mediated Inhibition of Filamentous-Growth Induction. *Eukaryotic Cell* 7.
153. Hall RA, Turner KJ, Chaloupka J, Cottier F, de Sordi L, Sanglard D, Levin LR, Buck J, Mühlschlegel FA. 2011. The Quorum-Sensing Molecules

- Farnesol/Homoserine Lactone and Dodecanol Operate via Distinct Modes of Action in *Candida albicans*. *Eukaryotic Cell* 10.
154. Lindsay AK, Deveau A, Piispanen AE, Hogan DA. 2012. Farnesol and Cyclic AMP Signaling Effects on the Hypha-to-Yeast Transition in *Candida albicans*. *Eukaryotic Cell* 11.
155. Cugini C, Morales DK, Hogan DA. 2010. *Candida albicans*-produced farnesol stimulates *Pseudomonas* quinolone signal production in LasR-defective *Pseudomonas aeruginosa* strains. *Microbiology* 156.
156. Raja M, Hannan A, Ali K. 2010. Association of Oral Candidal Carriage with Dental Caries in Children. *Caries Research* 44.
157. Ribeiro DG, Pavarina AC, Dovigo LN, Machado AL, Giampaolo ET, Vergani CE. 2012. Prevalence of *Candida* spp. associated with bacteria species on complete dentures. *Gerodontology* 29.
158. Sztajer H, Szafranski SP, Tomasch J, Reck M, Nimtz M, Rohde M, Wagner-Döbler I. 2014. Cross-feeding and interkingdom communication in dual-species biofilms of *Streptococcus mutans* and *Candida albicans*. *The ISME Journal* 8.
159. Silverman RJ, Nobbs AH, Vickerman MM, Barbour ME, Jenkinson HF. 2010. Interaction of *Candida albicans* Cell Wall Als3 Protein with *Streptococcus gordonii* SspB Adhesin Promotes Development of Mixed-Species Communities. *Infection and Immunity* 78.
160. Hoyer LL, Green CB, Oh S-H, Zhao X. 2008. Discovering the secrets of the *Candida albicans* agglutinin-like sequence (ALS) gene family – a sticky pursuit. *Medical Mycology* 46.

161. Holmes AR, McNab R, Jenkinson HF. 1996. *Candida albicans* binding to the oral bacterium *Streptococcus gordonii* involves multiple adhesin-receptor interactions. *Infection and Immunity* 64:4680–4685.
162. Bamford C v., d’Mello A, Nobbs AH, Dutton LC, Vickerman MM, Jenkinson HF. 2009. *Streptococcus gordonii* Modulates *Candida albicans* Biofilm Formation through Intergeneric Communication. *Infection and Immunity* 77.
163. Agudelo-Higueta NI, Huycke MM. 2014. Enterococcal Disease, Epidemiology, and Implications for Treatment, p. . *In* Gilmore, MS, Clewell, DB, Ike, Y, Shankar, N (eds.), *Enterococci: From Commensals to Leading Causes of Drug Resistant Infection*. Eye and Ear Infirmary, Boston.
164. Gullberg RM, Homann SR, Phair JP. 1989. Enterococcal Bacteremia: Analysis of 75 Episodes. *Clinical Infectious Diseases* 11.
165. Klotz SA, Chasin BS, Powell B, Gaur NK, Lipke PN. 2007. Polymicrobial bloodstream infections involving *Candida* species: analysis of patients and review of the literature. *Diagnostic Microbiology and Infectious Disease* 59.
166. Sutter D, Staglino D, Braun L, Williams F, Arnold J, Ottolini M, Epstein J. 2008. Polymicrobial Bloodstream Infection in Pediatric Patients. *Pediatric Infectious Disease Journal* 27.
167. Ferrari PHP, Cai S, Bombana AC. 2005. Effect of endodontic procedures on enterococci, enteric bacteria and yeasts in primary endodontic infections. *International Endodontic Journal* 38.
168. Hermann C, Hermann J, Munzel U, Ruchel R. 1999. Bacterial flora accompanying *Candida* yeasts in clinical specimens. *Mycoses* 42.

169. Cooper GS, Havlir DS, Shlaes DM, Salata RA. 1990. Polymicrobial bacteremia in the late 1980s: predictors of outcome and review of the literature. *Medicine* 69:114–123.
170. Valles J, Leon C. 1997. Nosocomial Bacteremia in Critically Ill Patients: A Multicenter Study Evaluating Epidemiology and Prognosis. *Clinical Infectious Diseases* 24.
171. Reuben AG, Musher DM, Hamill RJ, Broucke I. 1989. Polymicrobial Bacteremia: Clinical and Microbiologic Patterns. *Clinical Infectious Diseases* 11.
172. Vallés J, Rello J, Ochagavía A, Garnacho J, Alcalá MA. 2003. Community-Acquired Bloodstream Infection in Critically Ill Adult Patients. *Chest* 123.
173. Cruz MR, Graham CE, Gagliano BC, Lorenz MC, Garsin DA. 2013. *Enterococcus faecalis* inhibits hyphal morphogenesis and virulence of *Candida albicans*. *Infection and Immunity* 81:189–200.
174. Swe PM, Heng NCK, Ting YT, Baird HJ, Carne A, Tauch A, Tagg JR, Jack RW. 2007. ef1097 and ypkK encode enterococcin V583 and corynicin JK, members of a new family of antimicrobial proteins (bacteriocins) with modular structure from Gram-positive bacteria. *Microbiology* 153:3218–3227.
175. Dundar H, Brede DA, la Rosa SL, El-Gendy AO, Diep DB, Nes IF. 2015. The fsr quorum-sensing system and cognate gelatinase orchestrate the expression and processing of proprotein EF\_1097 into the mature antimicrobial peptide enterocin O16. *Journal of Bacteriology* 197:2112–2121.

176. Brown AO, Graham CE, Cruz MR, Singh K v, Murray BE, Lorenz MC, Garsin DA. 2019. Antifungal Activity of the *Enterococcus faecalis* Peptide EntV Requires Protease Cleavage and Disulfide Bond Formation. *mBio* 10:e01334-19.
177. Sherman F. 1991. Getting started with yeast *Methods Enzymology*. Academic Press.
178. Wong L, Sissions CH. 2001. A comparison of human dental plaque microcosm biofilms grown in an undefined medium and a chemically defined artificial saliva. *Archives of Oral Biology* 46:477–486.
179. Vylkova S, Lorenz MC. 2014. Modulation of Phagosomal pH by *Candida albicans* Promotes Hyphal Morphogenesis and Requires Stp2p, a Regulator of Amino Acid Transport. *PLoS Pathogens* 10:e1003995.
180. Gulati M, Lohse MB, Ennis CL, Gonzalez RE, Perry AM, Bapat P, Arevalo AV, Rodriguez DL, Nobile CJ. 2018. In Vitro Culturing and Screening of *Candida albicans* Biofilms. *Current Protocols in Microbiology* 50:e60.
181. Gillum AM, Tsay EY, Kirsch DR. 1984. Isolation of the *Candida albicans* gene for orotidine-5'-phosphate decarboxylase by complementation of *S. cerevisiae* *ura3* and *E. coli* *pyrF* mutations. *Mol Gen Genet* 198:179–182.
182. Shi W, Tian J, Xu H, Wang G, Zhou Q, Qin M. 2020. Carbon source utilization patterns in dental plaque and microbial responses to sucrose, lactose, and phenylalanine consumption in severe early childhood caries. *Journal of Oral Microbiology* 12.

183. Zhang Y, Zheng Y, Hu J, Du N, Chen F. 2014. Functional diversity of the microbial community in healthy subjects and periodontitis patients based on sole carbon source utilization. *PLoS ONE* 9.
184. Zhao Y, Zhong WJ, Xun Z, Zhang Q, Song YQ, Liu YS, Chen F. 2017. Differences in carbon source usage by dental plaque in children with and without early childhood caries. *International Journal of Oral Science* 9.
185. Arevalo AV, Nobile CJ. 2020. Interactions of microorganisms with host mucins: A focus on *Candida albicans*. *FEMS Microbiology Reviews* 44:645–654.
186. de Repentigny L, Aumont F, Bernard K, Belhumeur P. 2000. Characterization of Binding of *Candida albicans* to Small Intestinal Mucin and Its Role in Adherence to Mucosal Epithelial Cells. *Infection and Immunity* 68:3172–3179.
187. Donohue DS, Ielasi FS, Goossens KVV, Willaert RG. 2011. The N-terminal part of Als1 protein from *Candida albicans* specifically binds fucose-containing glycans. *Molecular Microbiology* 80:1667–1679.
188. Staab JF, Bradway SD, Fidel PL, Sundstrom P. 1999. Adhesive and Mammalian Transglutaminase Substrate Properties of *Candida albicans* Hwp1. *Science* 283:1535–1538.
189. Shen Y, Maupetit J, Derreumaux P, Tufféry P. 2014. Improved PEP-FOLD approach for peptide and miniprotein structure prediction. *Journal of Chemical Theory and Computation* 10:4745–4758.
190. Lamiable A, Thévenet P, Rey J, Vavrusa M, Derreumaux P, Tufféry P. 2016. PEP-FOLD3: faster de novo structure prediction for linear peptides in solution and in complex. *Nucleic acids research* 44:W449–W454.

191. Thévenet P, Shen Y, Maupetit J, Guyon F, Derreumaux P, Tufféry P. 2012. PEP-FOLD: An updated de novo structure prediction server for both linear and disulfide bonded cyclic peptides. *Nucleic Acids Research* 40:W288–W293.
192. Nobile CJ, Mitchell AP. 2005. Regulation of cell-surface genes and biofilm formation by the *C. albicans* transcription factor Bcr1p. *Current Biology* 15:1150–1155.
193. Nobile CJ, Fox EP, Nett JE, Sorrells TR, Mitrovich QM, Hernday AD, Tuch BB, Andes DR, Johnson AD. 2012. A recently evolved transcriptional network controls biofilm development in *Candida albicans*. *Cell* 148:126–138.
194. Moreno-Ruiz E, Galán-Díez M, Zhu W, Fernández-Ruiz E, D'Enfert C, Filler SG, Cossart P, Veiga E. 2009. *Candida albicans* internalization by host cells is mediated by a clathrin-dependent mechanism. *Cellular Microbiology* 11:1179–1189.
195. Martin R, Wächtler B, Schaller M, Wilson D, Hube B. 2011. Host-pathogen interactions and virulence-associated genes during *Candida albicans* oral infections. *International Journal of Medical Microbiology* 301:417–422.
196. Dalle F, Wächtler B, L'Ollivier C, Holland G, Bannert N, Wilson D, Labruère C, Bonnin A, Hube B. 2010. Cellular interactions of *Candida albicans* with human oral epithelial cells and enterocytes. *Cellular Microbiology* 12:248–271.
197. Park H, Myers CL, Sheppard DC, Phan QT, Sanchez AA, Edwards JE, Filler SG. 2005. Role of the fungal Ras-protein kinase A pathway in governing epithelial cell interactions during oropharyngeal candidiasis. *Cellular Microbiology* 7:499–510.



198. Brand A, Vacharaksa A, Bendel C, Norton J, Haynes P, Henry-Stanley M, Wells C, Ross K, Gow NAR, Gale CA. 2008. An internal polarity landmark is important for externally induced hyphal behaviors in *Candida albicans*. *Eukaryotic Cell* 7:712–720.
199. Hube B, Sanglard D, Odds FC, Hess D, Monod M, Schafer W, Schafer S, Brown AJP, Gow NAR. 1997. Disruption of Each of the Secreted Aspartyl Proteinase Genes SAP1, SAP2, and SAP3 of *Candida albicans* Attenuates Virulence. *Infection and Immunity* 65:3529–3538.
200. Naglik JR, Challacombe SJ, Hube B. 2003. *Candida albicans* Secreted Aspartyl Proteinases in Virulence and Pathogenesis. *Microbiology and Molecular Biology Reviews* 67:400–428.
201. Mayer FL, Wilson D, Hube B. 2013. *Candida albicans* pathogenicity mechanisms. *Virulence* 4:119–128.
202. Rangan SRS. 1972. A new human cell line (FaDu) from a hypopharyngeal carcinoma. *Cancer* 29:117–121.
203. Sun JN, Solis N v., Phan QT, Bajwa JS, Kashleva H, Thompson A, Liu Y, Dongari-Bagtzoglou A, Edgerton M, Filler SG. 2010. Host cell invasion and virulence mediated by *Candida albicans* Ssa1. *PLoS Pathogens* 6.
204. Blackwell JL, Miller R, Douglas JT, Li H, Reynolds PN, Carroll WR, Peters GE, Strong T v, Curiel DT. 1999. Retargeting to EGFR Enhances Adenovirus Infection Efficiency of Squamous Cell Carcinoma. *Arch Otolaryngol Head Neck Surgery* 125:856–863.

205. Sigurlásdóttir S, Engman J, Eriksson OS, Saroj SD, Zguna N, Lloris-Garcerá P, Ilag LL, Jonsson AB. 2017. Host cell-derived lactate functions as an effector molecule in *Neisseria meningitidis* microcolony dispersal. *PLoS Pathogens* 13.
206. Matthews BW. 1996. Structural and genetic analysis of the folding and function of T4 lysozyme. *The FASEB Journal* 10.
207. Wells JA. 1991. Systematic mutational analyses of protein-protein interfaces *Methods in Enzymology*.
208. Cunningham B, Wells J. 1989. High-resolution epitope mapping of hGH-receptor interactions by alanine-scanning mutagenesis. *Science* 244.
209. Graham C. 2017. Mechanism of *Candida albicans* biofilm and virulence inhibition by a bacterial secreted factor. Houston.
210. Craig TJ, Ciufo LF, Morgan A. 2004. A protein-protein binding assay using coated microtitre plates: Increased throughput, reproducibility and speed compared to bead-based assays. *Journal of Biochemical and Biophysical Methods* 60:49–60.
211. Fields GB. 2001. Introduction to Peptide Synthesis. *Current Protocols in Protein Science* 26:18.1.1-18.1.9.
212. Dmitrović V, Lenders JJM, Zope HR, de With G, Kros A, Sommerdijk NAJM. 2014. Library of Random Copolypeptides by Solid Phase Synthesis. *Biomacromolecules* 15.
213. Anderson QL, Revtovich A v., Kirienko N v. 2018. A high-throughput, high-content, liquid-based *C. Elegans* pathosystem. *Journal of Visualized Experiments* 137:e58068.

214. Diao L, Meibohm B. 2013. Pharmacokinetics and pharmacokinetic-pharmacodynamic correlations of therapeutic peptides. *Clinical Pharmacokinetics* 52:855–868.
215. Werle M, Bernkop-Schnürch A. 2006. Strategies to improve plasma half life time of peptide and protein drugs. *Amino Acids* 30.
216. Welch BD, Francis JN, Redman JS, Paul S, Weinstock MT, Reeves JD, Lie YS, Whitby FG, Eckert DM, Hill CP, Root MJ, Kay MS. 2010. Design of a Potent D-Peptide HIV-1 Entry Inhibitor with a Strong Barrier to Resistance. *Journal of Virology* 84.
217. Nattel S, Carlsson L. 2006. Innovative approaches to anti-arrhythmic drug therapy. *Nature Reviews Drug Discovery* 5.
218. Subramanian GM, Fiscella M, Lamoussé-Smith A, Zeuzem S, McHutchison JG. 2007. Albinterferon  $\alpha$ -2b: a genetic fusion protein for the treatment of chronic hepatitis C. *Nature Biotechnology* 25.
219. Verschraegen CF, Westphalen S, Hu W, Loyer E, Kudelka A, Völker P, Kavanagh J, Steger M, Schulz K-D, Emons G. 2003. Phase II study of cetorelix, a luteinizing hormone-releasing hormone antagonist in patients with platinum-resistant ovarian cancer. *Gynecologic Oncology* 90.
220. Herédi-Szabó K, Murphy RF, Lovas S. 2006. Is IGnRH-III the most potent GnRH analog containing only natural amino acids that specifically inhibits the growth of human breast cancer cells? *Journal of Peptide Science* 12.
221. Lorente L, Lecuona M, Jiménez A, Raja L, Cabrera J, Gonzalez O, Diosdado S, Marca L, Mora ML. 2016. Chlorhexidine-silver sulfadiazine– or rifampicin-

- miconazole-impregnated venous catheters decrease the risk of catheter-related bloodstream infection similarly. *American Journal of Infection Control* 44.
222. Camargo LFA, Marra AR, Büchele GL, Sogayar AMC, Cal RGR, de Sousa JMA, Silva E, Knobel E, Edmond MB. 2009. Double-lumen central venous catheters impregnated with chlorhexidine and silver sulfadiazine to prevent catheter colonisation in the intensive care unit setting: a prospective randomised study. *Journal of Hospital Infection* 72:227–233.
  223. Wang H, Tong H, Liu H, Wang Y, Wang R, Gao H, Yu P, Lv Y, Chen S, Wang G, Liu M, Li Y, Yu K, Wang C. 2018. Effectiveness of antimicrobial-coated central venous catheters for preventing catheter-related blood-stream infections with the implementation of bundles: a systematic review and network meta-analysis. *Annals of Intensive Care* 8.
  224. Fleitas Martínez O, Cardoso MH, Ribeiro SM, Franco OL. 2019. Recent Advances in Anti-virulence Therapeutic Strategies With a Focus on Dismantling Bacterial Membrane Microdomains, Toxin Neutralization, Quorum-Sensing Interference and Biofilm Inhibition. *Frontiers in Cellular and Infection Microbiology* 9.
  225. Rezzoagli C, Archetti M, Mignot I, Baumgartner M, Kümmerli R. 2020. Combining antibiotics with antivirulence compounds can have synergistic effects and reverse selection for antibiotic resistance in *Pseudomonas aeruginosa*. *PLOS Biology* 18.
  226. Shaw E, Wuest WM. 2020. Virulence attenuating combination therapy: a potential multi-target synergy approach to treat *Pseudomonas aeruginosa* infections in cystic fibrosis patients. *RSC Medicinal Chemistry* 11.

227. Shaban S, Patel M, Ahmad A. 2020. Improved efficacy of antifungal drugs in combination with monoterpene phenols against *Candida auris*. *Scientific Reports* 10.
228. Cui J, Ren B, Tong Y, Dai H, Zhang L. 2015. Synergistic combinations of antifungals and anti-virulence agents to fight against *Candida albicans*. *Virulence* 6.
229. Mundt JO. 1963. Occurrence of Enterococci in Animals in a Wild Environment. *Applied Microbiology* 11.
230. Martin JD, Mundt JO. 1972. Enterococci in Insects. *Applied Microbiology* 24.
231. Gilmore MS, Lebreton F, van Schaik W. 2013. Genomic transition of enterococci from gut commensals to leading causes of multidrug-resistant hospital infection in the antibiotic era. *Current Opinion in Microbiology* 16:10–16.
232. Tong Y, Tang J. 2017. *Candida albicans* infection and intestinal immunity. *Microbiological Research* 198:27–35.

## **Vita**

After Shane Alan Cristy completed his coursework at Randall High School, Amarillo, Texas in 2015, he entered Texas Tech University in Lubbock, Texas. He received the degree of Bachelor of Science with a major in biochemistry from Texas Tech in May, 2019. In August of 2019 he entered The University of Texas MD Anderson Cancer Center UTHHealth Graduate School of Biomedical Sciences.